



University of Genoa



Medical School University of Thessaly

Scuola di Dottorato di Ricerca in BIOLOGIA E MEDICINA

SPERIMENTALE, MOLECOLARE E CLINICA

Corso di Dottorato di Ricerca in BIOTECNOLOGIE

Indirizzo di BIOLOGIA E CHIRURGIA VASCOLARE

SPERIMENTALE E CLINICA

XXV Ciclo

PhD Thesis

**POSITRON EMISSION COMPUTED TOMOGRAPHY FOR THE  
EVALUATION OF ABDOMINAL AORTIC ANEURYSMS AND RISK  
OF RUPTURE**

Nikolaos Rousas MD, MSc

Supervisor:

Prof. Domenico Palombo and Prof. Athanasios Giannoukas

## INDEX

Ringraziamenti	V
Ευχαριστίες	Vii
Chapter I <i>Abdominal Aortic Aneurysm</i>	1
1. Introduction	1
1.1 Background	1
1.2 Historical perspectives	3
1.3 Risk Factors for AAA development	4
1.3.1 <i>Gender</i>	4
1.3.2 <i>Age</i>	5
1.3.3 <i>Smoking</i>	5
1.3.4 <i>Atherosclerosis</i>	6
1.3.5 <i>Hypertension</i>	7
1.3.6 <i>Cholesterol</i>	8
1.3.7 <i>Diabetes Mellitus</i>	9
1.4 Natural History	11
1.4.1 <i>Growth</i>	11
1.4.2 <i>Rupture</i>	12
Chapter II <i>Methods of Diagnosis</i>	14
2. Introduction	14
2.1 Ultrasound	15
2.1.1 <i>Limitations of Ultrasound</i>	17
2.2 Computed Tomography CT	19
2.3 Ultrasound verse CT	23
2.4 Role of Positron Emission Tomography (PET)	24
Chapter III <i>Treatment of AAA</i>	28
3. Introduction	28
3.1 Medical Therapy	28
3.2 Operative Treatment	29
3.2.1 <i>Intact AAA repair</i>	29
3.2.2 <i>Ruptured AAA repair</i>	32
Chapter IV <i>Rupture Criteria</i>	33
4. Introduction	33
4.1 Biomarkers	34
4.2 Biomechanical Analysis	36
Chapter V <i>Arterial Wall</i>	38
5. Introduction	38
5.1 Pathophysiology anatomy of Normal Aorta	38
5.2 Cells in the normal and aneurysmal aorta	41
5.3 Matrix of the Aorta	42
5.3.1 <i>Elastin</i>	43
5.3.2 <i>Collagen</i>	44
5.4 Proteases and their Inhibitors	45
5.4.1 Neutrophil elastase	46
5.4.2 Metalloproteinases	47
5.4.3 <i>Cathepsins, Trypsin, Chymase, Granzyme B</i>	50

Chapter VI <i>Our Study</i>	51
6. Introduction	51
6.1 Background	51
6.2 Objectives	53
6.3 Materials and methods Objective 1	54
6.3.1 Patient Population	54
6.3.2 PET/CT Acquisition	56
6.3.2a Image Analysis	56
6.3.2b Visual Analysis	56
6.3.2.c Quantitative Analysis	57
6.3.2.d Calcium Load Evaluation	60
6.3.2e Statistical Analysis	60
6.4 Materials and methods Objective 2	61
6.4.1 Patient Population	61
6.4.2 Biochemical assays	62
6.4.3 PET/CT Acquisition	62
6.4.3a In vivo image analysis	63
6.4.3b Autoradiographic image analysis	65
6.4.3.c Histology	65
6.4.3d Statistical analysis	66
6.5 Results Objective 1	68
6.5.1 Clinical Data	68
6.5.2 <i>PET/CT Evaluation of AAA</i>	71
6.6 Results Objective 2	74
6.6.1 Clinical Data	74
6.6.2 <i>PET/CT Evaluation of AAA</i>	77
6.6.3 <i>Histological correlates of FDG uptake in aortic aneurysm</i>	79
6.7 Discussion Objective 1	83
6.8 Discussion Objective 2	87
6.9 Conclusion	93
References	94

*Στο θεμέλιο της Ζωής μου*

*Ιωάννη κ Δήμητρα Ρούσα*

*Στην αδερφή μου*

*Σοφία Ρούσα*

*για τις Θερμοπύλες που κρατούσε*

## Ringraziamenti

Il mio primo ringraziamento appartiene di diritto ai miei colleghi ma soprattutto amici, **Pane Bianca** e **Giovanni Spinella** per il loro grande aiuto e sostegno che mi hanno mostrato in tutti questi anni e nella stesura di questa tesi. Questo traguardo appartiene anche a loro. Mi sento benedetto per l'esistenza di queste due persone che in tutti questi anni ho avuto come compagni in questa faticosissima e lunga strada. **Giovanni e Bianca** sono la prova lampante che la vera amicizia esiste. Si costruisce difficilmente ma si conserva a vita. Il migliore titolo che potrò mai vantare nella mia vita sarà quello di essere loro amico. E' un onore per me ragazzi . Vi ringrazio dal profondo dell'anima per questa *VERA AMICIZIA* che durerà per sempre, anche se la distanza potrà separarci, voi sarete sempre nel mio cuore.

Ringrazio di cuore il Professor **Domenico Palombo**, che per me sarà sempre il mio *Maestro*. Lo ringrazio non solo perché mi ha fatto innamorare di Chirurgia Vascolare ma per gli insegnamenti di vita che mi ha dato come: lavorare sodo, non lamentarti, guarda sempre avanti e prosegui per la tua strada, anche se è difficile, tenendo sempre fede alla parola data. Professore per me lei sarà sempre quello che il padre della medicina Ippocrate scrive «Ἠγήσασθαι μὲν τὸν διδάξαντά με τὴν τέχνην ταύτην ἴσα γενέτησιν ἐμοῖσι,....» (*di stimare il mio maestro di questa arte come mio padre..*)

Ringrazio il Professor **Athanasio Giannouka** che, come mio direttore in questi anni mi ha insegnato che la pazienza è la virtù dei forti. Spero mi perdoni se qualche volta, l'irruenza giovanile ha preso il sopravvento, ma imparo... La ringrazio per avermi accolto come suo figlio, per le innumerevoli opportunità che mi dà e soprattutto per la fiducia e l'affetto di cui mi sta circondando. Farò di tutto per non deluderLa.

Un ringraziamento speciale al professor **Miltiadi Matsagka**, per avermi onorato di partecipare come supervisore nella mia tesi. Per me è un grande onore, la sua presenza in quando lo apprezzo molto sia professionalmente sia come uomo.

Particolare menzione vorrei fare al Professor **Gianfranco Pane**, che ci ha lasciato troppo presto, per il sostegno e l'affetto che mi ha mostrato in tutti questi anni.

Vorrei ringraziare e chiedere scusa a tutti gli amici che ho angosciato e stancato durante la stesura di questa tesi. Specialmente a **Elena Xatzinikou**, per la sua pazienza e assistenza nella correzione della tesi. **Giorgio Sakouti**, per le ore improponibili di assistenza al PC ma anche per l'ottimo lavoro nella creazione del CD che trovate nella tesi.

A mia sorella **Sofia Rousa – Gkampoura** un enorme grazie, per le Termopili che hai tenuto tutti questi anni lasciandomi proseguire nel mio cammino senza preoccupazioni. Sofia respira ora....

Tutto questo non esisterebbe se Dio non mi dava il fondamento della mia vita, i miei genitori **Giovanni e Dimitra Rousas**. Non ci sono parole per esprimere la benedizione di avere queste persone per genitori. Da loro ho imparato in pratica cosa è l'amore incondizionato. Tutto questo faticoso lavoro è per LORO ed è il minimo che potrei fare per ripagarli di una vita vissuta per il loro figlio. Qualsiasi successo nella mia vita sarà dedicato a loro. Grazie. Mi auguro un domani di poter assomigliarvi e non deludervi mai.

## ΕΥΧΑΡΙΣΤΙΕΣ

Οι πρώτες μου ευχαριστίες δικαιοματικά ανήκουν στους συναδέλφους και φίλους μου **Bianca Pane** και **Giovanni Spinella** για την αμέριστη βοήθεια και υποστήριξη που μου δείξαν σε όλη αυτή τη δύσκολη περίοδο της συγγραφής της παρούσας Διατριβής. Νιώθω ευλογημένος για την ύπαρξη αυτών των δύο ανθρώπων που συνοδοιπόροι όλα αυτά τα χρόνια με στήριξαν στο μακρύ δρόμο μου. Είναι απόδειξη ότι οι αληθινές φιλίες κατακτώνται με κόπο αλλά διατηρούνται για μια ζωή. Ο καλύτερος τίτλος που θα μπορούσα ποτέ να αποκτήσω στη ζωή μου είναι αυτός να είμαι φίλος του. Και αυτή τη χαρά και τιμή, μου τη δώσανε ο Giovanni και η Bianca. Τους ευχαριστώ από την ψυχή μου και τους υπόσχομαι ότι αυτή η αληθινή φιλία θα έχει διάρκεια όσο και αν οι χιλιομετρικές αποστάσεις μας χωρίζουν γιατί η καρδιά μου θα είναι πάντα μαζί τους.

Θέλω να ευχαριστήσω από καρδιάς τον Καθηγητή **Domenico Palombo** που για πάντα θα είναι ο *Καθηγητής ο Δάσκαλος* μου. Ευχαριστίες όχι μόνο γιατί μου έμαθε την Αγγειοχειρουργική με σωστές βάσεις και δεδομένα αλλά γιατί μου δίδαξε ως άνθρωπος τι θα πει να εργάζεσαι σκληρά, να βάζεις στόχους, και να είμαι πάντα συνεπείς στο λόγο μου. Κύριε Καθηγητά για μένα θα είστε πάντα αυτό που αναφέρει ο πατέρας της Ιατρικής Ιπποκράτης «Ἦγήσασθαι μὲν τὸν διδάξαντά με τὴν τέχνην ταύτην ἴσα γενέτησιν ἑμοῖσι,....»

Ευχαριστώ θερμά τον Καθηγητή **Αθανάσιο Γιαννούκα** που ως διευθυντής μου αυτά τα χρόνια μου έμαθε ότι η υπομονή είναι το όπλο των ισχυρών. Ελπίζω να συγχωρέσει τον παρορμητικό μου χαρακτήρα μερικές φορές αλλά ως νέος ακόμα μαθαίνω. Τον ευχαριστώ που με δέχτηκε σαν δικό του παιδί μου, για τις αναρίθμητες ευκαιρίες που μου δίνει σε πολλαπλά πεδία και κύριος για την εμπιστοσύνη και στοργή με την οποία με έχει περιβάλει. Θα κάνω το παν για να μην σας απογοητεύσω.

Ιδιαίτερα ευχαριστώ τον Καθηγητή **Μιλτιάδη Ματσάγκα** για την τιμή που μου έκανε να παρευρεθεί ως επιβλέπων καθηγητής στη διατριβή μου. Για μένα είναι ιδιαίτερη τιμή η παρουσία του γιατί τον εκτιμώ τόσο για το επιστημονικό του έργο όσο και ως άνθρωπο.

Ιδιαίτερη μνεία θέλω να κάνω για τον Καθηγητή **Gianfranco Pane**, ο οποίος έφυγε από κοντά μας τόσο νωρίς, για την υποστήριξη και τη στοργή που μου έδειξε όλα αυτά τα χρόνια.

Θέλω να ευχαριστήσω και να ζητήσω συγνώμη από όλους τους φίλους που κούρασα και γκρίνιαξα κατά τη διάρκεια όλης αυτής της περιόδου. Ιδιαίτερα την **Έλενα Χατζηνίκου** για την υπομονή της και την βοήθεια της στην εκπόνηση αυτής της διατριβής. **Γιώργο Σακούτη**, για τις ώρες που μέσα στον πανικό μου τον καλούσα για να επισκευάσει των υπολογιστή και ήταν πάντα εκεί, όπως και για την καταπληκτική δουλειά που έκανε στην δημιουργία του CD της διατριβής.

Στην αδελφή μου **Σοφία Ρούσα-Γκαμπούρα** ένα τεράστιο ευχαριστώ για τις Θερμοπύλες που κράτησε τόσα χρόνια ώστε να μπορέσω απερίσκεπτα να ολοκληρώσω το έργο μου. Σοφία πάρε ανάσες τώρα..

Όλο αυτό το πόνημα δε θα μπορούσε να υπάρχει αν ο Θεός δε μου είχε δώσει το θεμέλιο της ζωής μου, τους γονείς μου **Ιωάννη** και **Δήμητρα Ρούσα**. Δεν υπάρχει λέξη ή τρόπος να εκφράσω την ευλογία που νιώθω έχοντας τέτοιους ανθρώπους για γονείς. Από αυτούς έμαθα εμπράκτως τι είναι ανιδιοτελής αγάπη. Όλος αυτός ο αγώνας και όλος αυτός ο κόπος τους αξίζει, είναι το λιγότερο που θα μπορούσα να κάνω για να τους ανταμείψω για μια ζωή που αφιέρωσαν για εμένα. Κάθε μου επιτυχία θα είναι αφιερωμένη σε εκείνους. Σας ευχαριστώ. Είθε ο Θεός να μου δώσει να μοιάσω έστω και στο ελάχιστο σε εσάς.



# Chapter I

## Abdominal Aortic Aneurysm

### 1.1 Background

The term aneurysm originates from the Greek word Ανεύρυσμα (Aneurysma), meaning a widening. An aneurysm is defined as a local, permanent dilatation of an artery at least 1.5 times its normal diameter (Figure 1.1). Any artery can become aneurysmal yet the infrarenal segment of the abdominal aorta is the most common site for development of Abdominal Aortic Aneurysms (AAAs).

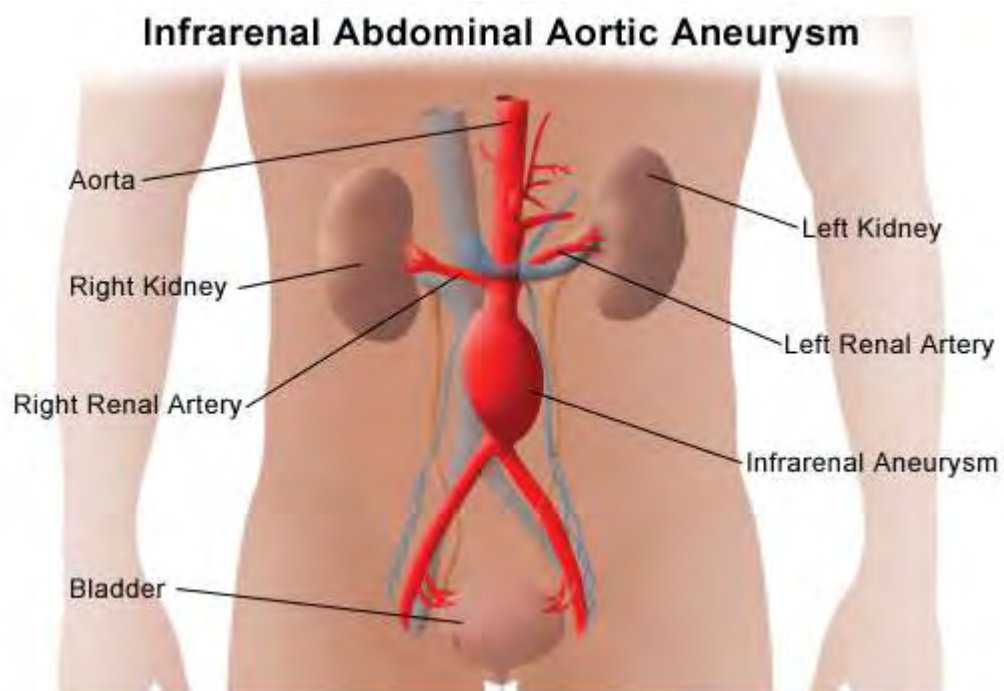


Figure 1.1 Anatomy of Abdominal Aortic Aneurysm

The prevalence of AAA is growing along with population age and according to different studies AAA rupture is the 13th most common cause of death in the United States (1) causing an estimated 15.000 deaths per year.

The incidence of AAA is 2-4 per cent in the adult population and it is growing with increase in the average population age. The risk of AAA in white males is elevated as compared to black males who have a hazard ratio of 0.57 compared to white men (2). In women the incidence of AAA is much lower, mostly likely due to hormonal differences.

AAA's are asymptomatic and are rarely detected until rupture. The incidence of asymptomatic AAA's appear to be 0.8% at age 50 and increase to 6% at age 65 in males (3). Rupture is defined as extravasion of blood or hematoma outside the AAA. (4). One third of untreated AAA's will rupture. Ruptured AAA's (rAAA) are responsible for 1.3% of all deaths among males between the ages of 65– 85 years. (5,6). Ruptured AAA's require emergency surgery and have an associated mortality rate of 65–85% half of which occur prior to surgery. It is more preferable to perform elective surgery on AAA's before they rupture. The mortality rate for elective AAA repair is 0%-9%, a rate significantly lower than emergency repair surgery. (6-12).

AAA's are mainly asymptomatic; therefore screening is required for diagnosis. Once diagnosed, the aneurysm size and growth can be kept under surveillance to assess the risk of rupture. An AAA of 5.5 - 6cm is considered as a risk of rupture. Once it is considered as a risk, elective surgery is recommended. Previous studies have shown that screening for AAA's is cost effective and can reduce the mortality rate. (6, 7, 13 - 16).

## **1.2 Historical perspectives**

Aneurysms might have been known in ancient Egypt, although Shushruta, a surgeon who lived in India, probably made the first written record sometime between 800 and 600 BC, in the treatise Sira Granthi, 'Tumours of the vessels' (Prakash 1978). Rufus of Ephesus (110-180 AD) advised treating an aneurysm with digital compression, torsion or ligation of the artery. Galen of Pergamon (129-201AD) described two types of aneurysms, one being a dilatation of the artery and the other a result of injury to an artery.

In the early Byzantine era (Byzantine Empire 395-1453 AD) Oribasios of Pergamon (325-403 AD) was the first to discuss operative indications, warning against hasty surgery on large aneurysms, especially those in the armpit groin and neck. He also referred to Antyllos who had earlier described complete exposure and ligation of non-traumatic aneurysms. At this time in history, the Greeks called an area being dilated; 'aneurysma'

The Belgian anatomist and physician Vesalius (1514-1564) was one of the first to describe an AAA. The treatment of aneurismal disease consisted primarily of ligation during the 18th and 19th century. Several innovative techniques such as external compression, wiring and electrocoagulation and cellophane wrapping were tried in the late 19th and first half of the 20th century.

The first successful reconstructive AAA repair was performed in 1951 by Freeman and Leeds (Freeman, 1951) and in the following years, the first repair of a rAAA was performed (Bahnson, 1953). Early on, freeze-dried homograft was used to replace the aorta (Dubost, 1952), which subsequently was replaced by more durable synthetic prostheses such as Vinyon-N cloth (Voorhees, 1952) and knitted Dacron (De Bakey, 1958). The innovative technique of endovascular aneurysm repair was first described by Volodos in the Russian medical literature (Volodos, 1986), and was later disseminated in clinical practice by Parodi (Parodi, 1991).

### 1.3 Risk Factors for AAA development

Abdominal Aortic aneurysm is a complex vascular condition with no one specific cause for its development. Risk factors for AAA formation include male sex, age, smoking, family history as well as atherosclerosis (3, 17).

#### 1.3.1 Gender:

Male sex is the most predominant risk factor. AAA's occur up to 5 times more in men than in women (3). With the incidence of AAA in women thought to be 0.7% compared to that of men, which is 3.9% (18, 19). However, the growth rate of AAA's is significantly higher in females than in males (20, 21). Women have smaller anatomies compared to men therefore the risk of rupture in females is at a smaller AAA size compared to males (6,16,22-24).

AAA's in males are reported at 65 years and older; where as AAA's in women occur in a later age group (75-80 years) (22). When women are diagnosed with AAA they usually have other co morbid conditions, making treatment of their AAA complicated. The risk of AAA in females compared to males appears to be similar to their risk for cardiovascular disease. Females are protected from such disease in their middle ages due to the high level of oestrogen in their system pre-menopause. A lab based study documented a decrease in AAA formation in male rats when they were treated with oestrogen, thus like other cardiovascular diseases, oestrogen may protect females from AAA formation until later in life (18)

Astrand *et al*/ reported that stress on the male abdominal aortic wall increases with age and its response to compensatory thickening is insufficient, unlike that of the female abdominal aorta (25)

### 1.3.2 Age:

The incidence of AAA increases with age from 0.8% in males at the age of 50 years to 6% of those aged 65 years (3). The risk of AAA formation and rupture increases with age, with the incidence peaking at 65-70 years in males (3, 26, 27), whereas in women it is at 70-80 years (19,21). AAA usually presents in women who are at an older stage of life compared to men (21, 24)

### 1.3.3 Smoking:

Smoking appears to be one of the strongest independent risk factors for AAA formation and growth (11, 12, 28, 29). Current smoking and duration of smoking are the most prevalent (12, 11, 30, 31).

Life-time male smokers are 2.5 times more likely to present with an AAA than non-smoking males (15). Patients who have been previous smokers have reduced risk of death compared to current smokers (15). Previous smoking still poses a risk, but at a lower incidence of 1.5 times that of non-smokers (3). A study by Lee *et al* of current and recent ex-smokers the likelihood of AAA was 3 times greater than ex-smokers of 5 years and more, than those who never smoked (28). Smoking has also been proven to be the biggest risk predictor for AAA in females (19). Studies have shown that smoking increases growth rates of AAA's by 15-20% and therefore increasing the risk of rupture (6, 28, 32).

The link between smoking and its strong association with AAA formation and growth appears unknown; however some studies suggest serum cotinine, a nicotine metabolite increases growth rate of AAA's (30). It is also thought that some components of smoking may inhibit the active site of  $\alpha_1$ -antitrypsin, leading to the degradation of elastin in the aortic wall by proteolytic enzymes (28, 30).

Receptors that can bind nicotine are not only present on neurons but also on lymphocytes and macrophages (53). Neutrophils exposed to nicotine increase their expression of elastase (54). Nicotine also activates matrix metalloproteinase (MMP2)

expression by smooth muscle cells in the vessel wall, enhancing AAA formation in animals in vivo. Studies in vitro indicate that tobacco smoke extracts cause death of human and animal smooth muscle cells, arterial and pulmonary endothelial cells, and human monocyte/macrophages (55, 56, 57).

The association of smoking and AAA formation and progression is much more pronounced than the association of smoking with coronary artery disease (CAD) (33). Long term smokers have a higher possibility of death from AAA's than CAD. This suggests that AAA formation is not independantly caused by the atherosclerotic process (28, 30, 33).

#### *1.3.4 Atherosclerosis:*

Atherosclerosis is associated with damage to the endothelial lining and lipid deposits in the tunica media. Increased lipid levels in the blood initiates the formation of atherosclerosis.

Atherosclerosis formation occurs with breakdown of the endothelial wall, promoting aggregation of platelets and also attracting phagocytes. Cholesterol and triglycerides collect at the injury site of the inner layer of the arterial wall. Macrophages arrive at the site due to the inflammatory process. Contact with platelets, lipids and other components of blood stimulate smooth muscle cells and collagen fibres in the arterial wall to proliferate abnormally. This occurs due to low levels of apolipoprotein- E (ApoE), which transports lipid in the blood and are quickly absorbed by body tissues or by high levels of low density lipoprotein which is slowly absorbed by the body. In response to this there is a build up of lipids and formation of atherosclerosis which causes a narrowing in the arterial wall and disturbance to the blood flow (34, 35).

The inflammatory process of atherosclerosis is linked with the AAA formation, enlargement and rupture cycle (36-38). One study implicates the inflammatory response as a potential cause of aneurysm rupture (39). Matrix metalloproteinase 9

(MMP9) is an enzyme when secreted presents a pathway for collagen degradation, AAA expansion and rupture. (40) However, this does not prove that atherosclerosis and an inflammatory response is a direct cause of AAA. A recent study examined the diabetic association of AAA and reports atherosclerosis as an associated feature and not a causative factor (41). (Figure 1.2)

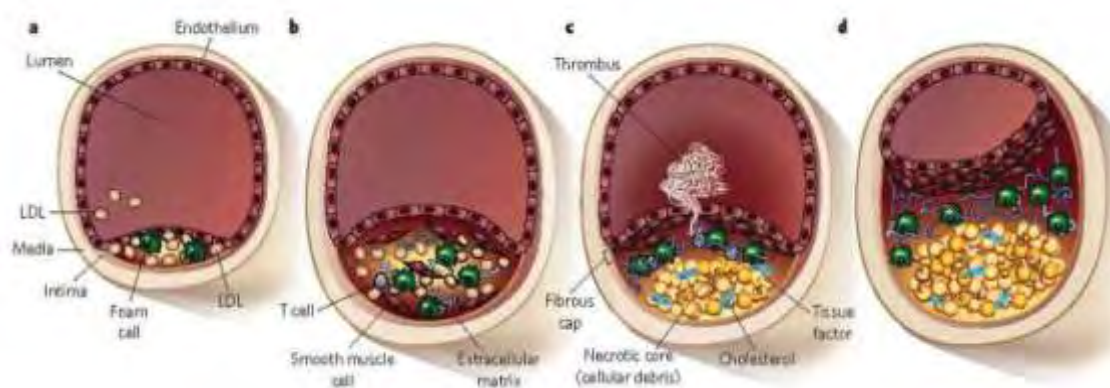


Figure 1.2 The inflammatory process involved in the formation of atherosclerosis

### 1.3.5 Hypertension

Hypertension (HTN) has been shown to pose a risk of AAA formation (28). There are conflicting studies which argue that HTN is risk of rupture rather than formation and growth of an AAA. While other studies have reported that there is no relationship between HTN and formation of AAA or increased expansion rates of existing AAA's (3, 12, 32).

HTN has been shown to be associated with AAA rupture due to its haemodynamic stress effect and its involvement in the up regulation of transcription factors (42, 25). The haemodynamic burden on the aortic wall depends on the mean blood pressure. An elevated burden is constantly putting pressure on the ever weakening aneurismal section causing the AAA to enlarge (15). In large and ruptured AAA's the wall stress at maximal systolic blood pressure is considerably higher than

in small AAA's (6, 25, 39, 43) which shows the association between HTN and rupture.

#### *1.3.6 The role of high cholesterol:*

Elevated LDL cholesterol, total cholesterol and triglycerides have been recorded in patients with AAA (12, 28). Studies have shown that cholesterol alone does not cause aortic enlargement (44, 45, 46). Significant association of plasma LDL and small aortic aneurysms has been shown (47). One study has shown that small LDL size is an independent risk factor for AAA (48). However, Golledge *et al* claims there is no association between LDL and AAA, but there is consistent association between low HDL and small AAA (49). HDL has anti-inflammatory and antioxidant properties and a low HDL level reduces its preventive properties and therefore may lead to inflammation of the abdominal aorta (49).



### 1.3.7 Relationship of Diabetes Mellitus and AAA:

Most studies have shown the inverse effect of Diabetes Mellitus (DM) on AAA formation and growth (19, 32, 41, 50).

One study has shown the association of the circulating marker of the glycation pathway, carboxymethyllysine (CML) and discovered levels of CML to be lower in patients with diabetes and AAA compared to patients with AAA and no diabetes (51). Another study suggests that hyperglycemia inhibits metalloproteinases (MMP) production, and therefore inhibiting MMP activity which is essential in AAA progression (52).

This is one explanation of the negative relationship of DM and AAA formation.

(Figure 1.3)

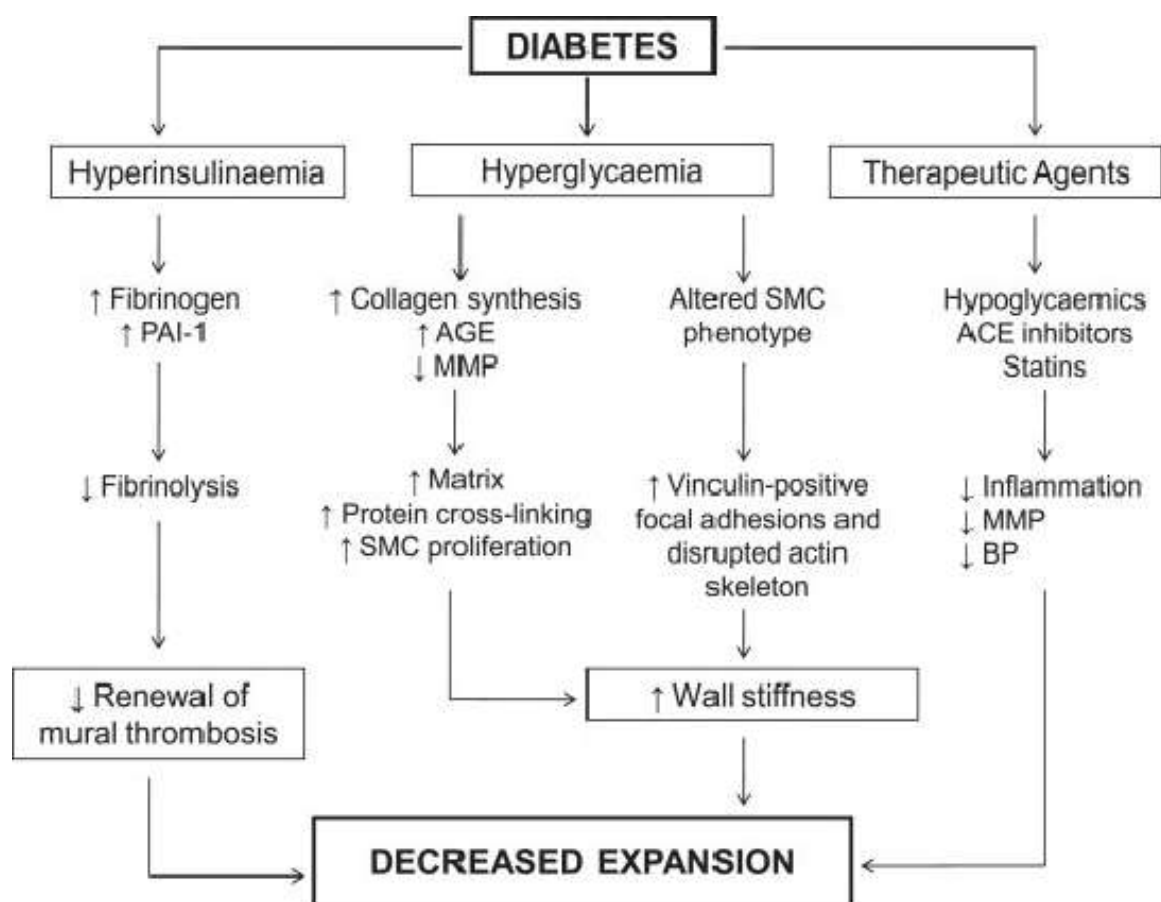


Figure 1.3 Effect of diabetes on AAA

The above diagram shows the inverse effect of diabetes in AAA expansion. In hyperinsulinaemia, decreased fibrinolysis leads to decreased mural thrombus formation which accumulates in an AAA. The less mural thrombus present prevents the AAA from expanding further.

Hyperglycaemia causes that arterial wall to stiffen due to an increase in matrix, protein crosslinking and vinculin positive focal adhesions. Due to this increased wall stiffness the aneurysm is unable to expand further.

The therapeutic agents given to diabetes sufferers, decrease inflammation, MMP levels and blood pressure. All of which are heavily involved in the formation and expansion of an AAA.

## 1.4 NATURAL HISTORY: GROWTH AND RUPTURE

### 1.4.1 Growth

It is generally assumed that the natural history of an AAA is continuous growth and eventual rupture. Growth and associated risk factors have been assessed in patients with small aneurysms or patients unfit for surgery. Annual AAA expansion rate is reported to be approximately 0.2-0.3 cm (9, 20, 32, 54-58) but there are substantial individual variations. In the United Kingdom Small Aneurysm Trial (UKSAT) and the Aneurysm Detection and Management (ADAM) trial the median annual growth rate was 0.3 cm in AAAs 4.0-5.5 cm.<sup>9,58</sup> Aneurysm with a diameter of 3.0-3.9 cm, followed outside the ADAM trial, had a median annual growth rate of 0.1 cm/year.<sup>(59)</sup>

Several conditions and diseases influence AAA growth. Large initial aneurysm diameter (9, 32, 54, 60), smoking (32, 55, 61) and age (61, 62,) have been reported to be risk factors for AAA growth. Presence of diabetes is associated with slower AAA growth.<sup>(9,32)</sup> The association between AAA growth and different manifestations of cardiovascular disease, such as suboptimal lipid profile, hypertension and low ankle/brachial pressure index are, however, less clear (32, 45, 55).

Female sex has been reported to be an independent risk factor for an increasing AAA growth rate (20, 54, 57) although contradicted by others (32, 55, 56). In two of the studies showing no association, few women were included. Nevertheless, this is an important subject of study, particularly when taking into account the reported higher rupture risk in female AAA patients.

Statin use and angiotensin converting enzyme inhibitor therapy have been reported to be associated with decreased AAA growth and lower rupture risk (57, 63). However, patients taking angiotensin converting enzyme inhibitors were recently reported to have faster aneurysm growth, in conflict with previous results (64).

Whether or not statin or angiotensin converting enzyme inhibitor therapy should be initiated to inhibit aneurysm expansion remains to be clarified.

#### *1.4.2 Rupture*

Aneurysm diameter is the currently used clinically predictor of rupture. Elective repair of AAA can prevent rupture but is associated with a non-negligible risk of mortality. In the large trials comparing patients with AAAs 4.0-5.5 cm kept under surveillance with prophylactic surgery, the UKSAT and the ADAM trial, elective repair of small aneurysms was not associated with superior survival (9, 65). These trials have had a strong influence on management of AAA patients in clinical practice.

The annual rupture rates for the surveillance groups were 0.6% in the ADAM trial and 1.0% in the UKSAT. In a study investigating the rupture rate of AAA of at least 5.5 cm in patients not planned for aortic intervention due to medical contraindications or patient refusal, the estimated yearly risk of rupture was markedly higher, 10.2% in patients with AAA  $\geq 6.0$  cm and 32.5% in patients with a diameter of 7.0 cm or more (66). Due to the study design it is difficult to generalize these results to an average AAA population.

Follow up of AAA patients aims to assess the risk of rupture versus risks associated with intervention. In a follow up of the UKSAT study population and an associated study of patients monitored for aneurysm growth, including totally 2257 patients of whom 21% were women, risk factors for rupture were investigated (6). Low forced expiratory volume in the first second (FEV1) and current smoking were associated with the risk of rupture. A higher mean arterial pressure (MAP) increased the risk slightly, adjusted hazard ratio was 1.02 (95% Confidence Interval (CI) 1.00-1.02 per mm Hg). A threefold increased risk of rupture was recorded in women after adjustment for initial aneurysm diameter, age and body size (6). The risk of aneurysm rupture was four times higher in women than men in the long-term follow up of the UKSAT (65) In a Finnish study of 221 patients (22% women) who died of

ruptured AAA, a higher proportion of women were found among patients with ruptured AAA smaller than 5,5 cm in diameter (67). In a study of 476 AAA patients (21% women) considered unfit for surgery, a four time higher risk for women with aneurysms 5.0-5.9 cm compared to men was recorded (24). Furthermore, a study from the United Kingdom of 210 subjects (22% women) showed that women with AAA have a shorter time to rupture compared to men with the same aneurysm diameter (68). In a report from the United States, based on the Nationwide Inpatient Sample, a higher percentage of women with AAA presented with rupture compared to men (69). It is clear that women have a more unfavorable aneurysm disease compared to men. The contributing causes to the increased risk of rupture among female AAA patients are not fully understood and further studies within the area are needed.

## **Chapter II**

### **Methods of Diagnosis of AAA:**

#### **2. Introduction**

Most AAA's are asymptomatic and are usually detected accidentally during physical examination. Large AAA's may be detected clinically by careful palpation or feeling of the abdomen, which may reveal an abnormally wide pulsation of the abdominal aorta. In overweight people, aneurysms can be very difficult to detect on physical examination.

Aneurysms on the verge of rupture when they are rapidly enlarging, they are often tender. Listening with a stethoscope may also reveal a bruit or abnormal sound from turbulence of blood within the aneurysm. Symptoms only occur near to or at point of rupture. These include lower abdominal, back or testicular pain, nausea and vomiting, feeling of coldness in the legs, profuse sweating and hypotension post rupture. (70)

An abdominal aortic aneurysm needs diagnostic imaging to be diagnosed and accurately measured. The first method of choice is ultrasound as it is non-invasive. Ultrasound has been shown to be a reliable and a cost effective method in the diagnosis of AAA.

## **2.1 Ultrasound for AAA diagnosis**

In a clinical setting Ultrasound is said to be the most practical, non-invasive and inexpensive modality in screening for and surveillance of AAA , with a sensitivity of 98.9% and specificity of 99.9% (9, 71,72). Ultrasound can reliably image the aorta in 99% of patients (73), however it is highly operator dependent.

Real-time ultrasound provides the examiner with a two-dimensional greys-scale image of the abdominal organs and vasculature. It is possible to image anomalies of arterial location and arterial course as well as pathologically dilated segments. Information can be gathered about the extent of aneurysms from cross-sectional measurements in different planes and these values can also be used in relevant follow-up examinations.

Significant portions of the abdominal aorta are not visualized on emergency due to non-fasting patients and the presence of bowel gas etc. This rate is higher than reported for fasting patients receiving elective ultrasound for evaluations of their aortas.

Ultrasound is not very accurate in determining the presence of a leak from an aneurysm. A rAAA can be indicated by the presence of free fluid in potential abdominal spaces. However, contrast enhanced CT is required for confirmation.

Duplex and colour flow Doppler ultrasound examinations of the abdominal cavity are highly dependent on the clear display of the tissues and vascular structure provided by B-mode ultrasound. B-mode is often used on its own in abdominal ultrasound to detect arteriosclerotic wall plaques and aneurysms of the abdominal aorta and pelvic arteries.

The more echogenic structures within the vascular lumen can be recognized due to their strong ultrasound reflection when compared to blood. This makes sonographic imaging of morphological wall changes of varying pathology possible as they occur in various types of aneurysm, including walls deposits (plaques) and also parietal thrombi.

Doppler mode and colour flow are not necessary tools in AAA diagnosis but can be helpful in identifying the iliac arteries. (Figure 2.1 Figure 2.2)

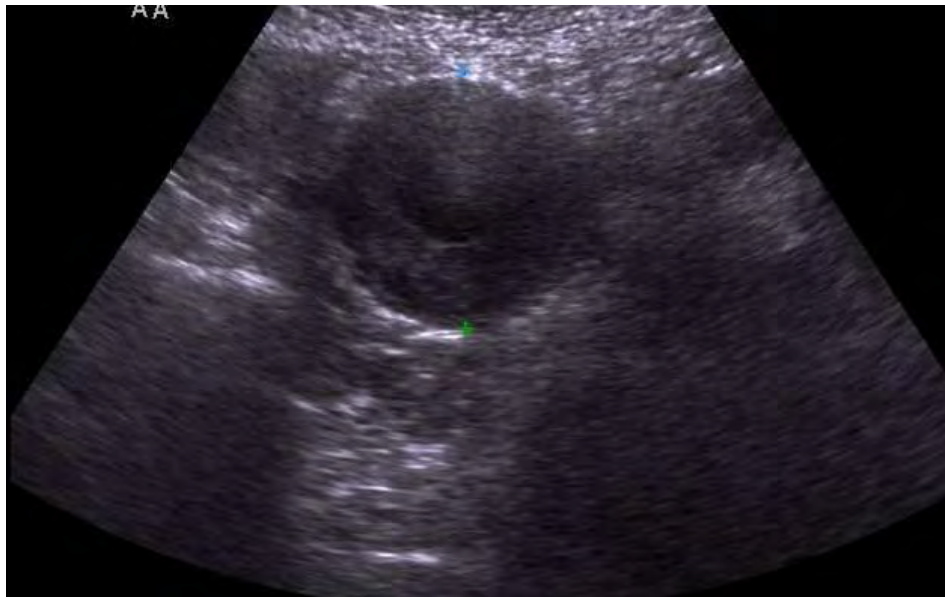


*Figure 2.1 Transverse B-mode image of an AAA, with an anterior posterior measurement.*

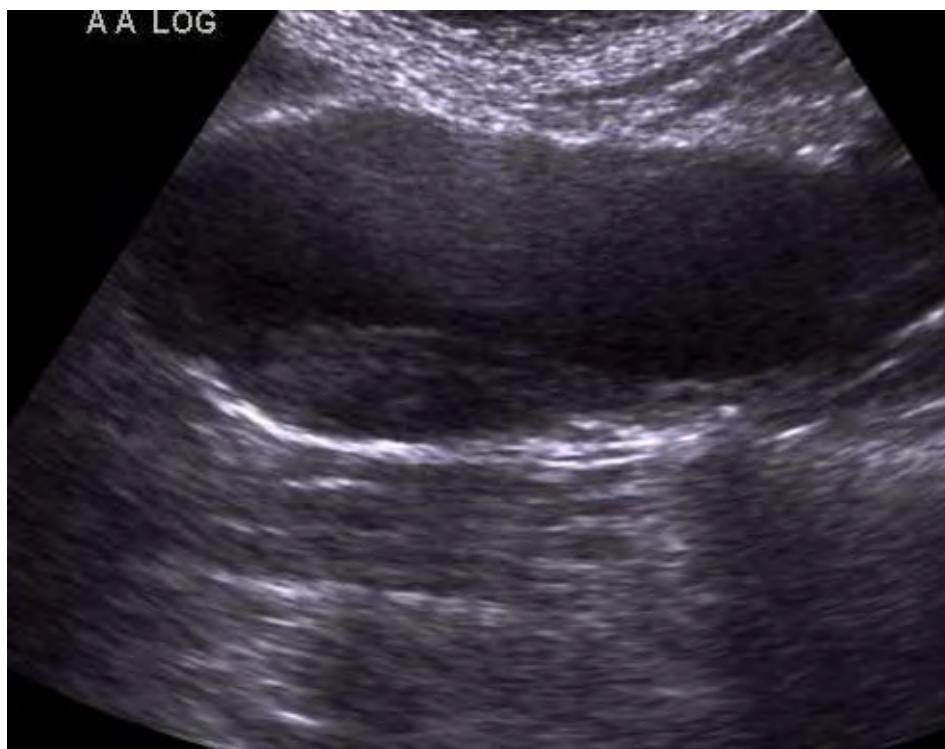


*Figure 2.2 Longitudinal B-mode image of an AAA*



### *2.1.1. Limitations of Ultrasound*

Major limitations with ultrasound are that it cannot travel through bone, air or gas. In AAA scanning is the presence of bowel gas and obesity can obscure the imaging. Patients who are obese are more difficult to image as the sound wave attenuates as it passes deeper into the body, therefore leading to suboptimal imaging and inaccurate measurements being obtained.

Intestinal gases also prevent visualization of deeper structures. Calcification of the artery can also obscure the image as the beam may not be able to penetrate the artery, therefore not giving a clear view of the arterial wall. Tortuosity can also impede the imaging, making it difficult to follow the course artery. The scan is also operator dependent, inter observer error can lead to inaccurate measurements of AAA and therefore maybe misleading in AAA growth on follow up scans. Performing an inter observer error test is vital to assess the error of measurement between fellow technologists in a scan center. Detailed knowledge of image optimization (the max amount of depth and width required to view the aorta etc) is also necessary to attain a clear image and accurate measurements. Therefore it is important that a full train vascular technologist performs the scanning in a screening setting. It is vital the machine settings are correct for the scan being performed. To ensure the best possible image is obtained.

In synthesis:

*Advantages:*

- Unlike CT, ultrasound does not use x-rays or any other kinds of potentially harmful radiation.
- Ultrasound equipment can produce moving images in real-time.
- Ultrasound has been used for abdominal examinations for about 40 years, and for standard diagnostic ultrasound there are no known risks or harmful effects to humans.
- Ultrasound is a cost-effective means of image acquisition in medicine.

*Disadvantages:*

- The patient has to undergo a slightly more intrusive session than is the case with a CT session, including the removal of clothes and application of the gel.
- The quality of the recorded images is dependent on the operator's skill of handling the equipment.

*Limitations:*

- Ultrasound imaging produces images that are far inferior in quality to CT. Proper identification of structures and regions in the finalized ultrasound images generally requires personnel with expertise and training to do so.

## 2.2 Computed Tomography (CT)

Computed Tomography is based on the principle of attenuation. It is composed of a large ring containing x-ray sources and arrays of detectors which rotate around the patient. Multiple X-ray fan-beam sources send out ionizing radiation into the patient's body. Attenuation occurs and the array detectors then process the beams post attenuation. The level of attenuation depends on the density of the medium (e.g. muscle is denser than blood). The arrays mathematically construct the image by numbering the attenuations detected. The larger the number, the more dense the medium and the lighter the shading on the image.

This method happens in 4 steps:

**Step 1:** The tube and detectors are rotated at a constant speed.

**Step 2:** The x-ray tube is energized and data collected for 360 degrees.

**Step 3:** The tube and detectors slow down and come to a stop.

**Step 4:** The table and patient are indexed to the next scanning position.

(Figure 2.3)

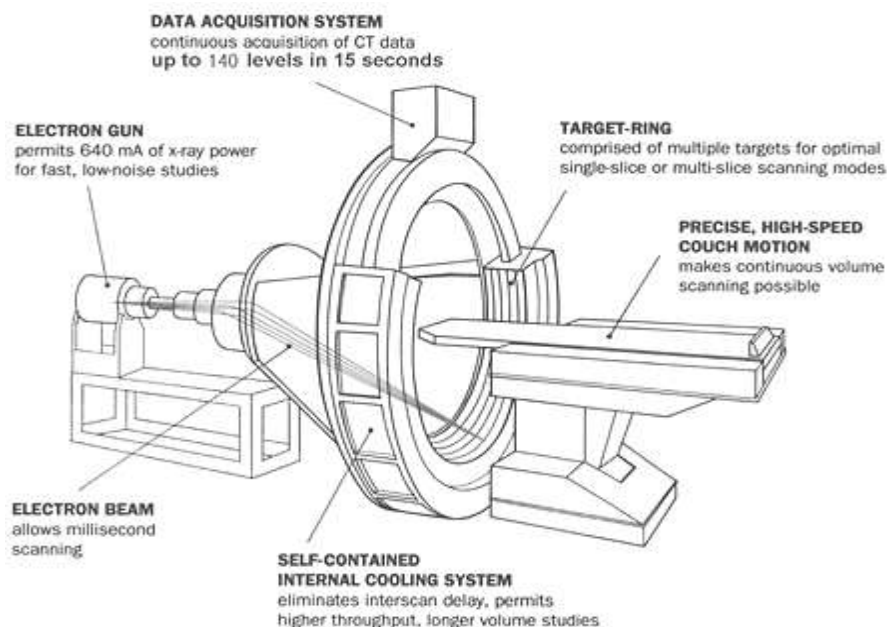


*Figure 2.3 Components of a CT machine*

CT gives a digital, transverse (trans axial) image. It is composed of slices of cross-section views. Computed tomography scanning creates superb images of the brain, bone, lung and soft tissue and it doesn't allow information from irrelevant locations to enter the acquired data. (Figure 2.4)

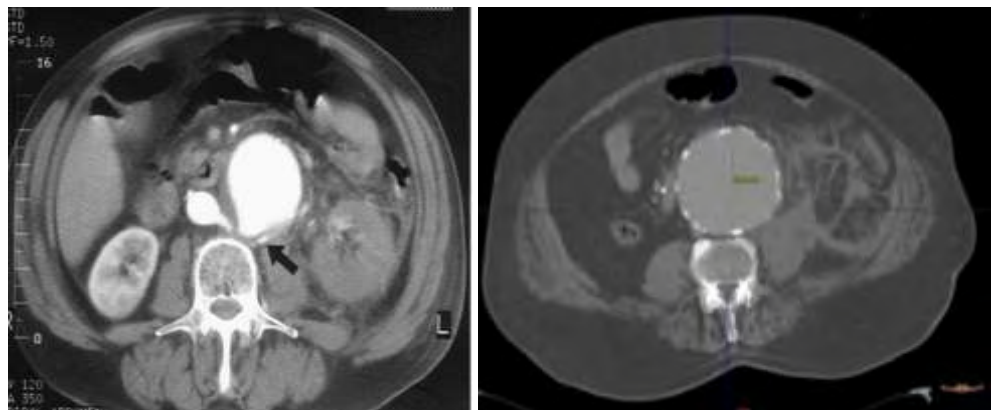


*Figure 2.4 CT image of an AAA*

Contrast-enhanced CT is widely used in the preprocedural imaging of AAA's. The 3-D images obtained from the CT are also used in the planning of endovascular procedures. It involves the use of CT and the injection of a high speed contrast media. This procedure is used in the assessment of the arterial tree, as the contrast agent highlights a narrowing in an artery. In AAA imaging it shows the dilation of the aorta, it allows the accurate measurement of the diameter of the aneurismal section and the length of the vessel involved. (Figure 2.5)

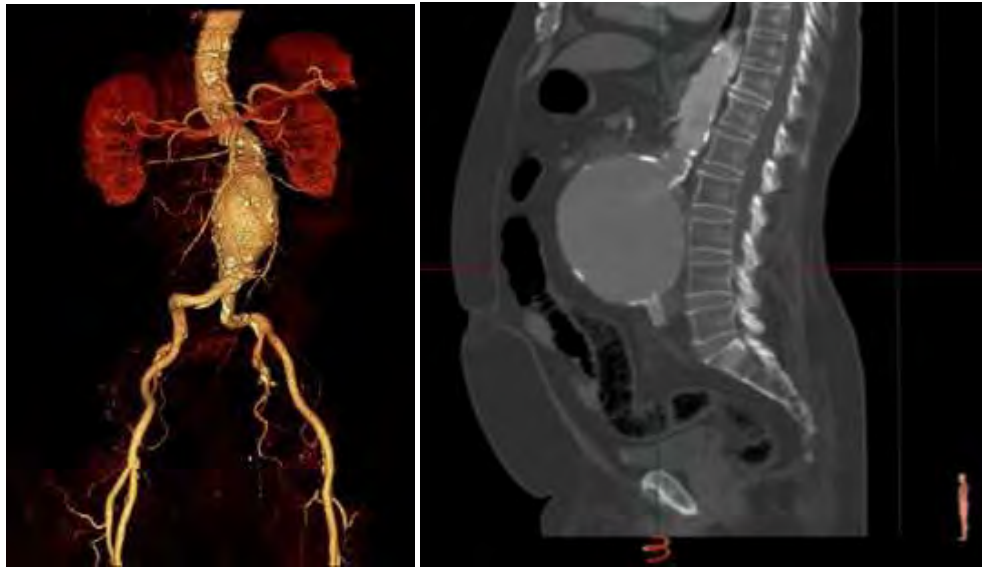


Figure 2.5 3-D reconstruction images of an AAA

The advantage of contrast-enhanced CT imaging is the accurate assessment of the blood vessels, giving detail to the location and length of the affected vessel.

However there are many disadvantages to CT contrast imaging:

1. It is highly invasive.
2. The patient may be allergic to the iodine contrast agent.
3. During CT imaging the patient is exposed to high doses of ionizing radiation.

In synthesis:

*Advantages:*

- CT examinations are fast and simple and can quickly reveal internal injuries and bleeding.
- CT imaging has been shown to be a cost-effective tool for a wide range of clinical problems.
- CT imaging offers detailed views of many different kinds of tissues.
- CT imaging is painless, noninvasive and accurate.
- Through use of CT scanning, it is possible to identify both normal and abnormal structures. This makes it a useful tool for guiding radiotherapy, needle biopsies and other minimally invasive procedures. In many cases this can eliminate the need for invasive surgery.

*Disadvantages:*

- CT involves exposure to radiation in the form of x-rays. The typical radiation dose from a CT exam is equivalent to the natural background radiation received over a year's time. Special care must be taken during x-ray examinations and the patient's abdomen and pelvis should normally be shielded by a lead apron.
- CT exams are generally not recommended for pregnant women.

*Limitations:*

- Very fine details in soft tissue cannot always be seen with CT imaging. In some situations, soft tissues may be obscured by bone structures. In these cases, magnetic resonance (MR) imaging may be preferable.
- Using CT imaging as a means of guidance during patient surgery is inconvenient, as the patient will have to be moved in and out of the CT scanner each time an updated image is needed.

### **2.3 Ultrasound verse CT**

Ultrasound is the method of choice in screening and AAA surveillance as it avoids high doses of radiation and minimizes costs compared to computed tomography (CT). (71, 74-76).

CT has been a widely used tool in the diagnosis and detection of AAA. However it is an expensive, time consuming method with high doses of radiation being given to the patient. Ultrasound is a quick, inexpensive and non-invasive method which is more suitable in diagnosis and screening for AAA (77). CT is gold standard preoperatively as it accurately measures the diameter of the proximal neck of aorta, diameter and length of the aneurysm, diameter of the aorta just before the bifurcation, length from the aneurysm to the bifurcation and diameters and length of the iliac and femoral arteries. The use of CT provides accurate configuration of stent grafts for the individual's anatomy. (78)

Ultrasound has also been shown to be the method of choice for measuring maximum AAA diameter. Ultrasound and CT do not always take the measurement on the same axis (77). CT takes the max cross-sectional area at any point, ultrasound takes the largest diameter in anteroposterior or transverse aspects (71). CT takes an oblique cut of the aneurysm to measure the max diameter, if the AAA is angulated more than 25 °, the diameter measured by the CT will be overestimated. (71, 77). Ultrasound is less affected by a tortuous vessel as the probe can be tilted to get a more accurate cross sectional area. (71, 77).

## **2.4 Role of Positron Emission Tomography (PET)**

PET imaging was developed in the mid-1970s; like any nuclear medicine imaging technique, it is based on the detection of photons emitted by the patient after administration of a radio-labelled tracer. Several physical characteristics of PET constitute a major advantage over monophotonic scintigraphy. Most importantly, the tracers are labelled with positron-emitting radionuclides. The two photons resulting from the disintegration of the positron are emitted in opposite directions (i.e., at 180° from each other) and recorded in coincidence by the detectors surrounding the subject. A detailed description of the specific technical and methodological features of PET imaging is obviously beyond the scope of this article and may be found in Phelps (78). In short, PET imaging increases the count rate (i.e., the number of photons that are detected) and improves the spatial resolution, that is, lesion detectability. In addition, the images can be fully corrected, in particular for attenuation, which allows for an accurate and reproducible quantitation of tracer distribution.

Depending on the radiotracer, a wide variety of physiological and pathological processes can be studied at the molecular level using this technique. However, in routine clinical practice, vast majority of PET studies are performed using 18-F-fluorodeoxyglucose (FDG), which reflects glucose uptake and metabolism resulting from cellular activity.

FDG is a glucose analogue, transported into cells using glucose transporters. Once inside the cells, FDG is phosphorylated to FDG-6-phosphate, which is not a substrate for the enzymes of the glycolytic chain, and hence FDG-6-phosphate accumulates within the cell. FDG-PET recognizes increased metabolic activity and is mainly used for cancer imaging. Indeed, cell glucose metabolism is significantly increased in most types of cancer (79) due to increased expression of membrane transporters, increased hexokinase activity or both. Nevertheless, FDG uptake is not



specific for tumours. Increased uptake is observed in many nonneoplastic physiological and pathological conditions (80).

Usually, the level of FDG uptake by inflammatory cells in the resting state is low in comparison with tumour cells. However, when activated, these cells may show significant increases in glucose uptake and metabolism. This has been evaluated in various experimental settings, including skin transplantation, turpentine-induced inflammation, concavalin- A activation of T lymphocytes in bacterial abscesses or in B lymphocytes after viral infection. The lack of specificity for tumours provides a powerful tool for using PET to evaluate inflammatory and infectious diseases as well as during the monitoring of vascular graft infection (81-83). It should be noted, however, that FDG uptake is often seen in the arterial wall, in the absence of any known inflammatory vascular disease. Yun et al. evaluated two series of patients who underwent PET imaging for oncological or other indications. They found that the rate of positive vessel uptake approached 50% and increased with age (84). They also showed that hypercholesterolaemia and age were the only parameters correlated with the presence of such uptake, among all major risk factors for atherosclerosis (85).

With the advent of modern PET/CT, the procedure has been considerably shortened and simplified. Usually, patients are asked to fast for 6 h prior to injecting FDG, which is of particular importance when investigating inflammatory processes, as glucose loading significantly decreases glucose transporter expression (and FDG uptake) in inflammatory lesions (86). Modern hybrid scanners are coupled with CT for attenuation correction and anatomical mapping. Attenuation correction is usually performed using data from continuous, enhanced, low-dose body CT from the skull base to the thighs. Intravenous contrast enhancement can be used with limited effects on attenuation correction and uptake quantification in order to provide additional information on the thrombus, surrounding tissues and vessels.

Wu et al. (87) demonstrated the uptake of  $^{18}\text{F}$ -FDG in the unstable atherosclerotic carotid plaque and correlated this with levels of circulating matrix metalloproteinase 1 (MMP-1). Other workers have shown the high uptake of FDG into vulnerable atherosclerotic plaque and the reduction of carotid FDG uptake after statin therapy. This suggests that PET imaging might have clinical utility in monitoring atherosclerotic arterial disease (88).

Using autoradiographic techniques, Rudd et al. showed increased tracer accumulation in the regions of the plaque with the highest density of macrophages (89). Indeed, enhanced uptake has been reported in various inflammatory diseases involving the large vessels. Giant cell arteritis and Takayasu arteritis both show significantly increased glucose metabolism in the wall of the affected arteries (i.e., aorta, subclavian arteries or carotid arteries). Furthermore, FDG uptake has been found in large arteries in the presence of active atheromatous plaques (84, 85).

In a pilot study, Sakalihasan et al. observed an association between  $^{18}\text{F}$ -FDG uptake by the aneurysm wall and rapid expansion of the aneurysm in some cases (90). Indeed, five of the nine operations on patients with positive PET imaging were performed on an urgent basis. In the 16 PET negative patients, aneurysmal repair was delayed for the convenience of the patient from one to several months. None of these patients developed aneurysm-related symptoms in the interval.

FDG uptake in the aneurysm wall reflects the presence of increased metabolic activity, probably associated with a high density of inflammatory cells (macrophages, lymphocytes, etc.) in the adventitia, as previously described (91). These preliminary observations have been confirmed recently in a study by Reeps et al. (92) where they observed a correlation between increased FDG uptake and patients with a very high macrophage activity and symptomatic AAA. However, in agreement with earlier reports (90) Reeps et al. failed to find a correlation between the maximum standard uptake value (SUV) and maximum cross-sectional infra-renal AAA diameter (92). These studies could suggest a possible correlation between

increased FDG uptake by the aneurysm wall and inflammatory cell biology leading to rupture.

Therefore, PET scanning with FDG uptake offers a new tool for exploring adventitial immuno-inflammatory responses in atherosclerosis and AAA.

## Chapter III

### Treatment of AAA's

#### 3. Introduction

AAA's are generally asymptomatic and are usually diagnosed as incidental findings during physical examinations for other conditions. The treatment of AAA varies depending on the size of the AAA and the risk factors of the individual patient.

##### *3.1 Medical Therapy*

At present there are no pharmacological treatments available to prevent AAA formation, growth and rupture. However, treating cardiovascular risk factors has been shown to prevent AAA's or reduce the progression of an already existing AAA.

When treating the risk factors, there are conflicting arguments whether statins are beneficial in slowing the growth of AAA's. Statins are generally used to lower cholesterol by inhibiting the enzyme involved in the synthesis of cholesterol in the liver. Studies have reported the use of statins to reduce the inflammatory response of macrophages, T lymphocytes and MMP and thus reducing AAA progression (57, 94, 95). Other studies show that lipid lowering drug treatments can delay growth in small AAA's (56). While others report that the use of statins, do not help in reducing AAA growth or changes in AAA wall composition (16, 46, 96).

### *3.2 Operative Treatment*

Surgical repair of AAAs can be classified according to symptoms prior to surgery in five groups: 1) elective asymptomatic, 2) elective symptomatic, 3) emergent repair without rupture, 4) rupture without clinical shock and 5) rupture with clinical shock (97). Perioperative mortality is lowest in group 1 and highest in group 5. In practice, AAA repairs are often divided into elective AAA repair (groups 1 and 2) and emergent AAA repair (groups 3-5), or into Intact Abdominal Aneurysm (iAAA) repair (groups 1-3) and Ruptured Abominal Aneurysm (rAAA) repair (groups 4 and 5).

#### *3.2.1 Intact AAA repair.*

The adequate AAA size at which elective repair is recommended in asymptomatic patients has been established to 55 mm in two large, randomized multi-centre studies (58, 66, 98). However, an individual approach is recommended, where the operative risk of the patient is balanced against risk of rupture and expected long-term survival.

Elective operative treatment is associated with a perioperative mortality of 2-5% in large randomized or population-based studies (56, 66, 99). National variations in perioperative mortality after AAA repair exist in register data (100). Short-term outcome is highly dependent on patient comorbidities, and mortality is increased in patients with renal dysfunction, cardiac disease and pulmonary dysfunction (101). In addition, increased age and female gender are associated with higher short-term mortality. Most but not all (8) reports indicate a reduced operative mortality after iAAA repair over time (102, 103). A minority of iAAA repairs are performed in symptomatic patients e.g. with tender aneurysms. In these cases operation is performed as an urgent intervention, and the perioperative mortality is approximately twice as high as in elective asymptomatic repair (100).

Based on the Swedvasc, time-trends for AAA repair in Sweden between 1994 and 2005 were recently reported (104). During this period, the incidence as well as the total crude number of operations performed for iAAA increased significantly. This was mainly due to the introduction of Endovascular Aneurysm Repair (EVAR), as discussed below. In addition, patient demography changed over time with an increase in mean age of AAA patients and a higher proportion of octogenarians being treated. The 30-day mortality rate decreased steadily over the studied time-period, both after iAAA and rAAA repair. Changes in patient demography could, however, affect long-term survival after AAA repair, potentially reducing the expected benefit for the patients. Long-term survival is fundamental for surgical decision-making, and has an important health economic implication when evaluating the cost-effectiveness of a new treatment (e.g. EVAR) or health intervention (e.g. screening for AAA).

There are two different methods for treatment of AAA: open reaper (OR) and Endovascular Aneurysm Repair (EVAR). There are advantages and disadvantages with both techniques. OR is associated with a higher perioperative mortality and morbidity, as well as longer ICU and hospital stay than EVAR (99, 105). While EVAR has several advantages in lower perioperative mortality and morbidity, this treatment is associated with a higher rate of re-interventions and need for close follow-up (99). Due to the novelty of the method and the rapid development of the endovascular technique, long-term durability of EVAR is not as well-known as after OR. In addition, EVAR is associated with certain requirements in aneurysm morphology, most importantly a need of an aneurysm neck as a proximal sealing zone for the endovascular stent graft.

Approximately 30-50% of all AAAs are currently regarded as not possible to treat with EVAR (although this varies considerably between centers), and future development of the technique might decrease this proportion (99, 105). Current practice at many centers is to select patients to OR or EVAR based on aneurysm

morphology as well as patient age and comorbidities. Patients treated with EVAR are typically older and have more comorbidities than those treated with OR (104).

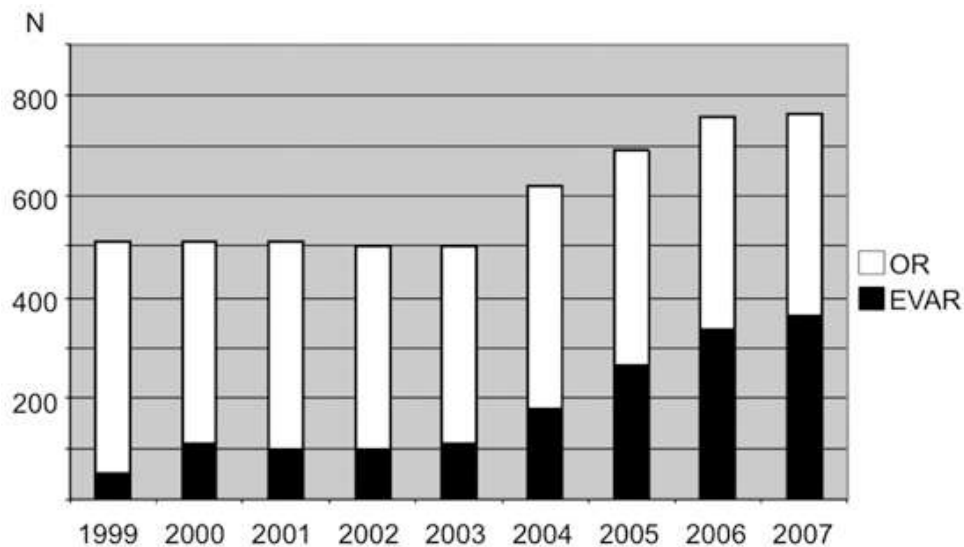


Figure 3.1 Number of elective AAA repairs in Sweden with open (OR) and endovascular (EVAR) technique (Swedvasc, 2008).

Since the introduction of EVAR in 1986, an increasing proportion of AAA patients are being treated with endovascular technique. Data from the Swedvasc indicate an increase of 53% in the total number of elective repairs and 189% in the number of EVARs in Sweden over the years 2003-2007, Figure 3.1 (106). In 2008, 53% of all elective AAA repairs in Sweden were performed with EVAR (106).

### *3.2.2 Ruptured AAA repair*

The operative mortality after rAAA repair is approximately 35% (104). However, only 1/3 of patients with AAA rupture undergo operation while the remaining patients die without surgical attempt.

The overall mortality after AAA rupture is thus around 80% (58). Some groups have reported stable mortality rate after rAAA repair (8, 21, 102), whereas others have found a decreasing mortality over time (103, 104). Endovascular repair for ruptured aneurysm is increasing and constituted 25% of all rAAA repairs in Swedvasc 2008 (106). The feasibility of endovascular technique in an emergency setting has been established in several reports. There is a great variety in use of EVAR for rAAA, and some centers treat a high proportion of all ruptures with this technique (Holst, 2009). However, it is difficult to compare the results of emergency EVAR to OR due to the effect of patient selection and the difficulty to perform randomized clinical trials in this acute setting. Large randomized clinical trials comparing OR and EVAR for rAAA are in progress.



## Chapter IV

### Rupture criteria in a clinical setting

#### 4. Introduction

The indication for elective repair is strongly related to the aneurysm's risk of rupture, and although maximum diameter is the current criteria for treatment, no general consensus exists on the critical size beyond which elective repair is recommended. In each case, the risk of rupture must be weighed against operation morbidity. Therefore, a single threshold diameter is not appropriate for every patient hence the assessment of the risk of rupture should ideally be individualized to better manage aneurysm patients.

Current clinical practice recommends to repair large AAA, with maximum transverse diameter larger than 55 mm, or to regularly monitor smaller AAAs (diameter less than 55 mm) with ultrasound. However, small aneurysms can also rupture, with an associated mortality rate of up to 50% (107). Moreover, the 12-year follow-up of the UK Small Aneurysm Trial reported an overall mortality of 67.3% for the surveillance group (98).

These findings question the ability of maximum diameter criterion to assess AAA risk of rupture. Several reports demonstrated the existence of a risk of rupture of AAA below 55 mm in diameter and showed that rapid aneurysm expansion is associated with increased rupture risk independently of their size (108).

In common clinical practice expansion rate of an AAA is generally defined as the change in maximum aortic diameter over time.

Limet et al. (109) associated the risk of rupture of AAAs with aneurysm expansion rate and different studies reported an increased mean expansion rate in patients with ruptured AAAs (24, 66).

Realistic AAAs have complex, tortuous, and asymmetric shapes with local changes in surface curvature (110-112) and the maximum-diameter measures at two time points only provides limited information regarding aneurysm growth. Specifically, it might miss regions of fast diameter growth, it cannot quantify axial growth, and it cannot capture shape changes of potential interest for EVAR-related decisions (113).

Stenbaek et al. (114) investigated the ILT growth as a potential rupture risk predictor and concluded that a rapid increase in ILT area may be a better predictor of AAA rupture than an increase in maximum transverse diameter.

So far, both aneurysm rupture and growth are unpredictable by the diameter alone. Better predictors for rupture and growth are required and may be found in a more extended patient-specific analysis, based on biomarker and biomechanical information. This may lead to an optimization of both the follow-up plan and the moment of aortic repair.

#### *4.1 Biomarkers*

More insight in the pathogenic pathways of aneurysm formation and progression may be gathered by evaluating circulating biomarker concentrations (115, 116). Circulation matrix metalloproteinase-9 (MMP-9) concentrations have been investigated most frequently in association with AAA.

As we see in the next chapter MMP-9 is involved in the breakdown of the extracellular matrix and, in most studies, was found to be elevated in AAA's compared to healthy subjects (115). Also, the tissue inhibitor of MMP 1 (TIMP-1) was found to be increased in AAA patients compared to healthy controls (117).

The markers of inflammation interleukin-6 (IL-6) and C-reactive protein (CRP) are frequently studied in cardiovascular disease and were found to be elevated in the presence of AAA in most studies (115). Besides, serum CRP concentration was also associated with the size of AAA (118).

Also, AAA growth was investigated in relation to biomarkers. Again, MMP-9 was correlated with AAA expansion rate (119). In the same study was found that alpha 1-antitrypsin ( $\alpha$  1-AT) was weakly correlated with AAA expansion rate (119).

$\alpha$  1-AT is an inhibitor of alpha 1-trypsin, which inhibits elastase. Elastase, on its turn, actively breaks down elastic fibers in the aortic wall.

Biomarkers as predictor for AAA rupture have been relatively little investigated.

Engstrom et al. (120) concluded that the incidence of fatal or repaired AAA was associated with a higher number and levels of inflammation-sensitive plasma proteins. CRP levels in patients with symptomatic or ruptured AAA's were significantly higher than in patients with an asymptomatic AAA (121). Also, MMP-1 and MMP-9 were elevated in the plasma of ruptured AAA versus non-ruptured AAA and elevation of MMP-9 was associated with ruptured AAA related 30-day mortality (122).

Numerous studies have focused on measuring biomarker concentrations in order to predict AAA presence, growth or rupture, but most studies have not assessed the value of these markers as diagnostic tests for AAA (115, 116, 118).

Biomarkers may play a role in the identification of small AAA's. Additionally, when biomarkers associated with AAA are identified, targeted medical treatment may be developed to slow down AAA progression. For now, sensitivity and specificity appear inadequate for the use of single biomarkers alone in diagnosis (115).

Using multiple biomarkers in combination with other AAA related factors may in the future prove to be of value in the diagnostics of AAA.

#### *4.2 Biomechanical Analysis*

From a biomedical engineering point of view, biomechanics play an imminent role in rupture of the AAA wall. When the stress on the AAA wall, caused by the blood pressure, locally exceeds the strength of the wall, rupture of the wall occurs. The law of Laplace states that the wall stress in a thin-walled cylinder linearly increases with increasing diameter and transmural pressure, and decreases for increasing wall thickness. However, due to the complex geometry of most AAA's, the wall stress is determined by the local AAA geometry and wall thickness, and can therefore not be predicted by the law of Laplace, or be based on simplified geometrical models (123).

Recent studies showed that peak wall stress (PWS) in AAAs is a more reliable parameter than maximum transverse diameter for aneurysm rupture prediction (124-127). Simulations of anatomically realistic AAA models were performed to compare PWS between ruptured or symptomatic and unruptured aneurysm cases (124, 128). These studies found a significant difference between the two groups. The PWS for ruptured aneurysms is about 60% higher than for non-ruptured and the location of the PWS correlates with the site of rupture (127).

However, it is necessary to underline that wall stress alone is not sufficient to predict rupture risk; regional estimations of wall strength would also be necessary (130). It has previously been shown that wall strength differs significantly from patient-to-patient and within the same aneurysmatic sac (129, 130). In addition, Di Martino et al. (131) found that the strength of the aneurysmatic wall from ruptured AAA cases is considerably lower than that for electively repaired ones. In this regard, Vande Geest and colleagues (129) have proposed a statistical model to noninvasively evaluate the wall strength distribution in AAA taking into account factors such as gender, age, family history, AAA size and local ILT thickness.

However, based on the principles of material failure knowledge of both, AAA wall stress distribution and wall tissue strength are necessary to assess rupture

potential, and different biomechanical rupture risk indicators have been suggested in literature (125, 129, 132).

Another factor of significant importance in AAA rupture risk prediction is the non-uniformity of the wall thickness. In fact, AAA wall has considerable regional variation in wall thickness with a reduction in wall thickness near the rupture site. Moreover a significant difference in wall thickness was found between ruptured and electively repaired aneurysms, as well as an inverse correlation between wall thickness and local tissue strength (131, 133).

Due to the inability to measure wall thickness noninvasively, a uniform thickness is typically assumed in biomechanics modeling of AAAs. Other significant limitations of previous studies include the use of isotropic tissue constitutive law (134) and of a load-free reference configuration.

Although an ILT is known to be an important solid structure that influences AAA wall stress distribution it has been disregarded in many biomechanical AAA models.

Advances in medical imaging, provide good information to perform patient-specific vascular geometries reconstructions (135, 136) and an accurate characterization of the aneurysm shape with the variation of wall thickness (110, 127) need to be accounted for the assessment of AAA rupture. In particular the assumption of constant distribution of wall thickness causes an underestimation of the PWS (138, 139). Moreover, accounting for the ILT and the non-homogeneous distribution of tissue strength and wall thickness in AAA models, reinforced the predictability of FE simulations, which allowed for a statistically significant discrimination between ruptured and non-ruptured AAAs (125).

## **Chapter V**

### **Arterial Wall**

#### **5.1. Pathophysiology Anatomy of the normal aorta and regional features that predispose to aneurysm**

The walls of every artery, including the aorta, consist of 3 layers: the tunica intima, tunica media, and tunica adventitia (usually called the intima, media, and adventitia).

The intima is the innermost layer, right next to the flowing blood. This layer is composed of a single layer of endothelial cells anchored by connective tissue to the layer immediately below, which is the media. The media consists of smooth muscle cells and elastin fibers, collagens, and other connective tissue molecules. The third and outermost layer, the adventitia, consists of fibroblasts, various hematopoietic cells, neurons, small capillaries, and connective tissue. The cells of the aortic wall are provided with nutrition and oxygen via small capillaries called vasa vasorum. Aortic vasa vasora, however, are present in the thoracic region, but not below the renal arteries. Instead, the cells in the wall of the abdominal section of the aorta are supplied by diffusion from luminal blood.

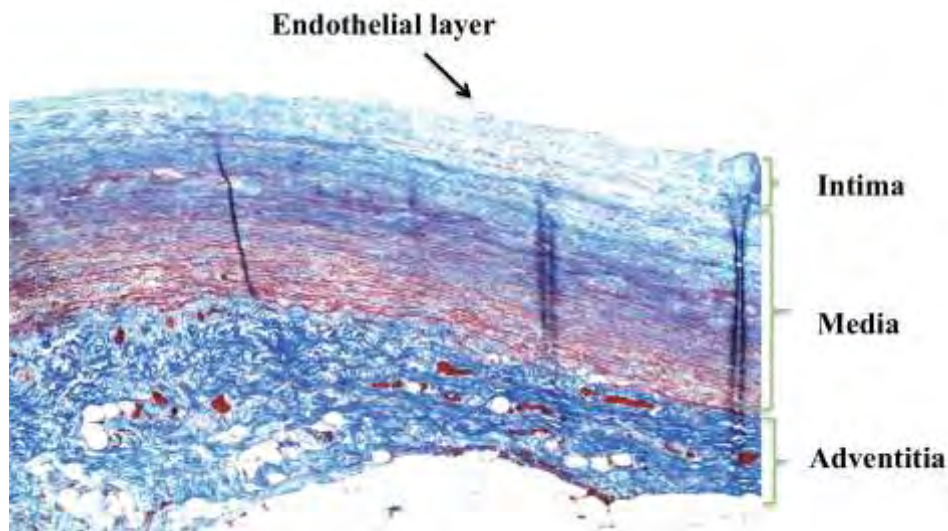


Figure 5.1: A section of normal aorta stained with Masson's Trichrome technique, in which smooth muscle cells appear red, collagen stains light blue, and the cell nucleolus appears dark blue. 10 times magnification.

It has been suggested that different segments of the aorta arise from different embryonic origins. In a study of murine embryos, vascular smooth muscle cells in various sections of the vasculature had different embryonic origins. In particular, the abdominal aorta diverges from the thoracic aorta. Smooth muscle cells in abdominal region of the aorta originate from mesoangioblasts, while smooth muscle cells from the abdominal aorta and femoral arteries originate from somites and various stem cells respectively (145, 146). Whether the different origins of vascular smooth muscle cells affect the characteristics of these cells and the predisposition to aortic diseases are not known. Nevertheless, some authors have speculated that the embryonic origins of the abdominal aorta may partly explain why it is far more likely to become aneurysmal than its neighboring sections.

In addition, the amount of elastin is not uniform along the length of aorta. The further from the heart, the fewer the elastin fibers there are in the aorta (147). This observation was first made in 1928, when Alfred Benninghoff investigated the

amount of elastin along the length of the human aorta and discovered a decrease in the amounts of elastin and collagen from proximal to distal aorta. Benninghoff estimated 60-80 layers of elastin in the ascending aorta, but only 20 layers in the infrarenal aorta.

In a later study, the infrarenal aorta was reported to have 58% fewer elastin layers, compared to the suprarenal aorta, and the infrarenal aorta exhibited the lowest proportion of elastin to collagen (148). These observations provide an additional explanation why most aortic aneurysms are seen in the infrarenal region.

Further evidence for structural weakness in the abdominal aorta comes from a study, in which the researchers used ultrasound to compute wall stress in the abdominal aorta and common carotid arteries of 111 healthy individuals between ages 25-70 years. Measurement of luminal diameter and intima-media thickness of these vessels showed that age was associated with increasing diameter of all of these arteries, but was compensated by additional thickness of the wall of the common carotid arteries, and so wall stress in these vessels remained constant with age. Some wall thickening was seen in abdominal aortae of older men, but was insufficient to fully compensate for the stress from increased vessel diameter. Thus, wall stress in the abdominal aorta increased with age in men and may contribute to the development of AAA in elderly men (149).



## 5.2. Cells in the normal and aneurysmal aorta

The normal aortic wall contains endothelial cells, smooth muscle cells, and fibroblasts.

Histological studies show that segments of AAA are not lined with endothelial cells (e.g., see Figure 5.2).

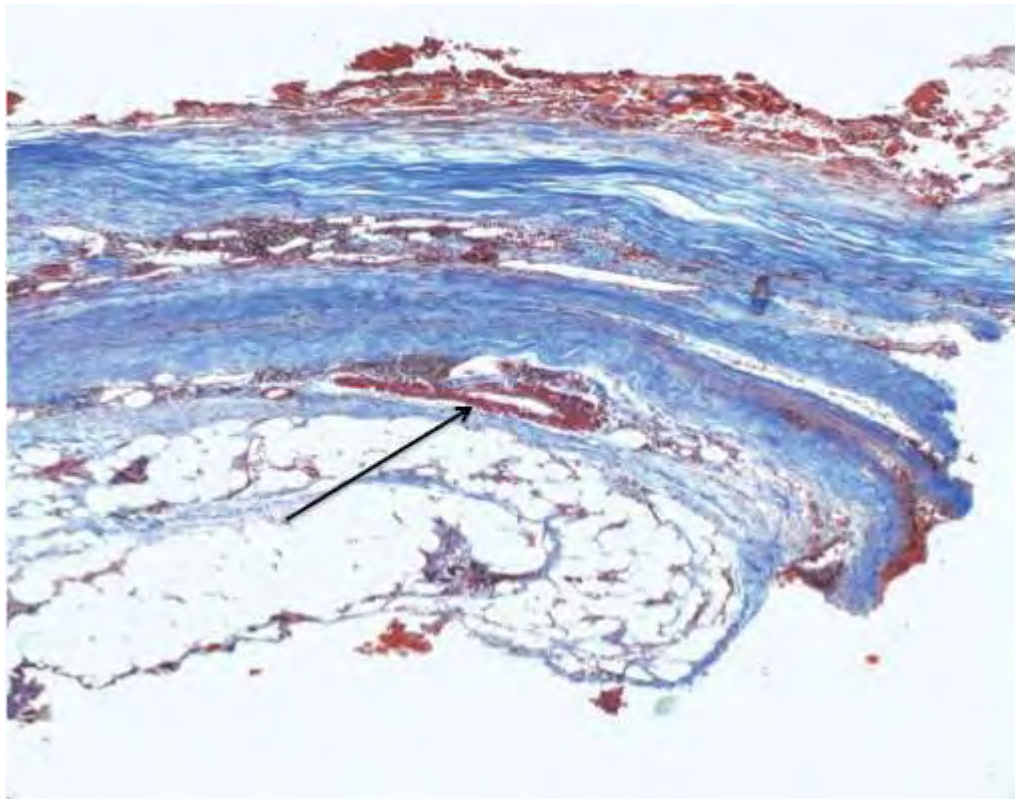


Figure 5.2: A section of aneurysmal abdominal aorta stained with Masson's Trichrome technique. Compared to the normal segment in Figure 5.2, smooth muscle (red) is decreased, and collagen (light blue) is increased. 10-times magnification. The arrow indicates neovascularization. The red region on the outer right surface is the remnant of an intraluminal thrombus, the majority of which had been removed during open repair.

Aneurysmal vessels contain smooth muscle cells, but in decreased amounts (150), and mRNA expression of alpha actin is lower in AAA vessels compared to healthy vessels (151). Importantly, AAA segments contain platelets and inflammatory cells, particularly macrophages, neutrophils, and mast cells. These cells are rarely found in normal aorta. Platelets together with inflammatory cells produce proteases that may further damage the vessel (152).

A comparison between Figure 5.1 and 5.2 shows clearly that the aneurysmal wall is distorted, and the number of smooth muscle cells (red) is decreased substantially, while collagen (blue) is initially overproduced.

### **5.3. Matrix of the Aorta**

There are several macromolecules comprising the extracellular matrix of the aorta. Among them are laminin, various types of proteoglycans, fibronectin, collagen, and elastin. The relevant macromolecules are elastin and collagen types I and III. These molecules provide elasticity and strength to the aortic wall, enabling it to store energy by distending during systole, and then recoil back during diastole, thereby maintaining systemic blood pressure while the left ventricle is relaxing and the aortic valve is closed.

While elastin provides physiological strength in the form of elasticity to the vessel wall, collagen is required for mechanical strength at higher pressure and provides rigidity to the vessel. It has been shown that canine models of AAA induced by treatment of the aorta with elastase show dilatation without rupture, whereas treatment with collagenases resulted in less dilatation but was followed by rupture (66).

### 5.3.1 *Elastin*

Elastin, a macromolecule in the medial layer of the aorta, enables the vessel to absorb the pulsatile energy from the heart, to increase aortic diameter at systole and regain its initial shape during diastole. Elastin is produced at early stages of infancy and must last throughout lifetime of an individual. Production of elastin in the aorta later in life has not been detected. Elastin has a high threshold for environmental assaults i.e. temperature and chemicals and has a half-life of 40 years (154).

It has been suggested that the first event in the onset of AAA is loss of elastin (155). Histological studies show that AAA walls contain markedly reduced amounts of elastin, which is a result of the activity of elastases. The presence of neutrophil elastase (NE) originating from polymorphonuclear cells in AAA tissue has been shown to cause degradation of elastin (156). In addition, matrix metalloproteinases (MMPs) and cathepsins (157) also have the ability to degrade elastin (158). It has been suggested that all the above-mentioned proteases have a role in loss of elasticity of the aortic wall and the increase of AAA diameter (159, 160).

Elastase-derived peptides (EDPs), which are produced by degradation of elastin, show an increased abundance in AAA compared to normal aorta (161). Moreover, EDPs have been shown to recruit inflammatory cells, which in turn produce more proteases that continue the degradation of elastin, leading to a vicious cycle (62, 163). The imbalance between protease and inhibitor exacerbates the progression of AAA (164).

Two experimental mouse models of AAA rely on artificial damage to aortic elastin. In the elastase model, the infra-renal abdominal aorta of mice is briefly clamped off, porcine elastase is injected into the lumen, and after a brief incubation, the elastase is rinsed out and normal blood flow restored. This manipulation induces

aneurysm formation and lasting within 2 weeks of the procedure (165). In the calcium chloride (CaCl<sub>2</sub>) model, the aorta is exposed to a CaCl<sub>2</sub> solution placed briefly on the adventitial surface. The CaCl<sub>2</sub> provokes an inflammatory reaction that disrupts the elastic network, leading to degradation of elastin (165). The aorta becomes aneurismal, but in the mouse, it is reversible, and the aneurysm regresses to its original size after 6 weeks.

### *5.3.2 Collagen*

Another major component of the connective tissue that gives the aorta its strength and rigidity is collagen. There are several types of collagen, but collagen types I and III are the predominant types in blood vessels. Degradation of collagens is a result of the activity of collagenases, such as MMP1, MMP8, and MMP13, all of which have been found in AAA tissue (166). Collagenases are capable of initiating the degradation of intact, triple-helical collagen. Once collagen degradation has begun, a second set of enzymes, called gelatinases, are able to digest partially degraded, denatured collagen.

Gelatinases include MMP2 and MMP9 (167). Degradation of elastin and collagen triggers the production of collagen in the AAA wall (168, 169), and so there is an initial increase in aortic collagen content (see Figure 5.2). As AAA progresses, however, the degradation of collagen overwhelms its production, leading to rupture (170).

During the development of AAA, the structure of the vessel wall is disrupted and the wall weakens (Figure 5.2). At later stages, production of extracellular matrix is decreased owing to apoptosis of smooth muscle cells, while at the same time, continued degradation of elastin and collagen renders the AAA wall thin (150).

Rupture occurs when the components of the disrupted aortic wall fail to withstand the mechanical stress from pulsatile blood flow.

#### 5.4 Proteases and their inhibitors

Some of the most important proteases are introduced in Table 1, below, along with their inhibitors and known substrates.

Table 1: Proteases studied in this thesis, their inhibitors, and substrates (Brew and Nagase 2010; Shiomi, Lemaitre et al. 2010)

<b>Protease</b>	<b>inhibitor</b>	<b>substrate</b>
Elastase	$\alpha$ -1 antitrypsin	Elastin, Fibrin
MMP1	TIMP1-4	Collagens I, II, III, VII, X, entacin, aggrecan, perlecan,
MMP2	TIMP1-4	Gelatins, collagens IV, V, VII, X, XI, Fibronectin, Laminin,
MMP9	TIMP1-4	Gelatins, collagens III, IV, V, elastin, aggrecan, vitronectin
MMP13	TIMP1-4	Collagen I, II, III, IV, IX, X, XIV, Fibronectin, Laminin,
ADAM10	TIMP1-3	ProTNF- $\alpha$ , delta, collagen IV, gelatin Myelin basic protein,
ADAM17	TIMP1-3	ProTNF- $\alpha$ , ProTGF- $\alpha$ , TNF-p75 receptor, TRANCE,

#### *5.4.1 Neutrophil elastase: its role in coagulation/fibrinolysis and its inhibition by $\alpha$ -1-antitrypsin*

Neutrophil elastase (NE) is a serine protease produced by polymorphonuclear neutrophilic leukocytes (neutrophils) and stored in their azurophilic granules. This protein is released during inflammation and has the capacity to degrade extracellular matrix, especially elastin. It also has anti bacterial activity. Elastin derived peptides (EDP) in AAA attract neutrophils to the AAA site (171).

Coagulation factors, such as factor XIII, are degraded by elastase, while factors VII, VIII, IX, and XII are inactivated by elastase (172, 173). Normally, tissues are protected by inhibitors of this protease. The major inhibitor for NE is  $\alpha$ -1-antitrypsin, which is a serine protease inhibitor generated by the liver and released into the blood in high amounts. The other inhibitor of elastase is called elafin, which is produced by epithelial cells in lung and skin. Inflammatory processes and involvement of matrix metalloproteinases can block the activity of  $\alpha$ -1-antitrypsin, despite its saturating concentrations in the blood.

Cigarette smoke and its major component, nicotine (141), increase NE activity and at the same time impair the ability of  $\alpha$ -1-antitrypsin to inhibit elastin. These two effects lead to more activity of NE (174). Impairment in the ability of  $\alpha$ -1-antitrypsin to inhibit NE is mediated by oxidation of one amino acid in the active site of  $\alpha$ -1-antitrypsin, which makes its attachment to NE less effective (175).

NE is capable of degrading fibrin in ILT (176). Fibrin, however, is degraded mostly by plasmin/mini-plasminogen, and the degradation products are different arrangements of 2 core fibrin fragments, fragment D and E. DD, DDE and E, with the major product being, DD also called D-Dimer. Plasma levels of D-dimer have been showed to correlate with growth of AAA (177). NE degrades fibrin into a peptide, called the NE degraded product (XDP), that differs from D-dimer by a few amino

acids and can be separately assayed (178). NE is capable of cleaving plasminogen to “diss Kringle 1-4” also called mini-plasminogen. Mini-plasminogen activated to mini-plasmin in a faster rate than the activation of plasminogen to plasmin. Mini-plasminogen is resistant to inhibition compared to plasminogen and also more effective at degrading fibrin. Therefore, NE can degrade fibrin directly or indirectly by activating mini-plasminogen (179).

Consequently neutrophils leucocytes associated with thrombi contribute to fibrinolysis (176).

Several fibrinolysis and coagulation factors, such as thrombin-antithrombin III complex (TAT) and fibrin/fibrinogen-degraded products (FDP) have shown to correlate with size of AAA. Another component of fibrinolysis investigated in AAA is plasminogen activator inhibitor type 1 (PAI-1), which is an inhibitor of fibrinolysis.

PAI-1 acts by inhibiting tissue plasminogen activator (tPA) and urokinase plasminogen activator (uPA), which are activators of plasminogen (180). It has been shown that NE is capable of inactivating PAI-1, which is yet another mechanism to enhance fibrinolysis. This degradation will facilitate bleeding into the ILT and increases the risk of rupture.

#### *5.4.2 Metalloproteinases and their inhibition by TIMPs*

Matrix metalloproteinases (MMPs) are proteins with a zinc-binding motif in their catalytic domain and are responsible for degrading collagens, gelatins, and elastin in the aortic wall of AAA. These proteases are involved in several biological events, such as reproduction, development, morphogenesis, and wound healing. They also play a role in protection against bacterial invasion (181). Metalloproteinases are zymogens and need cleavage of their pro domain to be

activated. Plasmin, a protein involved in fibrinolysis, is considered to be an activator of metalloproteinases (182).

The major collagenases are MMP1, MMP8 and MMP13. These proteases are able to degrade triple helical domain of collagens at physiological pH. The major gelatinases are MMP2 and MMP9 and are capable of digesting denatured collagen.

Tissue inhibitors of metalloproteinases (TIMPs) have many biological roles, such as modulation of cell proliferation, anti-angiogenesis, anti- and pro-apoptosis, signaling, and cell migration (183), but the most studied function of TIMPs is the inhibition of metalloproteinases. TIMPs 1-4 inhibit MMPs (181, 183). In one study, Lipp et al showed that TIMPs 1-3 in human AAA are suppressed compared to control aorta (184). The elastase-induced model of AAA produces a more severe phenotype in mice lacking expression of TIMP1 (185). Because TIMPs have anti-angiogenic properties (183), a lack of TIMPs in AAA tissue could promote angiogenesis. In a recent study, the thickness of the ILT was correlated with the concentration of TIMP1 and active MMP9 in the aortic wall of AAA and that showed to be independent of other variables, such as statin use, age, and gender (185).

The rupture site of AAA shows an increase in the concentrations of MMPs, such as MMP8 and MMP9 (187). In the elastase-induced model of AAA, mice deficient in MMP9 (*Mmp9*<sup>-/-</sup>) showed attenuation of AAA progression compared to wild-type *Mmp*<sup>+/+</sup> controls.

MMP9 activity is preserved when the protein binds neutrophil gelatinase-associated lipocalin (N-GAL), because degradation of MMP9 is halted (188). Thus, N-GAL enables MMP9 to continue to degrade collagen and elastin of AAA wall.

ADAMs (A Disintegrin And Metalloprotease) are a group of proteases belonging to the metalloproteinase family, but several members of this group have a trans-membrane domain. Similar to other MMPs, ADAMs also contain a zinc-binding



domain in their active site. ADAMs are produced as zymogens and are activated in the cytoplasm before they are transported to the cell membrane, where they are anchored in the phospholipid bilayer by their trans-membrane domain (189).

ADAM10 and ADAM17, which are studied in this thesis, cleave other membrane proteins, causing them to become activated or shed. Tumor necrosis factor alpha (TNF $\alpha$ ) is one of the proteins activated by ADAMs that possess TNF $\alpha$  converting enzyme (TACE) activity, especially ADAM10 and ADAM17 (190).

TNF $\alpha$  is a cytokine produced by activated macrophages and other cells. TNF $\alpha$  has a major role in the induction of inflammation and apoptosis (191). In the elastase-induced model of AAA, mice lacking receptors for TNF $\alpha$  showed only limited development of AAA. TNF $\alpha$ , together with c-JNK N-terminal kinase JNK and NonO, (a 54 kDa nuclear RNA and DNA binding protein) inhibit the expression of prolyl-4 hydroxylase (P4H), an enzyme required for synthesis of all collagens. Inhibition of P4H decreases collagen synthesis. TNF $\alpha$  and JNK also participate in the induction of genes, such as MMPs, that are responsible for matrix degradation

It has been shown that ADAM17 (TACE) is up-regulated in the media and adventitia of the aneurysmal wall and that TNF $\alpha$  has a role in the pathogenesis of AAA (192).

In addition to TNF $\alpha$ , the substrates for ADAMs include other vessel-wall proteins, such as syndecan -1 and -4, collagen type XVII, ICAM-1 and VCAM-1 (193). Inhibitors of ADAM10 and ADAM17 include TIMPs 1-3

#### 5.4.3 Cathepsins, Trypsin, Chymase, Granzyme B

Other proteases that may play a role in the pathogenesis of AAA include cathepsins, trypsin, chymase, and Granzyme B.

Cathepsins are cysteine, aspartyl or serine proteases that are active mostly in the lysosomes of cells involved in protein degradation. Twelve members of this family have been identified. They are active at low pH and have been indicated to have a role in elastolysis (194).

In the elastase-induced model of AAA, mice deficient in cathepsin C (195) and L were resistant to developing aneurysms.

Active cathepsin D and cathepsin L were found in the aneurysmal wall, and their concentrations were higher in AAA than in healthy control aorta. The activity of these proteases was shown to be higher in the ILT of AAA compared to an in-vitro produced blood clot from donors (197). Shortly after, the same group showed that activity of other cathepsins, namely, cathepsin A, cathepsin D, and cathepsin G, were higher in the ILT than in the blood clot while activity of cathepsin B, cathepsin C and cathepsin E was only slightly higher in the ILT of AAA patients compared to the blood clot (196). In addition, plasma of AAA patients was reported to contain elevated concentrations and activity of cathepsin D compared to control plasma (196).

Another group showed that cathepsin originates from neutrophils and mast cells in AAA tissue (151). Mast cells also release trypsin and chymase during degranulation and are abundant in AAA. Both trypsin and chymase are involved in the activation of MMPs and cause apoptosis of smooth muscle cells in AAA .

Granzyme B is a protease produced by cytotoxic T-lymphocytes involved in antitumor and antiviral activities of host immune defense, and their presence in AAA tissue has been demonstrated (198).

## Chapter VI

### Our Study

#### 6.1 Background

Rupture is an acute and life-threatening complication of abdominal aortic aneurysm (AAA). Its risk increases with aortic diameter; however, it is not negligible in relatively smaller AAAs (sizing: 4.0- 5.5 cm) in which its incidence ranges from 1% to 5 % per year. Thus, although the time of surgery is currently delayed until the aneurysm reaches 5.5 cm in diameter, (199) predicting AAA rupture risk remains a major issue in vascular medicine. On one side, this task implies a model, that is, a complete comprehension of the factors contributing to the precipitation of this syndrome, of their interplay, and temporal sequence. On the other side, it also asks for the availability of methods able to describe the presence of these same factors and their activation in each single patient at risk. According to these considerations, several authors investigated the role of inflammation because these pathways underlie many of acute complications of atherosclerotic disorders and can worsen the effect of biomechanical forces acting on the diseased aorta. Actually, AAA development in experimental models is paralleled by the appearance of inflammatory infiltrates (37, 200) whose release of matrix metalloproteinases (MMPs) and proinflammatory cytokines ultimately results in an accelerated proteolysis of elastin and collagen of aortic wall. In recent years, this inflammatory paradigm of AAA rupture has been extended to the clinical arena, as the increased availability of positron emission tomography/ computed tomography (PET/CT) imaging systems permit the detection of focal arterial inflammation as areas of increased <sup>18</sup>F-fluorodeoxyglucose (FDG) (92, 201) caused by the elevated insulin independent glucose consumption of infiltrating leukocytes (203). Actually, the high content of activated macrophages justifies the use of PET/CT imaging to identify vulnerable

plaques in a variety of acute complications of atherosclerosis (204). However, the pathologic features of AAA seem relatively unsuitable for this purpose, as the progression of aortic dilation is paralleled by a reduction in cell density and thus by a local reduction in the elements able to trap FDG (205). This consideration implies that PET/ CT might represent a relatively inaccurate method to identify the inflammatory activation in asymptomatic patients with AAA characterized by even a relatively low-diameter dilatation.

Conflicting results have been reported about the clinical value of fluorodeoxyglucose (FDG) imaging in predicting the risk of rupture of abdominal aortic aneurysm (AAA).

Actually, pathological evidence suggests that the progressive increase in aneurysmal diameter is paralleled by a reduction in cell density that might explain the inverse correlation between AAA size and FDG uptake with the possible confounding effect of nonspecific fluoride binding onto calcified arterial segments (206).

## 6.2 Objectives

In the present study, we planned to verify the prevalence of visible FDG uptake in aneurysmal walls, adopting a case control approach. To identify the possible role of this technique in the clinical setting, selection criteria were focused on those patients in whom the question about risk of rupture represents the main clinical factor able to identify surgical correction. Accordingly, patients with symptoms as well as patients with any evidence of aortic wall fissuration were excluded a priori (objective 1).

Moreover, we tested the hypothesis that with increasing AAA diameter cell density is too low to permit any visible FDG uptake. This limitation would particularly apply to asymptomatic patients bearing aortic dilatation with a size falling within a “grey zone” close to surgical indication but with uncertain therapeutic approach. For this purpose, we first tested the spatial agreement of radioactivity concentration with local cell density, type and mitotic activity by coregistering autoradiography with histological and immunohistochemical images. Then, to verify the specific nature of tracer binding, we tested the relationship between FDG uptake and glucose metabolism by modifying cell viability and biology via a preliminary freezing of aneurysmal samples (objective 2).

## 6.3 Methods Objective 1

### 6.3.1 Patient Population

This study included 40 males (mean age: 74 years, range: 59-93 years), consecutive, white Caucasian patients, with asymptomatic infrarenal AAA, selected by the outpatient clinic of Vascular and Endovascular Surgery Division of University Hospital “San Martino” Genoa Italy between January 2009 and 2010. All subjects were candidates to open surgical repair of AAA according to conventional morphological criteria: saccular aneurysm, aortic diameter  $\geq 5$  cm, or diameter increase  $>1$  cm in the last 6 months (Table II).

Table II. Indication to treatment of asymptomatic abdominal aortic aneurysm

Type of indication	Patients (n)	Mean diameter of aneurysms (cm)
Saccular aneurysm	11	4.9
Increase size of diameter		
( $>1$ cm/6 months)	19	5
Diameter $\geq 5$ cm	12	5.1
Total	42	5

Within the series of AAA with diameter  $<5$  cm under observation during the study period, the subgroups of cases characterized by rapid expansion or saccular aneurysm have been selected. The mean diameter of AAA was 4.9 cm (range: 4.8-5.4 cm), as measured by CT scan. Exclusion criteria were the presence of congestive heart failure, impaired renal function (serum creatinine,  $>1.5$  mg/dL), known intolerance to iodinated contrast media, or elevated blood glucose level ( $>130$  mg/dL).

Of 40 patients, 26 underwent open repair of AAA, 9 received endovascular treatment, and 5 refused the surgery. All patients provided written informed consent.

Patient demographic information included age, gender, smoking history (current, ex-smoker, no smoking), coronary heart disease, degree of carotid stenosis,

hypertension, renal insufficiency, and diabetes mellitus. Cardiovascular medication was also recorded (statin, B-blocker, antiplatelet). All patients with coronary heart disease and renal failure were evaluated as reported by international guidelines. These patients were considered as having moderate surgical risk and good life expectancy.

The following were measured before surgery: plasma glucose, triglycerides, high-density lipoprotein (HDL) cholesterol, low-density lipoprotein (LDL) cholesterol, uric acid, C-reactive protein, fibrinogen, D-dimer, N-terminal pro-brain natriuretic peptide (NT-proBNP), white blood cell count, lymphocyte count, monocyte count, and neutrophil count.

Control Subjects: Data were compared with findings obtained in 44 age-matched controls subjects (mean age: 71 years, range: 59-85 years, 24 males, 20 females) who were selected according to a case control criterion among a population of patients without any clinical evidence of atherosclerotic disease who were submitted to PET/CT scan as a part of the workup of characterization of neoplastic disease. Patients previously submitted to chemotherapy or radiotherapy, patients with aortic dilatation, as well as patients with suspected autoimmune disease were excluded.

### *6.3.2 PET/CT Acquisition*

After a minimum of 6-hour fasting, a dose of 4.8 to 5.2 MBq of FDG per kilogram body weight was injected through a peripheral vein catheter. The patient was placed in a quiet room and instructed not to move. Data acquisition started  $\geq 60$  minutes after intravenous tracer administration. Both patients and controls underwent simultaneous FDG-PET and CT imaging from the skull base to the femoral neck by using an integrated PET/CT scanner (Hirez; Siemens Medical Solutions, Knoxville TN). PET raw data were reconstructed by means of ordered subset expectation maximization, and attenuation correction was performed using the CT raw data (ordered subset expectation maximization).

The entire CT dataset was fused with the three-dimensional PET images using an integrated software interface (Syngo Image Fusion; Siemens Erlangen, Germany) to create anatomical images superimposed with FDG uptake in the arterial wall.

#### *6.3.2a Image Analysis*

To take account of presence and pathophysiological meaning of arterial hot spots as well as diffuse vascular wall hypermetabolism, both qualitative (visual) and quantitative (region of interest [ROI]- based) analyses were performed on PET/CT images.

#### *6.3.2b Visual Analysis*

Two independent readers carefully inspected images by performing a complete slice-by-slice analysis. Visual analysis aimed to search for the presence of hot spots of degree adequate to identify the aneurysmal arterial wall as well as all other vascular segments included in the PET/CT study.



### 6.3.2c Quantitative Analysis

To better characterize the metabolic pattern of the whole vascular tree and the peculiar aspects of AAA, a quantitative analysis was also performed. To this purpose, volumetric ROIs were placed on the anatomic CT images to identify aortic segments (ascending, arch, descending, and abdominal aorta), bilateral subclavian, common carotid, and iliac arteries (Figure 6.1 - 6.2).

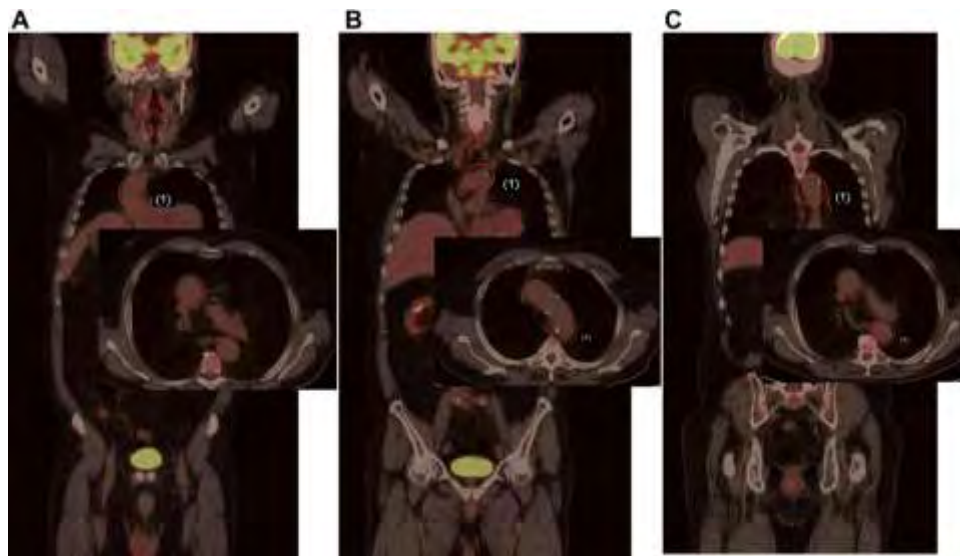


Figure 6.1 Image analysis on transaxial fused positron emission tomography/computed tomography (PET/CT) (coronal and transversal sections) of aortic segments: Circular regions of interest (ROIs) were drawn around different aortic segments: ascending (**panel A**), arch (**panel B**), and descending (**panel C**) aorta. PET image provided mean and maximum standardized uptake values (SUVs) within defined ROIs.  $^{18}\text{F}$ -fluorodeoxyglucose (FDG) uptake within each ROI was finally divided by circulating FDG (blood-pool ROI).

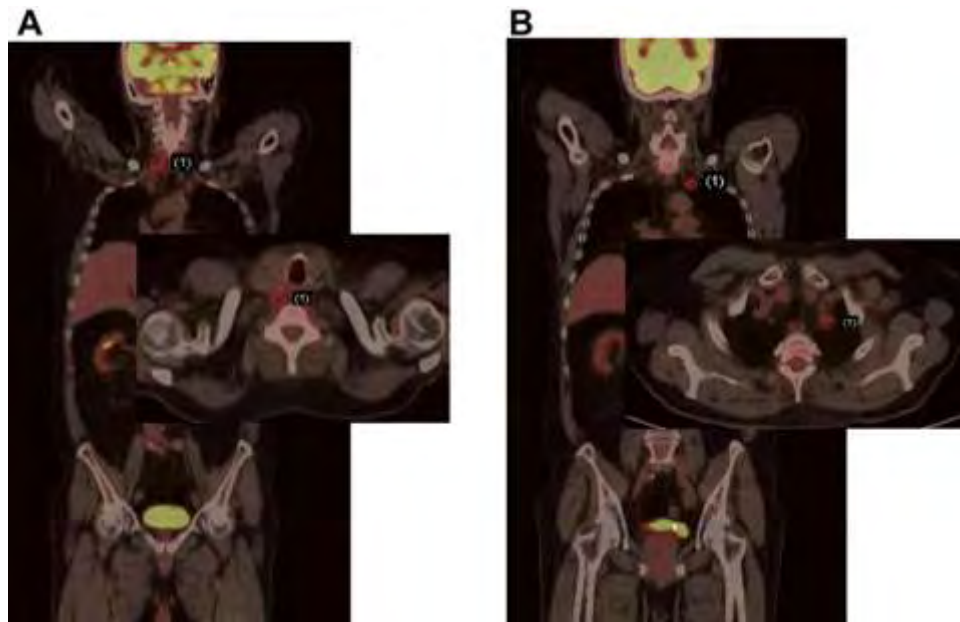


Figure 6.2 Example of image analysis on transaxial fused PET/CT (coronal and transversal sections) of right common carotid artery (**panel A**) and left subclavian artery (**panel B**). PET image provides mean and maximum SUVs within defined ROI. FDG uptake within each ROI was finally divided by circulating FDG (blood-pool ROI).

In all patients with AAA, a further ROI was drawn over the aneurysmal arterial walls (Figure 6.3B). Finally, two ROIs were drawn within the liver and the left ventricular chamber to estimate liver uptake and tracer concentration in the arterial blood, respectively (Fig. 6.4).

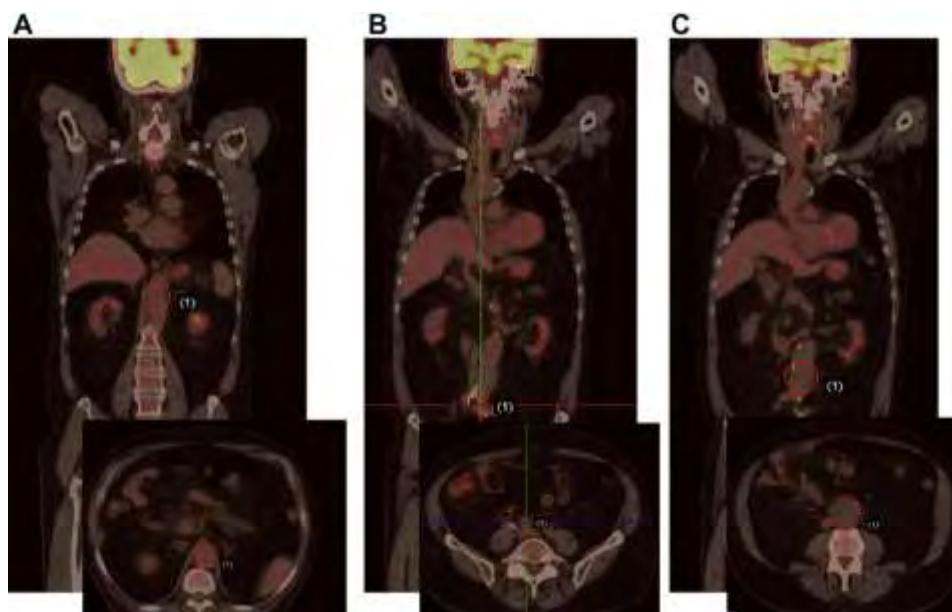


Figure 6.3 Image analysis on transaxial fused PET/CT (coronal and transversal sections) of abdominal aorta (panel A), abdominal aortic aneurysm (panel B), and iliac arteries (panel C). PET image provides mean and maximum SUVs within defined ROI. FDG uptake within each ROI was finally divided by circulating FDG (blood-pool ROI).

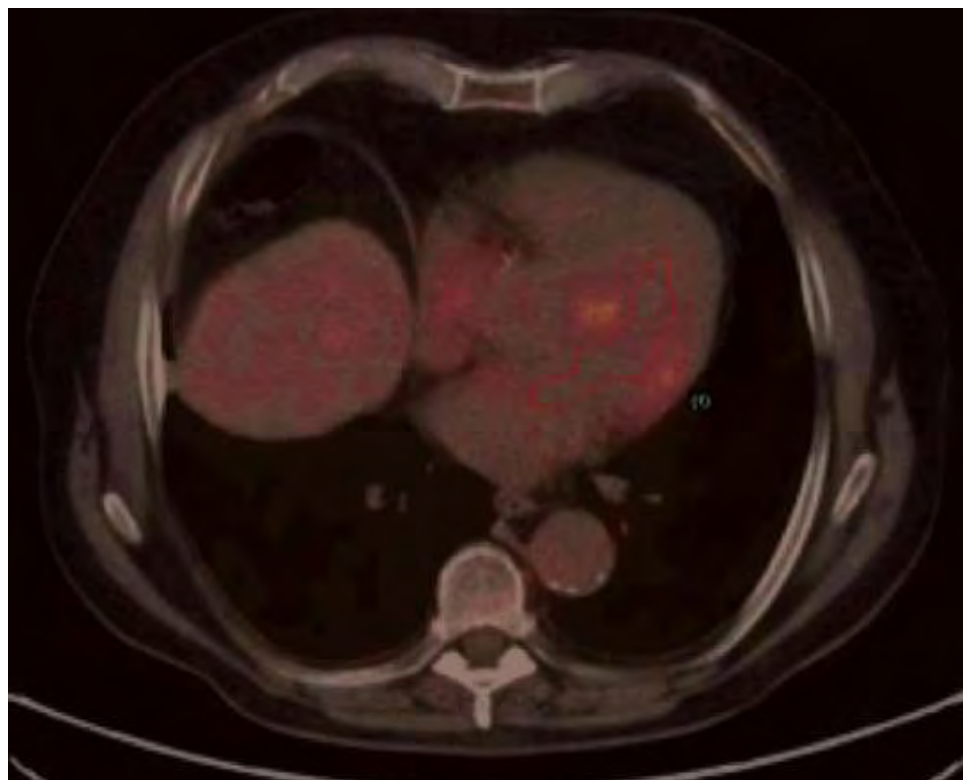


Figure 6.4 Liver and Blood-pool ROIs

FDG uptake was thus quantified by calculating the mean and maximal standardized uptake values (SUVs) within each ROI. Finally, these values were normalized for the blood-pool SUV, thus obtaining a target-to-background ratio and avoiding the confounding effect of circulating FDG. Bilateral measurements were averaged.

#### *6.3.2d Calcium Load Evaluation*

Total calcium load (ACL) was also estimated in the same arterial segments. To this purpose, two independent observers, blinded to the patient status, were asked to grade calcium density according to a semiquantitative five point scale based on percent calcification of the arterial ring documented in the transaxial views: (0= no calcific deposits, 1= 0-25%, 2= 25%-50%, 3= 50%-75%, and 4= 75%-100%).

#### *6.3.2e Statistical Analysis*

Intergroup differences in arterial mean and maximum SUVs were tested in each vascular segment by using Student t test for unpaired data and Bonferroni correction. Linear regression analysis was performed using the least squares method to assess the relationships between arterial wall metabolism in each artery and ACL or aneurysm maximum diameter.  $P < 0.05$  was considered significant.

## 6.4 Methods objective 2

### 6.4.1 Patients Population

The study included 12 consecutive patients (10 men, 2 women, mean age  $73 \pm 5$ , range 65–85 years) with asymptomatic AAA selected by the outpatient clinic of the Vascular and Endovascular Surgery Division of University Hospital “San Martino” Genoa Italy. All subjects were candidates for open surgical repair of AAA according to the evidence of diameter increase  $>10$  mm in the last 6 months. The maximum anteroposterior aneurysm diameter was measured by CT and ranged from 45 to 53 mm (mean diameter  $48 \pm 3.5$  mm) at the time of surgery. The main exclusion criteria included the presence of congestive heart failure, impaired renal function (serum creatinine  $>1.5$  mg/dl), known intolerance to CT-iodinated contrast media or elevated blood glucose level ( $>130$  mg/dl), significant concomitant diseases such as cancer, infections and, finally, autoimmune disorders.

Imaging data were compared with findings obtained in 12 age- and sex-matched subjects who were selected according to a case-control criterion among a population without cardiovascular risk factors or clinical evidence of cardiovascular disorders. All of these patients were submitted to PET/CT scan in the diagnostic workup of a suspected neoplastic disease. Patients previously submitted to either chemotherapy or radiotherapy, patients with aortic dilatation as well as patients with suspected autoimmune disease were excluded from the study. All patients signed the informed consent module to participate in the study that was approved by the local Ethics Committee.

#### *6.4.2 Biochemical assays*

Fasting blood samples were collected from all study subjects in the morning after resting in the supine position for 20 min during their outpatient clinical appointment.

Plasma glucose, lipid and renal profile, total protein, serum fibrinogen, C-reactive protein (CRP) and N-terminal probrain natriuretic peptide (NT-proBNP) were assessed using standard techniques. Similarly, leukocyte and monocyte counts were measured using automated cell counters.

#### *6.4.3 PET/CT acquisition*

After a 12-h fast, serum glucose level was measured before the intravenous injection of 4.8–5.2 MBq of FDG per kilogram of body weight. All of these procedures were performed 4–10 days before surgery, with the patient recumbent in a supine position in a quiet room and instructed not to move. FDG PET imaging, from the skull base to the femoral neck, started 60–90 min after tracer injection and was performed using an integrated PET/CT scanner characterized by a PET spatial resolution of 4 mm full-width at half-maximum (Hi-REZ, Siemens Medical Solutions, Knoxville, TN, USA).

CT aortic angiography was performed within 1 week from the FDG PET study using the same 16-slice CT scanner. Patients were placed in a supine position, and topograms in the anteroposterior view were obtained from the diaphragm to the pelvis. Intravenous contrast medium was injected into an antecubital vein, using an automatic injection system via a 20-gauge cannula. Synchronization between the passage of contrast and baseline arterial phase was conducted in real time using an automatic fire detection system on the upper abdominal aorta (Bolus Tracking, Siemens Medical Solutions, Erlangen, Germany). The control sequence was activated 10 s after the start of contrast injection and implied the acquisition of one image every second. The start of the study was triggered automatically when the

intensity level of contrast reached 180 HU, within a region of interest (ROI) placed on the abdominal aorta. In all cases, the craniocaudal direction was used.

#### *6.4.3a In vivo image analysis*

PET raw data were reconstructed by means of ordered subset expectation maximization (OSEM) and attenuation correction was performed using the CT raw data. The entire CT data set was fused with the three-dimensional PET images using an integrated software interface (Syngo Image Fusion, Siemens Medical Solutions, Erlangen, Germany) to create anatomical images superimposed with FDG uptake in the investigated body districts.

Volumetric regions of interest (VROIs) were placed on the anatomical CT images to identify four aortic segments (ascending, arch, descending and abdominal aorta), common carotid arteries and iliac arteries. In the case of bilateral branches, the mean value was considered. Two further VROIs were drawn in the liver and in the left ventricular chamber using the PET image to estimate liver uptake and arterial tracer concentration, respectively. Finally, in all patients with AAA, an additional VROI was drawn over the aneurysmal arterial walls.

FDG uptake was quantified by the maximum standardized uptake value (SUV) within each VROI according to the recently published guidelines (207). To account for the contribution of blood FDG activity, all SUVs were divided by the corresponding value in the blood pool as proposed by Rudd et al. (208, 209). In no case was correction for partial volume effect attempted due to the absence of clearly visible areas of focal uptake within the analysed vascular segments (210).

The degree of arterial calcification was measured from the takeoff of renal arteries to bifurcation of aorta into common iliac arteries. For this purpose, we used dedicated software (OsiriX) providing Agatston scores whose values were adjusted to account for slice width as previously published by Ellison et al. (211). In the aneurysmal walls, arterial calcium load was estimated according to the

semiquantitative method proposed by Siegel et al. (212). For this purpose, two independent observers, blinded to the patient status, were asked to grade calcium density according to a semiquantitative 5-point scale based on per cent calcification of the arterial ring documented in the transaxial views: (0=no calcific deposits, 1=0–25%, 2=25–50%, 3=50–75% and 4=75–100%).

Autoradiographic analysis of abdominal aneurysmal artery samples At the time of the surgical repair, the biodistribution of FDG within the aortic tissue was studied with digital autoradiography. Immediately after harvesting, the aneurysmal abdominal aorta was taken to the pathology lab of our hospital. The specimen was dissected, blood was washed with saline and the surrounding connective tissue and fat were removed. The AAA sample was then divided into three sequential blocks, from A to C. Blocks A and C were used for autoradiography, while block B was submitted to immunohistochemistry. The thickness of each block ranged from 3 to 5 mm for a weight of 150–450 mg.

Block A was frozen in isopentane chilled with dry ice for sectioning with a cryomicrotome, according to the procedure described by Laitinen et al. (206). Starting from the cutting border with block B, a minimum of three sequential sections were cut at  $-15^{\circ}\text{C}$  and thaw-mounted onto microscope slides. Slice thickness was set at 5  $\mu\text{m}$  to optimize image spatial resolution. The sections were then warmed to room temperature, incubated in saline for 20 min and, thereafter, immersed in 20 ml of saline containing 2–3 MBq/ml of FDG for 30 min. Thus, the slices were washed twice with ice-cold saline, rinsed in distilled water and air-dried (with a hair dryer for 10 min).

By contrast, the whole fresh block C was first incubated in the same tracer solution, for the same time and under the same experimental conditions used for the sections from block A. Thus, the specimen was washed, dried and then frozen in isopentane chilled with dry ice for sectioning with the cryomicrotome with the same



procedure used for block A, again obtaining a minimum of three sequential sections, 5  $\mu\text{m}$  thick, starting from the cutting border with block B.

Thereafter, all slides were exposed to an imaging plate (Cyclone, PerkinElmer Analysis Facilities) that provides an image resolution of 50  $\mu\text{m}$ . Different times of exposure were sequentially utilized in all experiments: 2, 5, 15, 30 and 60 min. At the end of the procedure, all aortic sections were stained using the haematoxylin and eosin technique.

#### *6.4.3b Autoradiographic image analysis*

Plates were scanned and images were analysed for count densities (photostimulated luminescence per unit area, PSL/ $\text{mm}^2$ ) with a dedicated image analysis software (OsiriX). For this purpose, a minimum of four ROIs were manually drawn in each image to identify hot and cold areas, respectively. Each region was thus saved to be exported for blind histological analysis.

For freshly incubated specimens, an exposure to the imaging plate longer than 5 min systematically prevented the analysis of FDG distribution due to saturation effect. On the contrary, for previously frozen slices, an exposure time shorter than 30 min consistently prevented an adequate analysis due to poor image statistics.

FDG uptake in samples incubated before or after freezing was estimated by comparing the number of PSD (counts) normalized for the different acquisition times (5 vs 30 min) and the consequent effect of  $^{18}\text{F}$  physical decay, according to the conventional formulations.

#### *6.4.3c Histology*

The central block B was fixed in 10% formalin solution and embedded in paraffin to optimize immunohistochemical analysis. Thereafter, two series of five—5  $\mu\text{m}$  thick—paraffin sections were obtained, starting from both cutting borders facing

toward either block A or block C. This procedure ensured that each autoradiography, regardless of its provenience, had a direct immunohistochemical counterpart obtained in the adjacent tissue.

Starting from each cutting border, block B sections were always stained, according to the same order, to allow the sequential analysis of the following variables: (1) tissue structure, (2) cells under any phase of active cell cycle, (3) leukocyte nature of cellular infiltrates and, finally, (4) T and B lymphocytes.

No histological analysis was performed on autoradiography slices to avoid the relative loss in image quality affecting previously frozen sections. Immunohistochemistry evaluation was performed using a panel with CD3 (Ventana), CD20 (Ventana) and Ki-67/MIB-1 (Dako) antibodies, in a ready-to-use formulation, on the paraffin-embedded and formalin-fixed slides. The standard avidin-biotin complex technique was employed for all immunostains; antibodies were optimized for use on an automated slide stainer in combination with Ventana detection kits. Heat pretreatment (microwave) and endogenous biotin blocking were performed for all of the abovementioned antibodies. Finally, all slides were counterstained with haematoxylin for 4 min.

A report was completed by two experienced pathologists, who described the specimens on a standard reporting form that included degree of atherosclerosis (graded 0–3) (213), plaque and vessel calcification as well as degree of medial and adventitial inflammation (density of inflammatory cells). For the coregistration study, pathology readers were blinded to the results of autoradiography and, in particular, were left unaware of ROI nature (hot or cold). ROI borders, saved in TIFF format, were reported on all of the histological images formatted in the same matrix.

#### *6.4.3d Statistical analysis*

Intergroup differences in maximal arterial SUV were tested in each vascular segment using Student's t test for unpaired data. Intersegment variability in arterial

SUV was tested in each patient using the t test for paired data and Bonferroni correction. Linear regression analysis was performed using the least-squares method. A p value <0.05 was considered significant.

## **6.5 Results objective 1**

### *6.5.1 Clinical Data*

The main clinical and metabolic characteristics of the study group are reported in Tables III and IV, respectively.

Surgical intervention was successfully completed in 35 patients, and no complication occurred in the postoperative period.

Table III. Clinical characteristics of patients with asymptomatic abdominal aortic aneurysm (n =42)

<i>Patients Characteristics</i>	
Mean age (years)	74.0
Sex (M/F)	40/0
Mean diameter (cm) 4.9 cm	4,9 cm
Hypertension	35/5
Systolic blood pressure (mm Hg)	144 ± 18
Diastolic blood pressure (mm Hg)	83 ± 9
Diabetes mellitus (yes/no) <sup>a</sup>	3/37
Coronary heart disease (yes/no)	10/30
Degree of carotid stenosis (right or left) <sup>b</sup>	
<50% (n)	9
>50% (n)	2
Degree of carotid stenosis (bilateral) <sup>b</sup>	
<50% (n)	20
>50 % (n)	8
Renal insufficiency (yes/no) <sup>c</sup>	5/35
Body mass index (kg/m <sup>2</sup> )	26.1 ± 3.2
Antiplatelet therapy (yes/no)	18/22
B-blocker (yes/no)	11/29
Statin (yes/no)	20/20

<sup>a</sup> Blood glucose level >130 mg/dL.

<sup>b</sup> Serum creatinine level <1.5 mg/dL.

<sup>c</sup> Degree of stenosis measured by North American Symptomatic Carotid Endarterectomy Trial.

Table IV. Metabolic characteristics of patients with asymptomatic abdominal aortic aneurysm (n = 42)

Circulating serum markers	Value $\pm$ SD
CRP (mg/dL)	8.8 $\pm$ 4.2
Fibrinogen (g/L)	412.1 $\pm$ 117.1
D-dimer (mg/L)	412.1 $\pm$ 225.5
LDL cholesterol (mg/dL)	138 $\pm$ 49.6
HDL cholesterol (mg/dL)	50.1 $\pm$ 13.6
Total cholesterol (mg/dL)	210 $\pm$ 55.1
Triglycerides (mg/dL)	230 $\pm$ 52.5
Uric acid (mg/dL)	6.17 $\pm$ 1.94
NT-proBNP	603 $\pm$ 204
White blood cell count ( $\times 10^9/L$ )	7,319 $\pm$ 2,225
Neutrophil count ( $\times 10^9/L$ )	5,230 $\pm$ 1,751
Monocyte count ( $\times 10^9/L$ )	467 $\pm$ 150
Lymphocyte count ( $\times 10^9/L$ )	1,565 $\pm$ 367

CRP, C-reactive protein; LDL, low-density lipoprotein; HDL, high-density lipoprotein; NT-proBNP, N-terminal pro-brain natriuretic peptide.

### 6.5.2 PET/CT Evaluation of AAA

On visual inspection, no patient showed an increased focal uptake of degree adequate to identify the aneurysmal arterial wall. Main descriptors of systemic FDG kinetics were similar in the patient and control groups (liver average SUV:  $2.3 \pm 0.5$  vs.  $2.2 \pm 0.4$ ,  $P = \text{no significant}$ ; the blood-pool average SUV:  $2.1 \pm 0.8$  vs.  $2 \pm 0.6$ ,  $P = \text{no significant}$ ). Arterial wall metabolism was similar in all aortic segments and in the subclavian arteries in the two groups, although both common carotid arteries and iliac branches displayed a significantly higher SUV in patients compared with controls (carotid arteries: patients,  $0.79 \pm 0.2$ ; controls,  $0.65 \pm 0.2$ ;  $P < 0.02$  and iliac arteries: patients,  $0.80 \pm 0.2$ ; controls,  $0.67 \pm 0.2$ ;  $P < 0.05$ . See Figure 6.5 for further details).

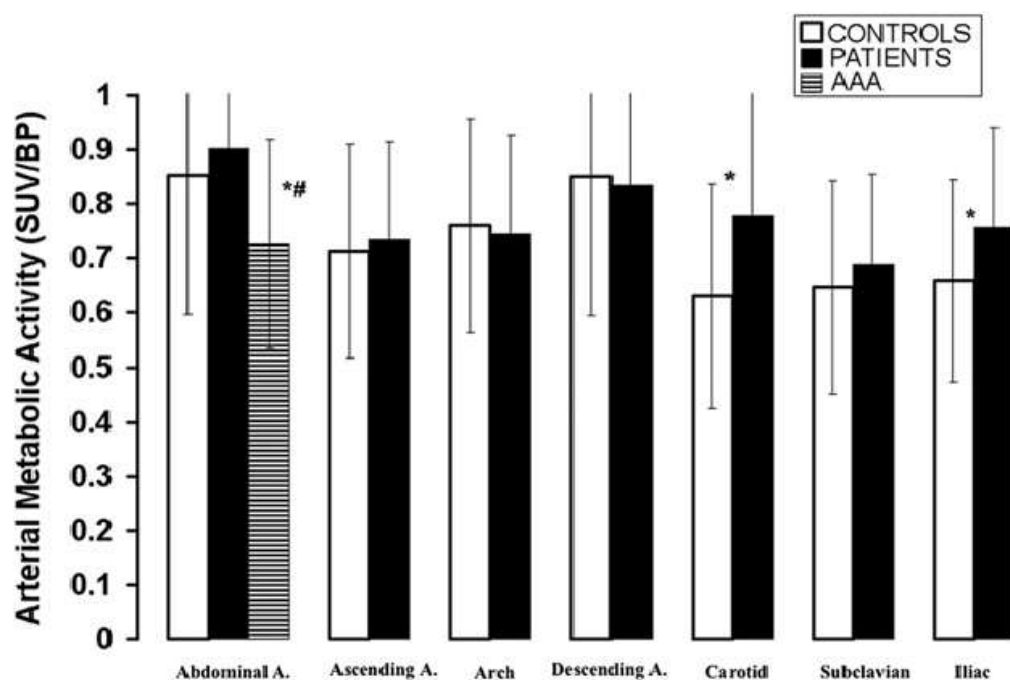


Figure 6.5 Wall metabolic activity (mean SUV/blood pressure) in the analyzed vascular districts. Metabolic activity in the aneurysmal aortic segment was lower with respect to both nonaneurysmal aorta of patient group ( $P < 0.001$ ) and the corresponding arterial segments of control subjects ( $P < 0.01$ ). On the contrary, both common carotid arteries (\* $P < 0.02$ ) and iliac branches (\* $P < 0.05$ .) displayed a significantly higher wall metabolic activity in patients compared with controls.

On the contrary, average metabolic activity in the aneurysmal aortic segment was even lower with respect to both the adjacent -non aneurysmal- aorta of patient group and the corresponding arterial segments of control subjects ( $0.7 \pm 0.2$ ,  $1 \pm 0.3$ , and  $0.9 \pm 0.3$ , respectively;  $P < 0.001$  versus non aneurysmal segment of the same patient and  $P < 0.01$  versus the same segment of control subjects Figure 6.5).

Analysis of maximum SUV replicated the same results with lower values in aneurysmal wall compared with normal abdominal aorta of patients and controls ( $0.9 \pm 0.3$ ,  $1.1 \pm 0.3$ , and  $1 \pm 0.2$ , respectively;  $P < 0.01$ ). Again, uptake by carotid arteries was higher in patients with respect to controls ( $1 \pm 0.2$  vs.  $0.78 \pm 0.2$ ,  $P < 0.01$ ).

Finally, no correlation was observed between FDG uptake in aneurysmal walls and AAA diameter. Atherosclerotic involvement was documented in AAA, as these patients showed significantly higher values of ACL than controls in ascending aorta and subclavian and iliac arteries ( $0.8 \pm 0.4$  vs.  $0.2 \pm 0.1$  for ascending aorta,  $0.5 \pm 0.3$  vs.  $0.3 \pm 0.1$  for subclavian arteries, and  $2.1 \pm 1.2$  vs.  $1.3 \pm 1$  for iliac arteries;  $P < 0.01$  in all cases).

Finally, only in AAA patient group, a significant correlation was present between values of ACL in iliac arteries (Figure 6.6) and abdominal aorta (Figure 6.7) and wall metabolic activity in the same arteries ( $P < 0.05$ ).



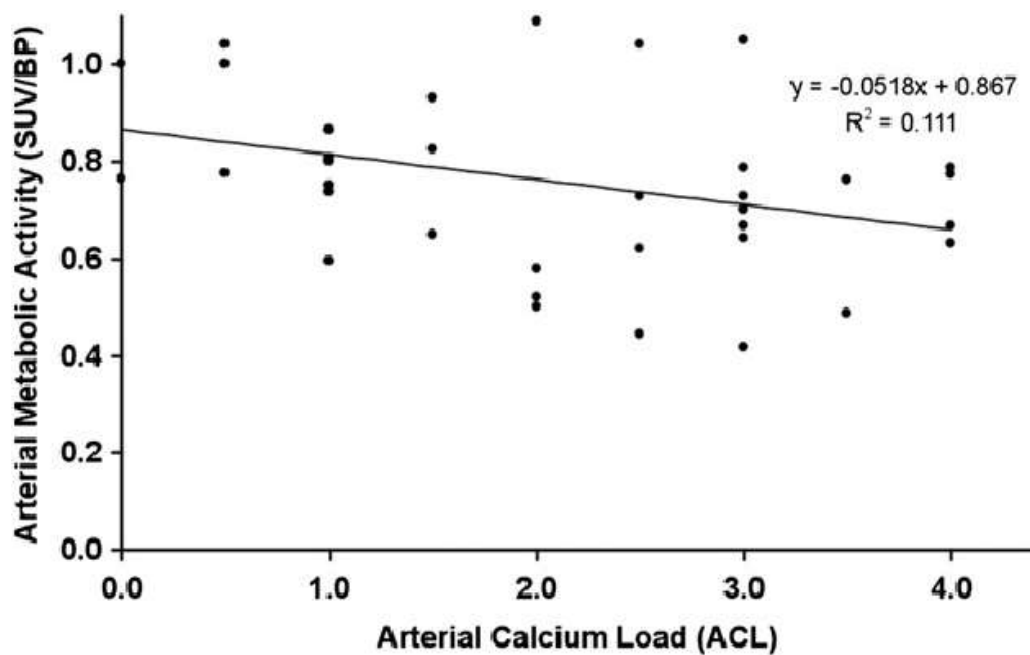


Figure 6.6 Inverse correlations between metabolic activity in iliac artery wall and calcium load.

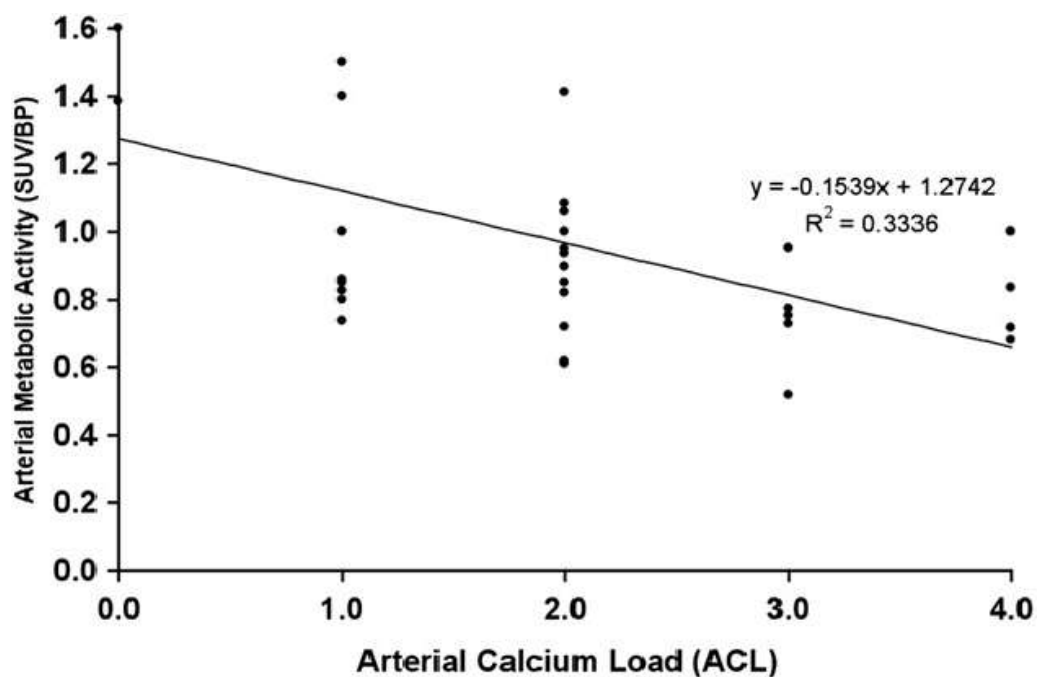


Figure 6.7 Inverse correlations between metabolic activity in abdominal aortic aneurysm wall and calcium load.

## 6.6 Results Objective 2

### 6.6.1 Clinical data

The main clinical and metabolic characteristics were similar in patients and controls as reported in Tables V and VI, respectively. Surgical intervention was successfully completed in all patients and no complication in the postoperative period occurred. An AAA example is reported in Figure 6.8, where the image fusion of CT angiography and FDG PET clearly shows, on one side, the vascular dilatation associated with the presence of calcium load and, on the other, the low metabolic activity of the aneurysmal walls.

Table V Demographics and treatment of study subjects

	AAA patients (n=12)	Controls (n=12)
Age (years)	73±5	73±4
M/F	11/1	11/1
Body mass index (kg/m <sup>2</sup> )	24.5±0.4	22.2±0.4
History of smoking (%)	10/12 (83%)	7/12 (58%)
Hypertension (%)	11/12 (92%)	8/12 (67%)
Hypercholesterolaemia (%)	8/12 (67%)	—
ACE 1 or AT1 inhibitors (%)	10/12 (83%)	6/12 (50%)
β-Blockers (%)	2/12 (17%)	1/12 (8%)
Aspirin or ticlopidine (%)	11/12 (92%)	5/12 (42%)
Age (years)	73±5	73±4

Table VI Laboratory tests of study patients

	AAA patients (n=12)	Controls (n=12)
Blood glucose (mg/dl)	96.2±9.0	88±12
Total serum cholesterol (mg/dl)	176.4±14.6	—
Triglycerides (mg/dl)	84±12	—
Uric acid (mg/dl <sup>-1</sup> )	5.4±0.4	—
Creatinine (mg/dl <sup>-1</sup> )	1.02±0.11	0.96±0.14
Total protein (g/dl <sup>-1</sup> )	7.8±0.2	—
Serum fibrinogen (mg/dl <sup>-1</sup> )	327±50	—
CRP (mg/l <sup>-1</sup> )	6.4±4.1	—
NT-proBNP (pg/ml)	118±57.2	—
White blood cell count (mm <sup>-3</sup> )	6,943±411	6,712±582
Neutrophil count (mm <sup>-3</sup> )	4,712±264	4,221±291
Monocyte count (mm <sup>-3</sup> )	452±71	411±62

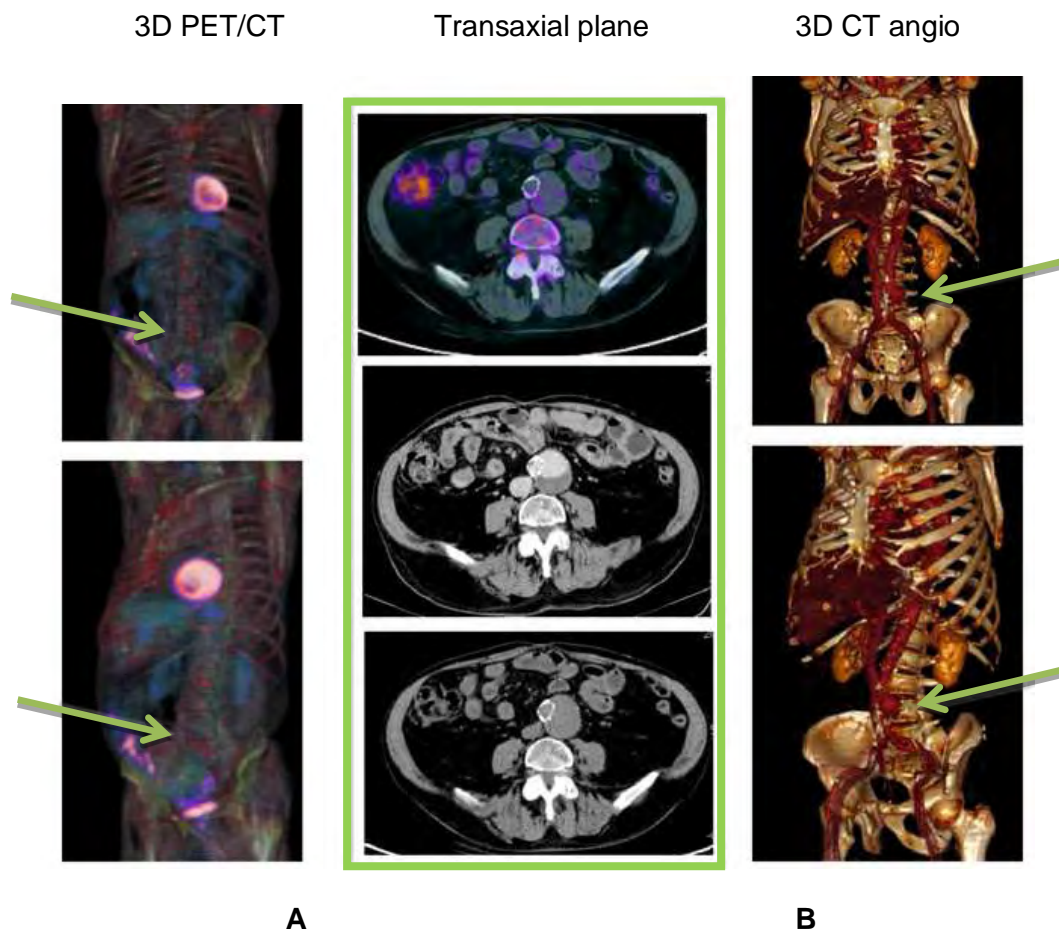


Figure 6.8 **A:** display 3-D 3D PET/CT Transaxial plane 3D CT angio reconstructions of PET/CT data and document the absence of any visible FDG uptake in the abdominal aortic region. CT transaxial plane (bottom, centre panel) displays the presence of an aortic aneurysm that is partially occupied by thrombotic material as documented by contrast CT angiography as well as by the absence of any visible FDG uptake at PET/CT coregistration. **B:** display the 3-D reconstructions of CT aortic angiography showing the aneurysmal portion as indicated by the green arrows

### 6.6.2 PET/CT evaluation of AAA

The main descriptors of systemic FDG kinetics did not differ in the two populations. In fact, the average SUV was similar in patients and in controls both in liver ( $2.2 \pm 0.4$  vs  $2.1 \pm 0.5$ , respectively,  $p=NS$ ) and in left ventricular blood ( $2.0 \pm 0.5$  vs  $2.1 \pm 0.6$ , respectively,  $p=NS$ ). As shown in Figure 7.2, no differences were observed in glucose metabolism in all non-diseased segments of aorta, common carotid arteries and iliac branches in the two groups. On the contrary, aneurysmal FDG uptake was significantly lower with respect to the corresponding arterial regions of control subjects ( $0.91 \pm 0.16$  vs  $1.54 \pm 0.39$ , respectively,  $p < 0.01$ , Figure 6.9). Compared to control subjects, AAA patients showed no significant differences in calcium load (Figure 6.10) both in the whole infrarenal abdominal aorta (modified Agatston score:  $3,845 \pm 2,000$  vs  $3,595 \pm 1,461$ , respectively,  $p=NS$ ) and in the aneurysmal segment (semiquantitative scoring system:  $2.9 \pm 1.2$  vs  $2.4 \pm 1.1$ , respectively,  $p=NS$ ).

Autoradiographic features of aortic aneurysm Independently of sample processing protocol, overall FDG distribution was largely heterogeneous with spots of clearly visible radioactivity surrounded by large areas characterized by low tracer content. Thrombi, when present, were always characterized by the absence of any visible radioactivity.

The different processing protocols resulted in marked differences in glucose metabolism. Despite the fact that the two samples were incubated with the same tracer solution for an identical incubation time, the history of recent transient freezing decreased FDG uptake by almost 8 times in hot regions, i.e. from  $30.5 \pm 8.7 \times 10^3$  PSL/mm<sup>2</sup> min<sup>-1</sup> (in freshly incubated samples) to  $3.7 \pm 1.1 \times 10^3$  PSL/mm<sup>2</sup> min<sup>-1</sup> (in previously frozen specimens, respectively,  $p < 0.001$ ). On the contrary, in cold areas tracer retention accounted for  $3.5 \pm 0.9 \times 10^3$  PSL/mm<sup>2</sup> min<sup>-1</sup> vs  $1.9 \pm 0.9 \times 10^3$  PSL/mm<sup>2</sup> min<sup>-1</sup> in fresh and previously frozen samples, respectively ( $p < 0.001$ ).

Thus, after the thermal shock, FDG uptake dramatically decreased by  $87\pm5\%$  within hot regions and by only  $34\pm 35\%$  in the cold ones ( $p<0.001$ ). This differential effect obviously affected image quality by modifying the tracer distribution throughout the slice. In fact, the ratio between hot and cold areas was  $9.2\pm2.7$  in freshly incubated samples vs  $2.2\pm0.7$  in previously frozen ones ( $p<0.001$ ).

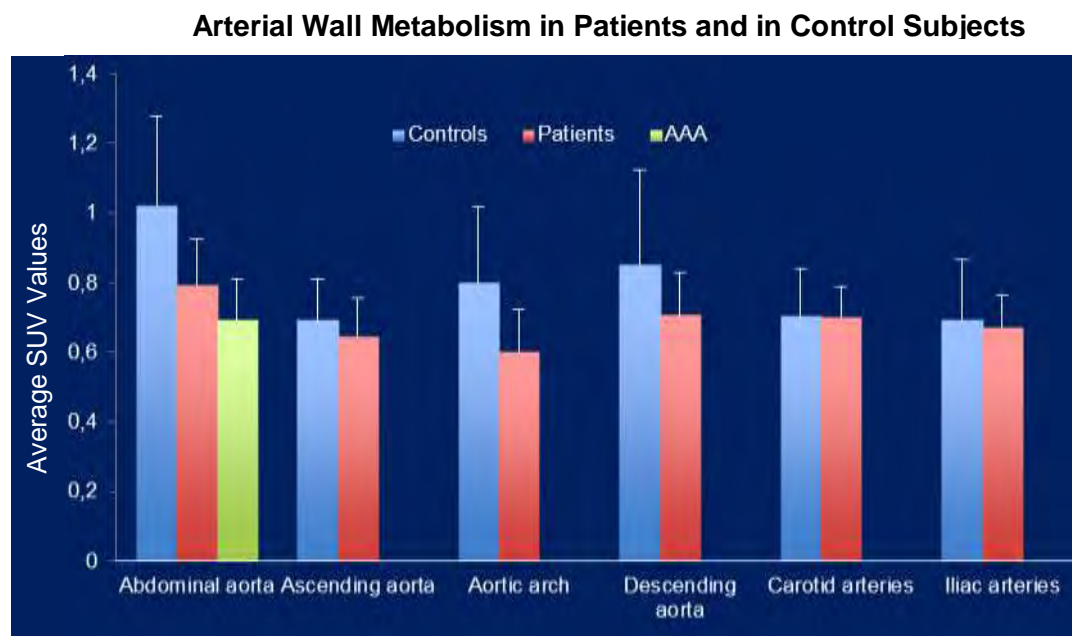


Figure 6.9 SUVs in the different arterial segments of patients and control subjects. The SUV was similar in all vascular segments in both groups (blue and red columns, respectively). Interestingly, FDG uptake was significantly lower in aneurysmal aortic segments with respect to controls subjects (green column).

### Arterial Calcium Load in Patients and in Control Subjects

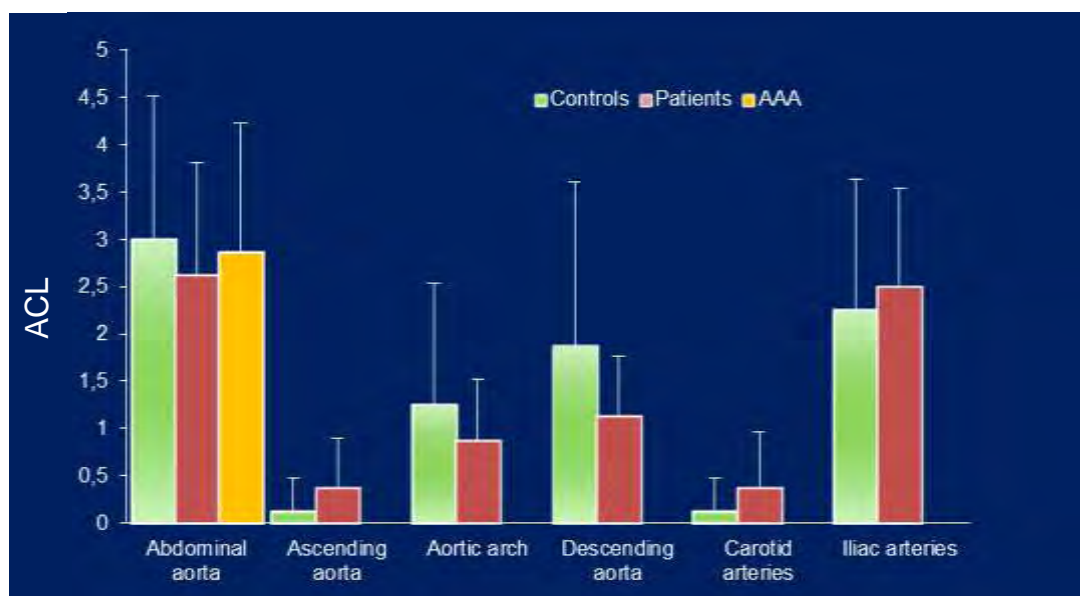


Figure 6.10 Total calcium load (ACL) was similar in patients and in control subjects

#### 6.6.3 Histological correlates of FDG uptake in aortic aneurysm

Aneurysm samples showed evidence of extensive atherosclerosis, graded 2–3, in all biopsies with necrosis, lipid deposits and/or calcifications. Evidence of ulcerated plaque occurred in 10 of 12 cases within the anatomical piece. Adhesive thrombus within the histological specimen occurred in 6 of 12 patients.

Haematoxylin and eosin staining of AAA specimens documented a loss of wall structure and a marked reduction in overall cell density. As expected, histological analysis documented a moderate inflammatory infiltration that encompassed the entire arterial wall although it was particularly evident in its outer layers. Representative examples of the extent of arterial wall inflammation are shown in Figure 6.11. Immunohistochemistry showed that the majority of cells (>85%) in both adventitia and media were leukocytes as documented by CD45 staining in all cases, with a striking prevalence of CD3 and CD20 lymphocytes (>80%). On the contrary, granulocytes and macrophages were rarely found. Prevalence of cells in all phases of the active cycle was documented by Ki-67 expression and was  $4.6 \pm 3\%$ . There was no evidence of bacteria or other unusual findings in any biopsies.

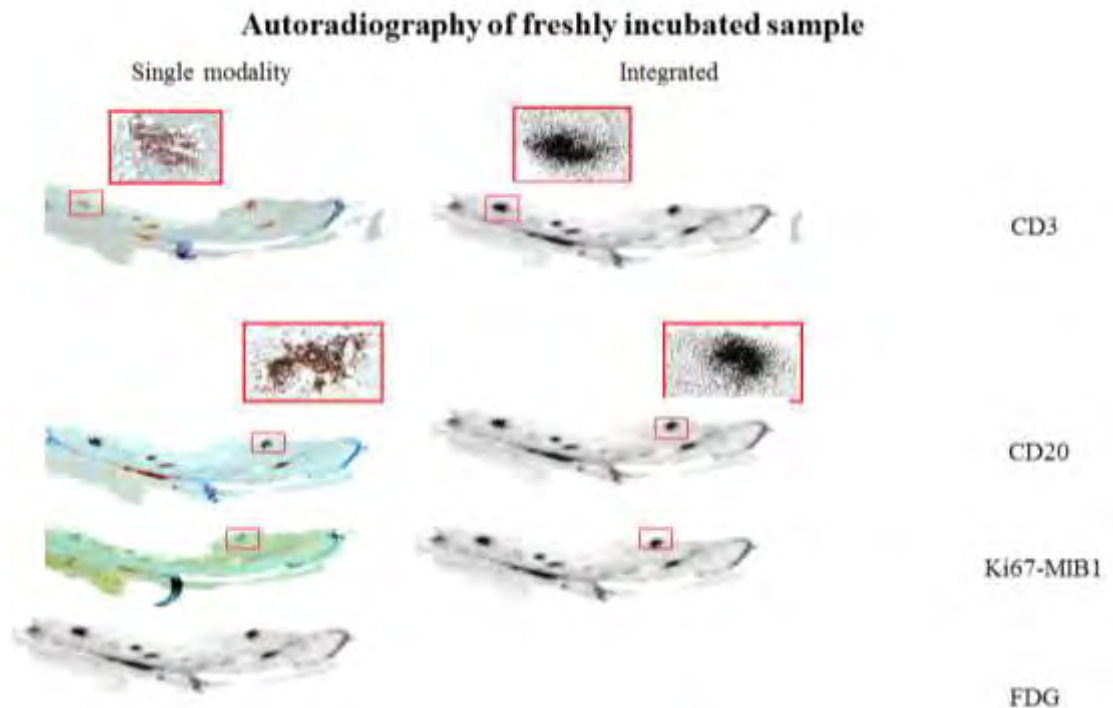


Figure 6.11 Immunohistochemical and autoradiographic analysis of a pathological sample of aortic aneurysm, incubated with FDG before cryotome application. Top right panel displays the autoradiographic image obtained from a slice cut from block C at its border with block B. Left panels display the immunohistochemical images of three sequential slices obtained after fixation from block B at its cutting border with block C. At the right of each image, its coregistration with autoradiography is shown. Starting from the top each row displays T lymphocytes recognized by CD3 staining, B lymphocytes identified on the basis of CD20 positivity and cells actively synthesizing DNA documented by Ki-67 expression. Despite the fact that these four images reflect the distribution of each marker in four sequential 5- $\mu$ m thick slices, the close agreement between cell density and metabolic activity is evident on the right panels and is confirmed by the details shown for the first two rows. Original magnification  $\times 200$

At coregistration analysis, the difference in tracer uptake was paralleled by an even more evident gap in cell density that was ten times higher in hot areas with respect to the cold ones without any differences between the two protocols ( $227 \pm 67$  vs  $27 \pm 21$  cells/mm<sup>2</sup> in fresh samples,  $212 \pm 70$  vs  $16 \pm 8$  cells/mm<sup>2</sup> in frozen samples, respectively,  $p < 0.001$ ). Moreover, all regions without any evidence of cells were



observed in cold ROIs. Similarly, the prevalence of cells actively synthesizing DNA, documented by their Ki-67 expression, was remarkably higher in hot than in cold regions both in freshly incubated samples ( $10\pm3\%$  vs  $1.8\pm 0.1\%$ , respectively,  $p<0.01$ ) and in slices incubated after freezing ( $8.3\pm3\%$  vs  $1.4\pm0.6\%$ ,  $p<0.01$ ).

Finally, as shown in Figures 6.12 and 6.13 a direct correlation was documented in each ROI between FDG concentration and density of both overall cells and cells in all phases of the active proliferation cycle. These correlations were more clearly evident for data obtained after incubation of fresh sample with respect to those provided by previously frozen slices.

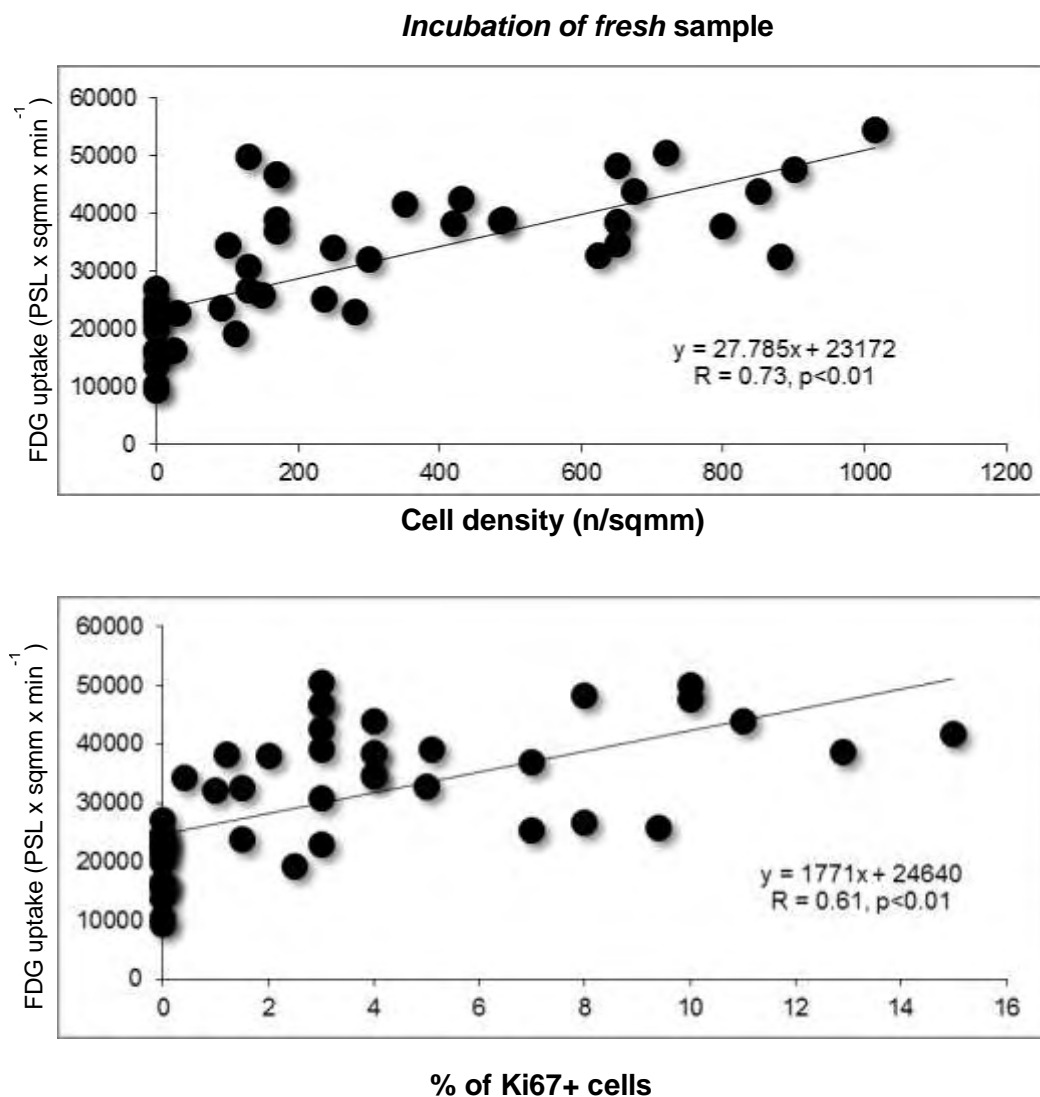


Figure 6.12 Tracer retention directly correlated with overall cell density and with prevalence of cells synthesizing DNA.

### Incubation of frozen slices

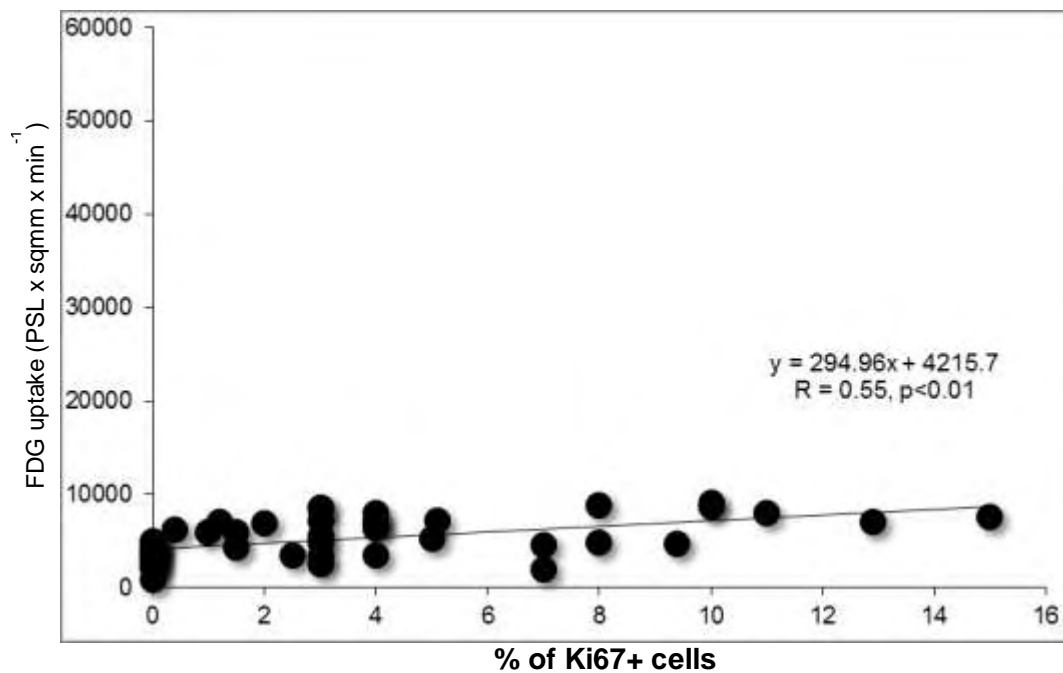
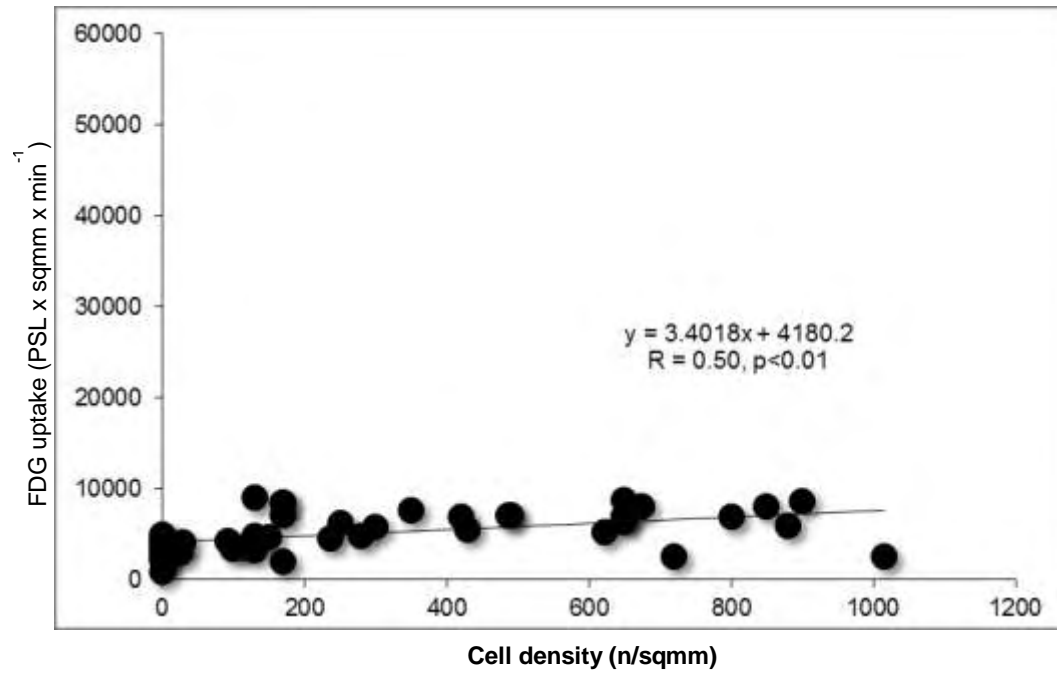


Figure 6.13 The metabolic nature of FDG uptake was confirmed by the selective effect of preliminary freezing that decreased tracer content by 90% in regions with high cell density and only by 34% in cold acellular areas

## **6.7 Discussion**

### **Objective 1**

The present study was designed to investigate whether imaging of the aneurysmal metabolism enables one to identify specific patterns among candidates to surgical abdominal repair of AAA.

No patient of this series showed any visible focal tracer uptake of degree adequate to identify the AAA. Similarly, the metabolic activity in the aneurysmal aortic segment was even lower compared with both the adjacent –nonaneurysmal- samples of the same patient and corresponding arterial segments of control subjects. By contrast, common carotid arteries and iliac branches displayed a significantly higher SUV in the AAA patients compared with controls.

AAA is the end result of a multifactorial process culminating in irreversible pathological remodeling of the aortic wall connective tissue (214). Aneurysm rupture was historically considered to be a simple physical process that occurs when hemodynamic wall stress exceeds the tensile strength of the aortic wall (215). When the rate of collagen degradation exceeds the rate of collagen synthesis, the tensile strength of the aortic wall declines and the risk of rupture increases. Recently, this model has been integrated by the evidence that AAA expansion and rupture also reflect a multifactorial process involving biochemical, cellular, and proteolytic influences (40). Among these factors, a key role is played by the release of MMPs produced or activated by inflammatory cells, causing degradation of elastin and collagen in the aneurysmal walls (216). Published findings seem to consistently indicate a great relevance for inflammatory wall digestion in both AAA progression and complication. Moreover, there is increasing evidence that MMPs and elastin degradation are implicated in the calcification process (217) that would reduce cell density in the aneurysmal wall. In keeping with these findings, the present study

reported an inverse correlation between arterial calcium load and wall metabolism in AAA.

Recently, a great attention has been paid to the possible role of functional imaging with PET/CT in the definition of inflammatory infiltration of aneurysmal aorta. The rationale behind this use is the fact that glucose metabolism is relatively insulin independent in activated leucocytes. Accordingly, imaging of FDG uptake under fasting conditions characterized by low serum concentrations of insulin might be able to visualize focal inflammation of different structures, including diseased aorta.

Reeps and coworkers reported slightly increased SUVs in 12 asymptomatic patients with relatively small aortic aneurysms ( $35 \pm 6$  mm) compared with 24 age-matched control subjects (92). This finding has been partially confirmed by Truijers et al, who documented that the slight SUV increase displayed by AAA walls was mostly evident in subjects with relatively small aneurysms (218).

Preliminary data in relatively larger aneurysms have been also provided. Kotze and colleagues reported an increased FDG uptake in 14 AAA patients in whom; however, the metabolic activity was not correlated with the recent growth rate (219). Finally, Sakalihasan et al. reported a positive FDG hot spot in the infrarenal aorta in 10 of 26 patients with an AAA ranging in size from 50 to 76 mm (90).

The present findings only partially disagree with this recent literature and rather extend these previous observations by documenting, in a larger population of 40 asymptomatic patients with AAA close to surgical indication, that a hot spot is an extremely rare finding in FDG imaging. On the contrary, tracer uptake in the diseased segment was even lower than that measured by the standard-method SUV in a population of subjects studied with a case control approach.

Together with the previously cited studies, this observation seems to indicate that focal PET signs of increased metabolic activity might be more frequent in AAAs of relatively small size. On the contrary, the prevalence of positive FDG hot spots seems to decrease with the enlargement of the aortic lesion. This finding reflects

both pathophysiological and technical phenomena related to the well documented reduction in cell density in large AAAs. In fact, low cell density is usually associated with low FDG uptake values just because of the small number of elements able to use glucose and thus to retain the tracer. On the other hand, the dispersed nature of these cell islands results in a frequent artifact of nuclear medicine, called partial-volume effect. This phenomenon implies a relevant underestimation of radioactivity concentration whenever the thickness of the source is less than twice the system spatial resolution. Because in most commercially available clinical systems, this parameter ranges from 4 to 7 mm, even large numbers of cells can be lost in PET imaging despite a high tracer uptake if they are dispersed in a large cellular matrix (220).

In the present study, images were acquired 1 hour after injection as per conventional protocols for both oncological and non-oncological PET studies. Previous studies suggested that a delayed acquisition time (3 hours (89) and 90 minutes (208) could be used for vascular inflammation imaging, as it would maximize the contrast between vascular wall and background (87). However, Menezes et al. (221) recently addressed this issue in 17 patients with atherosclerotic AAA and did not report any advantage compared with the most comfortable conventional timing. In the setting of our study, it seems extremely unlikely that waiting 2 hours more after injection would have resulted in a change of image pattern able to modify the main result of our experience, that is, visible FDG uptake is an extremely rare finding in patients with AAA close to surgical indication.

The lack of scientific evidence regarding the optimal acquisition time is paralleled by wide and variable range of choices regarding image analyses. Published studies based their analysis upon several different methods, ranging from a simple visual revision of the images (90) to an arbitrary choice of an SUV max cutoff for defining a high level of FDG uptake (222) or to a quantitative analysis of SUV max without normalization for circulating FDG (218).

From 2007 to 2008 Rudd et al. (208, 209) published a method of whole vessel analysis and a list of recommendation for atherosclerosis inflammation imaging. This analysis consists of arterial FDG uptake measure obtained by drawing an ROI around the artery on every slice of the coregistered transaxial PET/CT images; then, mean and maximum SUVs are calculated and divided for circulating FDG, thus obtaining the arterial target-to-background ratio. Authors proved high reproducibility of this method and proposed it as a reference for PET vascular imaging, especially when PET is used to tracking changes in plaque inflammation over time and after therapy as a surrogate end point in clinical trials.

The present analysis is in keeping with part of these recommendations (use of a PET/CT hybrid scanner, both mean and maximum SUV evaluation, and use of blood-pool activity for target uptake normalization). The lack of a so intensive evaluation might limit the reliability of the observation of normal glucose metabolism in the whole aorta. However, this limitation does not hamper the major finding of our study related to the low prevalence of visible FDG uptake in aneurysmal segment.

As a collateral finding, the present study documented a slightly, though significantly, higher FDG concentration in the carotid arteries of patients with respect to control subjects. Obviously, this finding does not yet retain any diagnostic relevance because the small value of the observed difference implies a data overlap that will prevent a diagnostic conclusion in any single patient. However, from the pathophysiological point of view, it strongly supports the inflammatory nature of atherosclerosis that represents an important target for diagnostic methods aimed to estimate the risk for cardiovascular events.

A limitation of this study was represented by relatively small aneurysm size (mean diameter of AAA was 5 cm) of patients. International guidelines suggest the surveillance with selective repair is generally most appropriate for older male patients with significant comorbidities. Good-risk patients aged <75 years and having a long

life expectancy with AAA between 5.0 and 5.4 cm may benefit from early repair (223).

## 6.8 Discussion

### Objective 2

The present study used an in vitro method to explain the low prevalence of positive findings at FDG PET imaging of asymptomatic AAAs with a size close to surgical indication. At this stage, diseased aortic walls typically display a marked reduction in cell density. Autoradiographic evaluation showed that radioactivity content was prevalently confined to populated islets being instead virtually absent in the residual, largely acellular, regions. The exposure to a transient thermal shock profoundly decreased cell tracer uptake, having only minor effect on the remaining acellular tissue. Altogether these data directly document that FDG retention accurately tracks glucose uptake being only modestly affected by unspecific binding. Accordingly, the extremely low FDG retention in these relatively large asymptomatic AAAs reflects the metabolic activity of an extremely low number of cells present within diseased arterial walls.

The capability of PET to visualize FDG uptake in vulnerable atherosclerotic plaques (89, 224) or large vessel vasculitis (225) has already been documented. On the contrary, the clinical value of this tool in asymptomatic AAA patients is less clear, since the high prevalence of positive scans in preliminary studies has not been confirmed by more recent reports (218, 226). This variability agrees with the current model of AAA progression (34, 200) characterized by the repetitive sequence of inflammatory damage and repair. However, when arterial diameter reaches values close to surgical indications, cell density is eventually reduced throughout the aneurysmal walls (162 227-230). This sequence of events might thus imply a cyclic variation in FDG uptake in early stages and a progressive reduction of tracer retention in later ones. Accordingly, positive PET findings should be more frequently encountered in aneurysms of small size or in those involved in large inflammatory



processes that are more frequently associated with symptoms and require direct surgical repair (92).

The micrometric analysis of FDG distribution and its coregistration with histology strongly corroborates this interpretation of the mechanisms underlying the reduced tracer retention in the diseased arterial segment. In fact, FDG uptake was extremely heterogeneous within the damaged arterial wall, with regions characterized by a “relatively preserved” metabolism clearly visible in the low background of the remaining vascular tissue. Metabolically inert areas were consistently located in fibrotic tissue, in endoluminal thrombus or in necrotic regions. These metabolic features agree with the pathological peculiarities of uncomplicated AAA characterized by the loss of smooth muscle cells and by the presence of infiltrating lymphocytes (227, 228) in contrast to the higher cell number and macrophage infiltration found in occlusive atherosclerosis (208) or in symptomatic AAAs complicated by inflammation (92).

This concept is further corroborated by the coregistration of autoradiography with immunohistochemistry: FDG uptake closely correlated with the number of lymphocytes under active mitotic cycle as documented by Ki-67 staining (231). Thus, this in-depth analysis of tracer handling by aneurysmal walls indicates that FDG actually tracks the local glucose consumption. However, the overall number of cells entrapping this tracer is excessively low to permit the *in vivo* diagnosis of AAA inflammation, at least in these asymptomatic patients, whose arterial dilatation falls in a grey zone close to surgical indication. This clinical condition might thus be better approached by evaluating more specific molecular pathways. In this line, the high prevalence of lymphocytes in cellular infiltrates of diseased walls might represent the basis for imaging with tracer targeted to interleukin 2 (232).

The technique of autoradiography is most often used to evaluate the distribution of tracers after their *in vivo* injection. However, under many experimental conditions, a direct incubation of biological samples is needed to verify the tissues

responsible for tracer uptake. In this setting, specimen physiology responds to an artificial environment in which signalling systems modulating cellular metabolism are lacking, oxygen tension is not preserved due to the absence of perfusion while tracer concentration remains relatively stable throughout the incubation period. Due to these considerations, this procedure does not permit testing of possible quantitative correlations between in vitro FDG uptake and in vivo SUV. On the contrary, it permits one to accurately verify the spatial distribution of the metabolic tracer within the analysed tissue.

In vitro autoradiography can be performed according to two procedures: direct incubation of tissue sample and subsequent freezing for slice preparation (162, 230-232) or preliminary freezing and sectioning followed by slice incubation (206, 233, 234). The former protocol offers the advantage of a relatively preserved physiology of the experimental specimen. The latter procedure (206) permits exposure of all cells to the same tracer concentration, thus avoiding the possible presence of gradients between inner and outer layers that can occur in a freshly incubated sample. Although incubation of previously frozen slices improves the accuracy of receptor binding studies (233, 234), the exposure to a thermal shock profoundly disrupts cellular biology and viability hampering the link between FDG uptake and glucose metabolism. In this line, preliminary freezing can be considered as a tool to estimate the contribution of unspecific tracer binding to the overall FDG distribution in analysed tissue. Cell tracer content eventually decreased to less than 15% in previously frozen slices with respect to values measured after incubation of the corresponding fresh specimen. On the contrary, preliminary freezing only modestly modified the radioactivity counts of necrotic and fibrotic regions. Thus, the selectivity of thermal shock effect documents that contamination from unspecific tracer binding plays a minor role in overall AAA FDG uptake. This finding extends previous observations reporting a high tracer uptake in acellular calcified regions in aortic specimens previously submitted to snap freezing (206). In this line, tracer uptake in

AAAwalls reflects both specific (metabolic) and unspecific binding mechanisms. The relative contribution of these two different pathways varies according to the stage of the lesion and thus to its cell density.

Aortic dilatation remains most often asymptomatic throughout its progression until it reaches a size that requires intervention. This usually precludes obtaining fresh specimens of uncomplicated AAA in earlier disease stages. Therefore, we cannot extend the present observations to describe the natural history of AAA progression. Similarly, the present study does not elucidate the potential of PET/ CT imaging of FDG distribution in predicting aneurysm inflammation and risk of rupture in patients with aneurysms of relatively smaller size presenting with suspicious but non-diagnostic clinical features.

However, the present study was planned to identify the biological mechanisms underlying FDG uptake in uncomplicated, asymptomatic AAA. In this line, the consistent nature of our findings, as well as their agreement with clinical studies in larger populations (226), permit us to explain the reason why asymptomatic patients with a relatively large aneurysm most often present an extremely low FDG uptake at PET imaging.

In the present study, immunohistochemical evaluation of diseased aorta did not include CD68 staining to recognize macrophage infiltration. This selection was motivated by the evidence that the large majority of infiltrating cells (>80%) were lymphocytes. This finding agrees with the inclusion criteria that aimed to exclude patients with suspected AAA inflammation. In this line, the evidence of such a large lymphocyte presence in asymptomatic AAA suggests these cells play a role in the natural history of the disease, even in phases not characterized by active inflammation.

Finally, the heterogeneous nature of cell populations in AAA specimens might partially reduce the agreement of data collected from different slices. This procedure was motivated by the fact that the short half-life of  $^{18}\text{F}$  implies an almost immediate

imaging of its distribution, while immunohistochemistry requires a long fixation time to obtain accurate image definition. To improve the accuracy of the coregistration procedure, great care was paid to ensure the contiguity of the slices submitted to autoradiography and immunohistochemistry. As a result, the correlation between tracer concentration and cell density was indeed robust enough as to document that FDG retention is modulated by its well-known determinants, i.e. local glucose uptake as an indirect index of cell density and metabolic activation.

## **6.9 Conclusion**

In conclusion, our results suggest that FDG uptake is most often very low and does not result in either hot spots or diffuse tracer retention in asymptomatic patients with AAA of diameter close to surgical indications.

The possible accuracy of metabolic imaging in patients with relatively smaller AAA cannot be defined by the present data and remains an open question.

AAA is the end result of a multifactorial process that is characterized by the progressive loss of cell populations associated with an irreversible remodelling of the arterial connective tissue eventually culminating in aortic rupture. These pathways are extremely complex and probably vary in the different disease stages. According to this concept, in AAAs whose size reaches a relatively large diameter, cell density is decreased to levels so low as to prevent any visible FDG uptake.

The match between FDG behaviour and cell density confirms this concept and offers a good explanation of the extremely low prevalence of “positive” PET/CT scans in these patients. Obviously, this pathological picture is just one snapshot in time and may not be representative of all pathophysiological mechanisms underlying aortic rupture or progressive dilatation. These data therefore corroborate the concept that PET/CT imaging might not represent an accurate screening tool to identify rupture risk in these asymptomatic patients. In particular, the profound agreement between cell density and FDG uptake suggests that care should be taken in considering a negative PET scan as an index of low risk. As AAA diameter enlarges, in fact, the marked loss of cells and tissue structure within the diseased walls might increase the risk of rupture caused by mechanical stressors and amplified by aortic dilatation.

## References

1. Patel, M.I., D.T.A. Hardman, C.M. Fisher, and M. Appleberg. Current views on the pathogenesis of abdominal aortic aneurysms. *J. Am. Col. Surg.* 181:371–382, 1995.
2. Iribarren, C., Darbinian, J. A., Go, A. S., Fireman, B. H., Lee, C. D., and Grey, D.P. Traditional and Novel Risk Factors for Clinically Diagnosed Abdominal Aortic Aneurysm: The Kaiser Multiphasic Health Checkup Cohort Study. *Annals of Epidemiology*, 17: 669-678, 2007.
3. Varulaki K.A, Walker N.M, Day N.E, Duffy S.W, Ashton H.A, Scott R.A.P. Quantifying the risks of hypertension, age, sex and smoking in patients with abdominal aortic aneurysm. *BJS* 2000;87:195-200
4. Acosta S, Ogren M, Bergqvist D, Lindbald B, Dencker M, Zdanowski Z. The Hardman index in patients operated on for ruptured abdominal aortic aneurysm: a systematic review. *J VascSurg* 2006;44:949-54
5. Sakalihasan N, Limet R, Defawe O.D. Abdominal Aortic Aneurysm. *Lancet* 2005; 365:1577-89
6. The UK Small Aneurysm Trial Participants, with Brown L.C AND Powell J.T. Risk factors for aneurysm rupture in patients kept under ultrasound surveillance. *Annals of Surgery* 1999;230:289-97
7. Multicentre Aneurysm Screening Study Group. The Multicentre Aneurysm Screening Study (MASS) into the effect of abdominal aortic aneurysm screening on mortality in men: a randomised controlled trial. *The Lancet* 2002;360:1531-39
8. Heller J.A, Weinberg A, Arons R, Krishnasastri K.V, Lyon R.T, Deitch J.S, Schulick A.H, Bush H.L Jr, Kent K.C. Two decades of abdominal aortic aneurysm repair: have we made any progress? *J Vasc Surg.* 2000;32:1091-100.
9. Lederle F.A, Wilson S.E, Johnson G.R, Reinke D.B, Littooy F.N, Acher C.W, Ballard D.J, Messina L.M, Gordan I.L, Chute E.P, Krupski W.C, Bandyk D, for the Aneurysm Detection and Management Veterans Affairs Cooperative Study Group, Immediate repair with surveillance of small abdominal aortic aneurysms. *N Engl J Med* 2002;346:1437-44
10. Kniemeyer H.W, Kessler T, Reber P.U, Ris H.B, Hakki H and Widmer M.K, Treatment of ruptured abdominal aortic aneurysm, a permanent challenge or a waste of resources? Prediction of outcome using a multi-organ-dysfunction score. *Eur J Vasc Endovasc Surg* 2000;19:190–196.

11. Ogata T, MacKean G.L, Cole C.W, Arthur C, Andreou P, Tromp G, Kuivaniemi H. The lifelong prevalence of abdominal aortic aneurysms among siblings of aneurysm patients is eightfold higher among siblings of spouses: An analysis of 187 aneurysm families in Nova Scotia, Canada. *J Vasc Surg* 2005;42:891-7
12. Wanhinen A, Bergqvist D, Boman K, Nilsson T.K, Rutegard Jorgen, Bjorck M. Risk factors associated with abdominal aortic aneurysm: A population-based study with historical and current data. *J Vasc Surg* 2005;41:390-6
13. Multicentre Aneurysm Screening Study Group. Multicentre aneurysm screening study (MASS): cost effectiveness analysis of screening for abdominal aortic aneurysms based on four year results from randomised controlled trial. *BMJ* 2002;325:1135
14. Norman P.E, Golledge J. Screening for Abdominal Aortic Aneurysms: More Benefit than Cost. *Eur J Vasc Endovasc Surg* 2006
15. The United Kingdom Small Aneurysm Trial Participants. Long-term outcomes of immediate repair compared with surveillance of small abdominal aortic aneurysms. *N Engl J Med* 2002;346:1445-52
16. Forsdahl S.H, Singh K, Solberg S, Jacobsen B.K. Risk factors for abdominal aortic aneurysms: a 7-year prospective study: the Tromso Study, 1994-2001. *Circulation* 2009 ; 119:2202-8.
17. Cole S, Walker R. and Norris R, Vascular laboratory practise IPEM, The Society for Vascular Technology of Great Britain and Ireland (2001) 42–67.
18. Cho B.S, Woodrum D.T, Roelofs K.J, Stanley J.C Differential Regulation of Aortic Growth in Male and Female Rodents Is Associated With AAA Development *Journal of Surgical Research* 2009;155: 330-338
19. DeRubertis B, Trocciola S, Ryer E et al Abdominal aortic aneurysm in women: Prevalence, risk factors, and implications for screening *J Vasc Surg* 2007;46:630-5
20. Solberg S, Singh K, Wilsgaard T, Jacobsen B.K. Increased growth rate of abdominal aortic aneurysms in women. The Tromsø study. *Eur J Vasc Endovasc Surg.* 2005; 29:145- 9.
21. Dillavou E.D, Muluk S.C, Makaroun M.S. A decade of e in abdominal aortic aneurysm repair in the United States: Have we improved outcomes equally between men and women? *J Vasc Surg* 2006;43:230-8
22. Harthun N.L, Current issues in the treatment of women with abdominal aortic aneurysms. *Gender Medicine* 2008;5:36-43

23. Katz D.J, Stanley J.C, Zelenock. Gender differences in abdominal aortic aneurysm prevalence, treatment and outcome. *J Vasc Surg* 1997;25:561-8
24. Brown P.M, Zelt D.T, Sobolev B. The risk of rupture in untreated aneurysms: the impact of size, gender, and expansion rate. *J Vasc Surg.* 2003; 37(2):280-4.
25. Astrand H, Ryden-Ahlgren A, Sandgren T, Lanne T. Age-related increase in wall stress of the human abdominal aorta: An in vivo study. *J Vasc Surg* 2005;42:926-31
26. Lederle F.A The natural history of abdominal aortic aneurysm. *Acta Chir Belg.* 2009; 109:7-12.
27. Alcorn H.G, Wolfson S.K, Sutton-Tyrrell K, Kuller L.H, O'Leary D. Risk factors for abdominal aortic aneurysms in older adults enrolled in the cardiovascular health study. *Arteriosclerosis, Thrombosis and Vascular Biology* 1996;16:963
28. Lee A.J, Fowkes F.G.R, Carson M.N, Leng G.C, Allant P.L. Smoking, atherosclerosis and risk of abdominal aortic aneurysm. *Eur Heart J* 1997;18:671-76
29. Blanchard J.F, Armenian H.K, Poulter Friesen P. Risk factors for abdominal aortic aneurysm: results of a case-control. *AJE* 2000;151:575-83
30. Wilmsink T.B.M, Quick C, Day NE. The association between cigarette smoking and abdominal aortic aneurysms. *Jour Vasc Surg* 1999;30:1099-1105
31. Bergoeing M.P, Arif B, Hackmann A.E, et al. Cigarette smoking increases aortic dilation without effecting matrix metalloproteinase -9 and -12 expression in a modified mouse model of aneurysm formation. *J of Vasc Surg* 2007;45:1217-1227
32. Brady A.R, Thompson S.G, Fowkes G.R, Greenhalgh R.M, Powell J.T on behalf of the UK Small Aneurysm Trial Participants. Abdominal aortic aneurysm expansion: Risk factors and time intervals for surveillance. *Circulation* 2004;110:16-21
33. Lederle F.A, Nelson D.B, Joseph A.M,. Smokers' relative risk for aortic aneurysm compared with other smoking-related diseases: A systematic review. *J Vasc Surg* 2003;38:329-34
34. Martini F.H, Natl J.L. *Fundamentals of Anatomy and Physiology.* Eighth edition 2009
35. Tortora G.J. *Principles of Human Anatomy* 2002



36. Sandford R.M., Bown M.J, London N.J and Sayers R.D The Genetic Basis of Abdominal Aortic Aneurysms: A Review *European Journal of Vascular and Endovascular Surgery* 2007;33:381-390
37. Daugherty A. and Cassis L.A, Mechanisms of abdominal aortic aneurysm formation, *Curr Atheroscler* 2002;4: 222-227
38. Kaschina E, Scholz H, Steckelings U.M, Sommerfeld M, Kemnitz U.R, Artuc M, Schmidt S, Unger T. Transition from atherosclerosis to aortic aneurysm in humans coincides with an increased expression of RAS components *Atherosclerosis*. 2009;205: 396-403.
39. Choke E et al. Whole genome-expression profiling reveals a role for immune and inflammatory response in abdominal aortic aneurysm rupture. *Eur J Vasc Endovasc Surg*. 2009;37:305-310
40. Wilson W.R, Anderton M., Schwalbe E.C, Jones J.L, Furness P.N and Bell P.R et al. Matrix metalloproteinase-8 and -9 are increased at the site of abdominal aortic aneurysm rupture *Circulation* 2006;113:438–445.
41. Shantikumar S, Ajjan R, Porter K.E, Scott D.J.A. Diabetes and the Abdominal Aortic Aneurysm. *Euro J of Vasc and Endovasc Surgery* 2010;39:200-207
42. Shiraya S, Miwa K and Aoki M et al. Hypertension accelerated experimental abdominal aortic aneurysm through upregulation of nuclear factor B and Ets. *Hypertension* 2006;48:628-36.
43. Truijers M., Pol J.A, SchultzeKool L.J, Van Sterkenburg S.M, Fillinger M.F and Blankensteijn J.D Wall Stress Analysis in Small Asymptomatic, Symptomatic and Ruptured Abdominal Aortic Aneurysms *European Journal of Vascular and Endovascular Surgery*, 2007;33:401-407
44. Kobayashi H. Matsushita M. Oda K. Nishikimi N. Sakurai T. The effects of atherosclerotic plaque on the enlargement of an experimental model of abdominal aorticaneurysms in rabbits. *Eur J of Vasc and Endovasc Surg* 2004;28:71-78
45. Lindholt J.S, Heegaard N.H.H, Vammen S. et al. Smoking , but not Lipids, Lipoprotein (A) and Antibodies Against Oxidised LDL, is Correlated in the Expansion of Abdominal Aortic Aneurysms. *Eur J Vasc and Endovasc Surg* 2001;21:51-56
46. Ferguson D.C, Clancy P, Brouke B, Walker P.J et al. Association of statin prescription with small abdominal aortic aneurysm progression. *American Heart Jour* 2010;159:307- 313

47. Hobbs S.D, Claridge M.W.C, Quick C.R.G, Day N.E, et al. LDL cholesterol is associated with small abdominal aortic aneurysms. *Eur J Vasc Endovasc Surg* 2003;26:618-622
48. Rizzo M, Kryenbuhl P.A, Pernice V et al. LDL size and subclasses in patients with abdominal aortic aneurysm *Int J of Card* 2009;134:406-408
49. Golledge J, Van Bockxmeer F, Jamrozik K, Mc Cann M, Norman P.E. Association between serum lipid proteins and abdominal aortic aneurysms *Am J Cardiol* 2010;105:1480-4
50. Vega de Ceniga M, Gomez R, Estallo L et al. Growth rate and associated factors in small abdominal aortic aneurysms. *Eur J Vasc Endovasc Surg* 2006;31:231-6
51. Norman P.E, Davis, W.A, Coughlan M.T, Forbes J.M, Golledge J, Davis T.M. Serum carboxymethyllysine concentrations are reduced in diabetic men with abdominal aortic aneurysms: Health in men study. *J of Vasc Surg* 2009;50:626-631
52. Miyama N, Dua M.M, Yeung J.J, et al. Hyperglycemia limits experimental aortic aneurysm progression. *J Vasc Surg* July 2010
53. Brady AR, Thompson SG, Fowkes FG, Greenhalgh RM, Powell JT. Abdominal aortic aneurysm expansion: risk factors and time intervals for surveillance. *Circulation*. 2004;110(1):16-21.
54. Mofidi R, Goldie VJ, Kelman J, Dawson AR, Murie JA, Chalmers RT. Influence of sex on expansion rate of abdominal aortic aneurysms. *Br J Surg*. 2007;94(3):310-314.
55. Thompson AR, Cooper JA, Ashton HA, Hafez H. Growth rates of small abdominal aortic aneurysms correlate with clinical events. *Br J Surg*. 97(1):37-44.
56. Schlosser FJ, Tangelder MJ, Verhagen HJ, van der Heijden GJ, Muhs BE, van dominal der Graaf Y, Moll FL. Growth predictors and prognosis of small abaortic aneurysms. *J Vasc Surg*. 2008;47(6):1127-1133. 78.
57. Schouten O, van Laanen JH, Boersma E, Vidakovic R, Feringa HH, Dunkelgrun M, Bax JJ, Koning J, van Urk H, Poldermans D. Statins are associated with a reduced infrarenal abdominal aortic aneurysm growth. *Eur J Vasc Endovasc Surg*. 2006;32(1):21-26.
58. Mortality results for randomised controlled trial of early elective surgery or ultrasonographic surveillance for small abdominal aortic aneurysms. The UK Small Aneurysm Trial Participants. *Lancet*. 1998;352(9141):1649-1655.

59. Santilli SM, Littooy FN, Cambria RA, Rapp JH, Tretinyak AS, d'Audiffret AC, Kuskowski MA, Roethle ST, Tomczak CM, Krupski WC. Expansion rates and outcomes for the 3.0-cm to the 3.9-cm infrarenal abdominal aortic aneurysm. *J Vasc Surg.* 2002;35(4):666-671.
60. Norman P, Spencer CA, Lawrence-Brown MM, Jamrozik K. C-reactive protein levels and the expansion of screen-detected abdominal aortic aneurysms in men. *Circulation.* 2004;110(7):862-866.
61. Chang JB, Stein TA, Liu JP, Dunn ME. Risk factors associated with rapid growth of small abdominal aortic aneurysms. *Surgery.* 1997;121(2):117-122.
62. Couto E, Duffy SW, Ashton HA, Walker NM, Myles JP, Scott RA, Thompson d SG. Probabilities of progression of aortic aneurysms: estimates and implications for screening policy. *J Med Screen.* 2002;9(1):40-42.
63. Hackam DG, Thiruchelvam D, Redelmeier DA. Angiotensin-converting enzyme inhibitors and aortic rupture: a population-based case-control study. *Lancet.* 2006;368(9536):659-665.
64. Sweeting MJ, Thompson SG, Brown LC, Greenhalgh RM, Powell JT. Use of angiotensin converting enzyme inhibitors is associated with increased growth rate of abdominal aortic aneurysms. *J Vasc Surg.* 52(1):1-4.
65. Long-term outcomes of immediate repair compared with surveillance of small abdominal aortic aneurysms. *N Engl J Med.* 2002;346(19):1445-1448.
66. Lederle FA, Johnson GR, Wilson SE, Ballard DJ, Jordan WD, Jr., Blebea J, Littooy FN, Freischlag JA, Bandyk D, Rapp JH, Salam AA. Rupture rate of large abdominal aortic aneurysms in patients refusing or unfit for elective repair. *JAMA.* 2002;287(22):2968-2972.
67. Heikkinen M, Salenius JP, Auvinen O. Ruptured abdominal aortic aneurysm in a well-defined geographic area. *J Vasc Surg.* 2002;36(2):291-296.
68. Wilson KA, Lee AJ, Hoskins PR, Fowkes FG, Ruckley CV, Bradbury AW. The relationship between aortic wall distensibility and rupture of infrarenal abdominal aortic aneurysm. *J Vasc Surg.* 2003;37(1):112-117.
69. McPhee JT, Hill JS, Eslami MH. The impact of gender on presentation, therapy, and mortality of abdominal aortic aneurysm in the United States, 2001-2004. *J Vasc Surg.* 2007;45(5):891-899.
70. Warrell D.A, Cox T.M, Firth J.D *Oxford Textbook of Medicine Vol 2* Fifth edition 2010

71. Sprouse L.R , Meier G.H, Parent F.N, DeMasi R.J, Glickman M.H and Barber G.A. Is Ultrasound More Accurate than Axial Computed Tomography for Determination of Maximal Abdominal Aortic Aneurysm Diameter? *Eur J Vasc Endovasc Surg.* 2004;28:28-35
72. C. Fleming, E.P. Whitlock, T.L. Beil and F.A. Lederle, Screening for abdominal aortic aneurysm: a best-evidence systematic review for the U.S. preventive services task force, *Ann Intern Med* 142 (3) (2005), pp. 203–211.
73. J.S. Lindholt, S. Vammen, S. Juul, E.W. Henneberg and H. Fasting, The validity of ultrasonographic scanning as screening method for abdominal aortic aneurysm, *Eur J Vasc Endovasc Surg* 17 (6) (1999), pp. 472–475.
74. Sandford R.M, Bown M.J, Fishwick G et al. Duplex ultrasound is reliable in detection of Endoleak following endovascular aneurysm repair. *Euro J of Vasc and Endovas Surg* 2006;32:537-541
75. Pages S., Favre J.P, Cerisier A. Comparison for colour duplex ultrasound and computed tomography scan for surveillance after aortic endografting. *Annals of Vasc Surg* 2001;15:155-162
76. Collins J.T, Boros M.J, Combs K. Ultrasound surveillance of endovascular aneurysm repair: A safe modality verses computed tomography. *Annals of Vasc Surg* 2007;21:671- 675
77. Sprouse R , Meier G., LeSar C, DeMasi R., Sood J, Parent F, Marcinyzck M and Gayle R. Comparison of abdominal aortic aneurysm diameter measurements obtained with ultrasound and computed tomography: is there a difference? *J Vasc Surg.* 2003;38:466- 71
78. *Phelps ME. PET: the merging of biology and imaging into molecular imaging. J Nucl Med* 2000;41:661-81.
79. *Hustinx R, Bénard F, Alavi A. Whole-body imaging in the management of patients with cancer. Semin Nucl Med* 2002;32: 35-46.
80. *Strauss LG. Fluorine-18 deoxyglucose and false-positive results: a major problem in the diagnostics of oncological patients. Eur J Nucl Med* 1996;23:1409-15.
81. *Zhuang H, Alavi A. 18-fluorodeoxyglucose positron emission tomographic imaging in the detection and monitoring of infection and inflammation. Semin Nucl Med* 2002;32:47-59.
82. *Belhocine T, Blockmans D, Hustinx R, Vandevivere J, Mortelmans L. Imaging of large vessel vasculitis with (18)FDG PET: illusion or reality? A critical review of the literature data. Eur J Nucl Med Mol Imaging* 2003;30:1305-13.

83. Wasse'lius J, Malmstedt J, Kalin B, Larsson S, Sundin A, Hedin U, et al. *High 18F-FDG uptake in synthetic aortic vascular grafts on PET/CT in symptomatic and asymptomatic patients. J Nucl Med* 2008;49:1601-5.
84. Yun M, Jang S, Cucchiara A, Newberg A, Alavi A. *18F FDG uptake in the large arteries: a correlation study with the atherogenic risk factors. Semin Nucl Med* 2002;32:70-6.
85. Yun M, Yeh D, Araujo LI, Jang S, Newberg A, Alavi A. *F-18 FDG uptake in the large arteries: a new observation. Clin Nucl Med* 2001 Apr;26(4):314-9.
86. Zhao S, Kuge Y, Tsukamoto E, Mochizuki T, Kato T, Hikosaka K, et al. *Fluorodeoxyglucose uptake and glucose transporter expression in experimental inflammatory lesions and malignant tumours: effects of insulin and glucose loading. Nucl Med Commun* 2002;23:545-50.
87. Wu Y-W, Kao H-L, Chen M-F, Lee B-C, Tseng WY, Jeng JS, et al. *Characterization of plaques using 18F-FDG PET/CT in patients with carotid atherosclerosis and correlation with matrix metalloproteinase-1. J Nucl Med* 2007;48:227-33.
88. Tahara N, Kai H, Ishibashi M, Nakaura H, Kaida H, Baba K, et al. *Simvastatin attenuates plaque inflammation. J Am Coll Cardiol* 2006;48:1825-31.
89. Rudd JH, Warburton EA, Fryer TD, Jones HA, Clark JC, Antoun N, Johnstro'm P, et al. *Imaging atherosclerotic plaque inflammation with [18F] fluorodeoxyglucose positron emission tomography. Circulation* 2002;105:2708-11.
90. Sakalihasan N, Van Damme H, Gomez P, Rigo P, Lapiere CM, Nusgens B, Limet R. *Positron emission tomography (PET) evaluation of abdominal aortic aneurysm (AAA). Eur J Vasc Endovasc Surg* 2002;23:431-6.
91. Defawe OD, Hustinx R, Defraigne JO, Limet R, Sakalihasan N. *Distribution of F-18 fluorodeoxyglucose (F-18 FDG) in abdominal aortic aneurysm: high accumulation in macrophages seen on PET imaging and immunohistology. Clin Nucl Med* 2005 May; 30(5):340-1.
92. Khan, J. A., M. N. Abdul Rahman, et al. (2012). "Intraluminal thrombus has a selective influence on matrix metalloproteinases and their inhibitors (tissue inhibitors of matrix metalloproteinases) in the wall of abdominal aortic aneurysms." *Ann Vasc Surg* 26(3): 322-329.

93. Kim H.C. Park S.W. Nam K.W. Determination of accurate stent graft configuration in abdominal aortic aneurysm using computed tomography: a preliminary study. *Clinical imaging* 2010;34
94. Luan Z. Chase A.J, Newby A.C. *Statins inhibit the secretion on metalloproteinases -1, -2, -3 and - 9 in vascular smooth muscle cells and macrophages.* *Arterioscler Thromb Vasc Biol.* 2003;5: 769-775
95. Kajimoto K, Miyauchi K, Kasai T et al. Short-term 20-mg atorvastatin therapy reduces key inflammatory factors including c-Jun N-terminal kinase and dendritic cells and matrix metalloproteinase expression in human abdominal aortic aneurysmal wall. *Atherosclerosis* 2009;206;505-511
96. Hurks R, Hoefer I.E, Vink A. et al. Different effects of commonly prescribed statins on abdominal aortic aneurysm wall biology. *European Journal of Vascular and Endovascular Surgery* 2010;39:569-576
97. Eriksson I, Hallen A, Simonsson N, Aberg T. Surgical classification of abdominal aortic aneurysms. *Acta Chir Scand* 1979;145:455-458.
98. Powell JT, Brown LC, Forbes JF, Fowkes FG, Greenhalgh RM, Ruckley CV, Thompson SG. Final 12-year follow-up of surgery versus surveillance in the UK Small Aneurysm Trial. *Br J Surg* 2007;94:702-708.
99. Prinssen M, Verhoeven EL, Buth J, Cuypers PW, van Sambeek MR, Balm R, Buskens E, Grobbee DE, Blankensteijn JD. A randomized trial comparing conventional and endovascular repair of abdominal aortic aneurysms. *N Engl J Med* 2004;351:1607-1618.
100. Gibbons C BM, Jensen LP, Laustsen J, Lees T, Moreno-Carriles R, Troëng T, Wigger P, Beiles B, Thomsen I, Venermo M, Menyhei G, Palombo D, Halbakken E, Kinsman R, Walton P. *The second vascular surgery database report.* Henley-on-Thames: European Society for Vascular Surgery, 2008.
101. Steyerberg EW, Kievit J, de Mol Van Otterloo JC, van Bockel JH, Eijkemans MJ, Habbema JD. Perioperative mortality of elective abdominal aortic aneurysm surgery. A clinical prediction rule based on literature and individual patient data. *Arch Intern Med* 1995;155:1998-2004.
102. Wainess RM, Dimick JB, Cowan JA, Jr., Henke PK, Stanley JC, Upchurch GR, Jr. Epidemiology of surgically treated abdominal aortic aneurysms in the United States, 1988 to 2000. *Vascular* 2004;12:218-224.
103. Cowan JA, Jr., Dimick JB, Henke PK, Rectenwald J, Stanley JC, Upchurch GR, Jr. Epidemiology of aortic aneurysm repair in the United States from 1993 to 2003. *Ann N Y Acad Sci* 2006;1085:1-10.

104. Wanhainen A, Bylund N, Bjorck M. Outcome after abdominal aortic aneurysm repair in Sweden 1994-2005. *Br J Surg* 2008;95:564-570.
105. Greenhalgh RM, Brown LC, Kwong GP, Powell JT, Thompson SG. Comparison of endovascular aneurysm repair with open repair in patients with abdominal aortic aneurysm (EVAR trial 1), 30-day operative mortality results: randomized controlled trial. *Lancet* 2004;364:843-848.
106. Swedvasc. Annual Report 2008. Swedish Society for Vascular Surgery; Available at [www.karlkirurgi.com/swedvasc.aspx](http://www.karlkirurgi.com/swedvasc.aspx) 2008.
107. Valentine RJ, Decaprio JD, Castillo JM, Modrall JG, Jackson MR, Clagett GP. Watchful waiting in cases of small abdominal aortic aneurysms appropriate for all patients? *J Vasc Surg* 2000;32:441– 448.
108. Glimaker H, Hollmberg L, Elvin A, Nybacka O, Almgren B, Bjorck CG., Eriksson I. Natural history of patients with abdominal aortic aneurysm. *Eur J Vasc Surg* 1991;5:125-130.
109. Limet, R., N. Sakalihasan, and A. Albert. Determination of the expansion rate and the incidence of rupture of abdominal aortic aneurysms. *J. Vasc. Surg.* 14:540-548, 1991.
110. Martufi G , Di Martino ES, Amon CH, Muluk SC, Finol, EA, 2009, Three dimensional geometrical characterization of abdominal aortic aneurysms: image-based wall thickness distribution, *Journal of Biomechanical Engineering*, 131(6):061015.
111. Sacks, M.S., D.A. Vorp, M.L. Raghavan, M.P. Federle, and M.W. Webster. In vivo three- dimensional surface geometry of abdominal aortic aneurysms. *Ann. Biomed. Eng.* 27:469–479, 1999.
112. Shum J, Martufi G, Di Martino ES, Washington CB, Grisafi J, Muluk SC, Finol EA, 2011, Quantitative assessment of abdominal aortic aneurysm shape, *Annals of Biomedical Engineering*, 39(1):277-286.
113. Martufi, G., Auer, M., Roy, J., Swedenborg, J., Sakalihasan, N., Panuccio, G., and Gasser, T.C., 2012, " Growth of Small Abdominal Aortic Aneurysms: A multidimensional analysis", submitted to *Journal of Vascular Surgery*.
114. Stenbaek, J., Kalin, B., Swedenborg, J., 2000. Growth of thrombus may be a better predictor of rupture than diameter in patients with abdominal aortic aneurysms. *European Journal of Vascular & Endovascular Surgery* 20, 466–469.
115. J. Golledge, P. S. Tsao, R. L. Dalman, and P. E. Norman. Circulating markers of abdominal aortic aneurysm presence and progression. *Circulation*, 118(23):2382– 2392, 2008.

116. S. Urbonavicius, G. Urbonaviciene, B. Honore, E. W. Henneberg, H. Vorum, and J. S. Lindholt. *Potential circulating biomarkers for abdominal aortic aneurysm expansion and rupture - a systematic review. Eur. J. Vasc. Endovasc. Surg.*, 36 (3):273–280, 2008.
117. M. Nakamura, R. Tachieda, H. Niinuma, A. Ohira, S. Endoh, K. Hiramori, and S. Makita. *Circulating biochemical marker levels of collagen metabolism are abnormal in patients with abdominal aortic aneurysm. Angiology*, 51(5):385–392, 2000.
118. T. Vainas, T. Lubbers, F. R. Stassen, S. B. Herngreen, M. P. Dieijen-Visser, C. A. Bruggeman, P. J. Kitslaar, and G. W. Schurink. *Serum C-reactive protein level is associated with abdominal aortic aneurysm size and may be produced by aneurysmal tissue. Circulation*, 107(8):1103–1105, 2003.
119. J. S. Lindholt, S. Vammen, H. Fasting, E. W. Henneberg, and L. Heickendorff. *The plasma level of matrix metalloproteinase 9 may predict the natural history of small abdominal aortic aneurysms. A preliminary study. Eur. J. Vasc. Endovasc. Surg.*, 20(3):281–285, 2000.
120. G. Engstrom, G. Borner, B. Lindblad, L. Janzon, and F. Lindgarde. *Incidence of fatal or repaired abdominal aortic aneurysm in relation to inflammation-sensitive plasma proteins. Arterioscler. Thromb. Vasc. Biol.*, 24(2):337–341, 2004.
121. H. Domanovits, M. Schillinger, M. Mullner, T. Holzenbein, K. Janata, K. Bayegan, and A. N. Laggner. *Acute phase reactants in patients with abdominal aortic aneurysm. Atherosclerosis*, 163(2):297–302, 2002.
122. W. R. Wilson, M. Anderton, E. C. Choke, J. Dawson, I. M. Loftus, and M. M. Thompson. *Elevated plasma mmp1 and mmp9 are associated with abdominal aortic aneurysm rupture. Eur. J. Vasc. Endovasc. Surg.*, 35(5):580–584, 2008.
123. J. Hua and W. R. Mower. *Simple geometric characteristics fail to reliably predict abdominal aortic aneurysm wall stresses. J. Vasc. Surg.*, 34(2):308–315, 2001.
124. Fillinger, M.F, M.L. Raghavan, S. Marra, J. Cronenwett, and F.E. Kennedy. *In vivo analysis of mechanical wall stress and abdominal aortic aneurysm rupture risk. J. Vasc. Surg.* 36:589-597, 2002.
125. Gasser, T.C., Auer, M., Labruto, F., Swedenborg, J., Roy, J., (2010). *Biomechanical rupture risk assessment of abdominal aortic aneurysms: Model complexity versus predictability of finite element simulations. European Journal of Vascular & Endovascular Surgery* 40, 176-185.



126. Heng M.S., Fagan M.J., Collier W., Desai G., McCollum P.T., Chetter I.C., (2008). *Peak wall stress measurement in elective and acute abdominal aortic aneurysms. Journal of Vascular Surgery* (47), 17-22.
127. Venkatasubramaniam, A.K., M.J. Fagan, T. Mehta, K.J. Mylankal, B. Ray, G. Kuhan, I.C. Chetter, and P.T. McCollum. *A comparative study of aortic wall stress using finite element analysis for ruptured and non-ruptured abdominal aortic aneurysms. Europ. J. Vasc. Surg.* 28:168-176, 2004.
128. Fillinger, M.F., S.P. Marra, M.L. Raghavan, and F.E. Kennedy. *Prediction of rupture risk in abdominal aortic aneurysm during observation: wall stress versus diameter. J. Vasc. Surg.* 37:724-732, 2003
129. Vande Geest JP, Wang DHJ, Wisniewski SR, Makaroun MS, Vorp DA. *A noninvasive method for determination of patient-specific wall strength distribution in abdominal aortic aneurysms. Annals of Biomedical Engineering* 2006a;34:1098–1106.
130. Wang DHJ, Makaroun MS, Webster MW, Vorp DA. *Effect of intraluminal thrombus on wall stress in patient-specific models of abdominal aortic aneurysm. Journal of Vascular Surgery* 2002;36:598–604.
131. Di Martino, E.S., A. Bohra, J.P. Vande Geest, N. Gupta, M. Makaroun and D.A. Vorp. *Biomechanical properties of ruptured versus electively repaired abdominal aortic aneurysm wall tissue. J. Vasc. Surg.* 43:570-576, 2006.
132. Doyle BJ, Callanan A, Walsh MT, Grace PA, McGloughlin TM. *A finite element analysis rupture index (FEARI) as an additional tool for abdominal aortic aneurysm rupture prediction. Vasc Dis Prev.* 2009;6:114–121.
133. Forsell, C., Swedenborg, J., Roy J., Gasser, T. C., 2012. *The quasi-static failure properties of the Abdominal Aortic Aneurysm wall estimated by a mixed experimental-numerical approach. Annals of Biomedical Engineering. Submitted for publication.*
134. Raghavan, M.L., and Vorp, D.A., 2000, "Toward a Biomechanical Tool to Evaluate Rupture Potential of Abdominal Aortic Aneurysm: Identification of a Finite Strain Constitutive Model and Evaluation of Its Applicability," *Journal of Biomechanics*, 33, pp. 475-482.
135. Auer M, Gasser TC. *Reconstruction and finite element mesh generation of abdominal aortic aneurysms from computerized tomography angiography data with minimal user interactions. IEEE Trans Med Imaging* 2010 Apr;29(4):1022-8.

136. Shum, J., Xu, A., Chatnuntawech, I., Finol, E.A. A framework for the automatic generation of surface topologies for abdominal aortic aneurysm models. *Annals of Biomedical Engineering* 39 (1) :249-259
137. Shum, J., E. S. DiMartino, A. Goldhammer, D. Goldman, L. Acker, G. Patel, Julie H. Ng, Giampaolo Martufi, Finol, E.A. Semi-automatic vessel wall detection and quantification of wall thickness in CT images of human abdominal aortic aneurysms. *Med. Phys.* 37:638–648, 2010.
138. Scotti, C.M., Jimenez, J., Muluk, S.C., and Finol, E.A., 2008, "Wall Stress and Flow Dynamics in Abdominal Aortic Aneurysms: Finite Element Analysis vs. Fluid-Structure Interaction," *Computer Methods in Biomechanics and Biomedical Engineering*, 11(3), pp. 301-322.
139. Shahrokh Zeinali-Davarani , Azadeh Sheidaei & Seungik Baek 2011. A finite element model of stress-mediated vascular adaptation: application to abdominal aortic aneurysms. *Computer Methods in Biomechanics and Biomedical Engineering* 14:9, 803-817.
140. Gahring, L. C. and S. W. Rogers (2005). "Neuronal nicotinic acetylcholine receptor expression and function on nonneuronal cells." *AAPS J* 7(4): E885-894.
141. Murphy, E. A., D. Danna-Lopes, et al. (1998). "Nicotine-stimulated elastase activity release by neutrophils in patients with abdominal aortic aneurysms." *Ann Vasc Surg* 12(1): 41-45
142. Raveendran, M., J. Wang, et al. (2005). "Endogenous nitric oxide activation protects against cigarette smoking induced apoptosis in endothelial cells." *FEBS Lett* 579(3): 733-740.
143. Hsu, C. L., Y. L. Wu, et al. (2009). "Ginkgo biloba extract confers protection from cigarette smoke extract-induced apoptosis in human lung endothelial cells: Role of heme oxygenase-1." *Pulm Pharmacol Ther* 22(4): 286-296.
144. Li, M., D. Yu, et al. (2010). "Tobacco smoke induces the generation of procoagulant microvesicles from human monocytes/macrophages." *Arterioscler Thromb Vasc Biol* 30(9): 1818-1824.
145. Jiang, X., D. H. Rowitch, et al. (2000). "Fate of the mammalian cardiac neural crest." *Development* 127(8): 1607-1616.
146. Majesky, M. W. (2007). "Developmental basis of vascular smooth muscle diversity." *Arterioscler Thromb Vasc Biol* 27(6): 1248-1258.

147. Ahmed, M. M. (1968). "Microscopic anatomy and the attenuation of elastic tissue in the aortic wall of slow loris (*Nycticebus coucang coucang*)."  
*Folia Primatol (Basel)* 8(3): 290-300.
148. Halloran, B. G. and B. T. Baxter (1995). "Pathogenesis of aneurysms."  
*Semin Vasc Surg* 8(2): 85-92.
149. Astrand, H., A. Ryden-Ahlgren, et al. (2005). "Age-related increase in wall stress of the human abdominal aorta: an in vivo study." *J Vasc Surg* 42(5): 926-931.
150. Kazi, M., J. Thyberg, et al. (2003). "Influence of intraluminal thrombus on structural and cellular composition of abdominal aortic aneurysm wall." *J Vasc Surg* 38(6): 1283-1292.
151. Mayranpaa, M. I., J. A. Trosien, et al. (2009). "Mast cells associate with neovessels in the media and adventitia of abdominal aortic aneurysms." *J Vasc Surg* 50(2): 388-395; discussion 395-386.
152. Sakalihasan, N., R. Limet, et al. (2005). "Abdominal aortic aneurysm." *Lancet* 365(9470): 1577-1589.
153. Dobrin, P. B., W. H. Baker, et al. (1984). "Elastolytic and collagenolytic studies of arteries. Implications for the mechanical properties of aneurysms." *Arch Surg* 119(4): 405-409.
154. Rucker, R. B. and D. Tinker (1977). "Structure and metabolism of arterial elastin." *Int Rev Exp Pathol* 17: 1-47.
155. Jacob, M. P. (2003). "Extracellular matrix remodeling and matrix metalloproteinases in the vascular wall during aging and in pathological conditions." *Biomed Pharmacother* 57(5-6): 195-202.
156. Fontaine, V., Z. Touat, et al. (2004). "Role of leukocyte elastase in preventing cellular re-colonization of the mural thrombus." *Am J Pathol* 164(6): 2077-2087.
157. Liu, J., G. K. Sukhova, et al. (2005). "Cathepsin L expression and regulation in human abdominal aortic aneurysm, atherosclerosis, and vascular cells." *Atherosclerosis*.
158. Herron, G. S., E. Unemori, et al. (1991). "Connective tissue proteinases and inhibitors in abdominal aortic aneurysms. Involvement of the vasa vasorum in the pathogenesis of aortic aneurysms." *Arterioscler Thromb* 11(6): 1667-1677.

159. Pearce, W. H. and V. P. Shively (2006). "Abdominal aortic aneurysm as a complex multifactorial disease: interactions of polymorphisms of inflammatory genes, features of autoimmunity, and current status of MMPs." *Ann N Y Acad Sci* 1085: 117-132.
160. Allaire, E., F. Schneider, et al. (2009). "New insight in aetiopathogenesis of aortic diseases." *Eur J Vasc Endovasc Surg* 37(5): 531-537.
161. Petersen, E., F. Wagberg, et al. (2002). "Serum concentrations of elastin-derived peptides in patients with specific manifestations of atherosclerotic disease." *Eur J Vasc Endovasc Surg* 24(5): 440-444.
162. Satta, J., A. Laurila, et al. (1998). "Chronic inflammation and elastin degradation in abdominal aortic aneurysm disease: an immunohistochemical and electron microscopic study." *Eur J Vasc Endovasc Surg* 15(4): 313-319
163. Hance, K. A., M. Tataria, et al. (2002). "Monocyte chemotactic activity in human abdominal aortic aneurysms: role of elastin degradation peptides and the 67-kD cell surface elastin receptor." *J Vasc Surg* 35(2): 254-261.
164. Cohen, J. R., C. Mandell, et al. (1988). "Elastin metabolism of the infrarenal aorta." *J Vasc Surg* 7(2): 210-214.
165. Chiou, A. C., B. Chiu, et al. (2001). "Murine aortic aneurysm produced by periarterial application of calcium chloride." *J Surg Res* 99(2): 371-376.
166. Panek, B., M. Gacko, et al. (2004). "Metalloproteinases, insulin-like growth factor-I and its binding proteins in aortic aneurysm." *Int J Exp Pathol* 85(3): 159-164.
167. Elmore, J. R., B. F. Keister, et al. (1998). "Expression of matrix metalloproteinases and TIMPs in human abdominal aortic aneurysms." *Ann Vasc Surg* 12(3): 221-228.
168. Carmo, M., L. Colombo, et al. (2002). "Alteration of elastin, collagen and their crosslinks in abdominal aortic aneurysms." *Eur J Vasc Endovasc Surg* 23(6): 543-549.
169. Abdul-Hussien, H., R. G. Soekhoe, et al. (2007). "Collagen degradation in the abdominal aneurysm: a conspiracy of matrix metalloproteinase and cysteine collagenases." *Am J Pathol* 170(3): 809-817.
170. Lindeman, J. H., B. A. Ashcroft, et al. (2010). "Distinct defects in collagen microarchitecture underlie vessel-wall failure in advanced abdominal aneurysms and aneurysms in Marfan syndrome." *Proc Natl Acad Sci U S A* 107(2): 862- 865.

171. Cohen, J. R., L. Keegan, et al. (1991). "Neutrophil chemotaxis and neutrophil elastase in the aortic wall in patients with abdominal aortic aneurysms." *J Invest Surg* 4(4): 423-430.
172. Schmidt, W., R. Egbring, et al. (1975). "Effect of elastase-like and chymotrypsin-like neutral proteases from human granulocytes on isolated clotting factors." *Thromb Res* 6(4): 315-329.
173. Nilsson, I. M., L. Holmberg, et al. (1980). "Characteristics of the factor VIII protein and Factor XIII in various factor VIII concentrates." *Scand J Haematol* 24(4): 340- 349.
174. Cohen, A. B. and H. L. James (1982). "Reduction of the elastase inhibitory capacity of alpha 1-antitrypsin by peroxides in cigarette smoke: an analysis of brands and filters." *Am Rev Respir Dis* 126(1): 25-30.
175. Li, Z., S. Alam, et al. (2009). "Oxidized {alpha}1-antitrypsin stimulates the release of monocyte chemotactic protein-1 from lung epithelial cells: potential role in emphysema." *Am J Physiol Lung Cell Mol Physiol* 297(2): L388-400.
176. Kolev, K., E. Komorowicz, et al. (1996). "Quantitative comparison of fibrin degradation with plasmin, miniplasmin, neutrophil leukocyte elastase and cathepsin G." *Thromb Haemost* 75(1): 140-146.
177. Golledge, J., R. Muller, et al. (2011). "Evaluation of the diagnostic and prognostic value of plasma D-dimer for abdominal aortic aneurysm." *Eur Heart J* 32(3): 354-364.
178. Kohno, I., K. Inuzuka, et al. (2000). "A monoclonal antibody specific to the granulocyte-derived elastase-fragment D species of human fibrinogen and fibrin: its application to the measurement of granulocyte-derived elastase digests in plasma." *Blood* 95(5): 1721-1728.
179. Gombas, J., K. Kolev, et al. (2004). "Impaired fibrinolytic potential related to elevated alpha1-proteinase inhibitor levels in patients with pulmonary thromboembolism." *Ann Hematol* 83(12): 759-763.
180. Louwrens, H. D., H. C. Kwaan, et al. (1995). "Plasminogen activator and plasminogen activator inhibitor expression by normal and aneurysmal human aortic smooth muscle cells in culture." *Eur J Vasc Endovasc Surg* 10(3): 289-293.
181. Shiomi, T., V. Lemaitre, et al. (2010). "Matrix metalloproteinases, a disintegrin and metalloproteinases, and a disintegrin and metalloproteinases with thrombospondin motifs in non-neoplastic diseases." *Pathol Int* 60(7): 477-496.

182. Allaire, E., D. Hasenstab, et al. (1998). "Prevention of aneurysm development and rupture by local overexpression of plasminogen activator inhibitor *Circulation* 98(3): 249-255.
183. Brew, K. and H. Nagase (2010). "The tissue inhibitors of metalloproteinases (TIMPs): an ancient family with structural and functional diversity." *Biochim Biophys Acta* 1803(1): 55-71.
184. Lipp, C., F. Lohoefer, et al. (2012). "Expression of a disintegrin and metalloprotease in human abdominal aortic aneurysms." *J Vasc Res* 49(3): 198-206.
185. Eskandari, M. K., J. D. Vijungco, et al. (2005). "Enhanced abdominal aortic aneurysm in TIMP-1-deficient mice." *J Surg Res* 123(2): 289-293.
186. Choke, E., M. M. Thompson, et al. (2006). "Abdominal aortic aneurysm rupture is associated with increased medial neovascularization and overexpression of proangiogenic cytokines." *Arterioscler Thromb Vasc Biol* 26(9): 2077-2082.
187. Fernandez, C. A., L. Yan, et al. (2005). "The matrix metalloproteinase-9/neutrophil gelatinase-associated lipocalin complex plays a role in breast tumor growth and is present in the urine of breast cancer patients." *Clin Cancer Res* 11(15): 5390- 5395.
188. Edwards, D. R., M. M. Handsley, et al. (2008). "The ADAM metalloproteinases." *Mol Aspects Med* 29(5): 258-289.
189. Hiraoka, Y., K. Yoshida, et al. (2008). "Ectodomain shedding of TNF- $\alpha$  is enhanced by nardilysin via activation of ADAM proteases." *Biochem Biophys Res Commun* 370(1): 154-158.
190. Locksley, R. M., N. Killeen, et al. (2001). "The TNF and TNF receptor superfamilies: integrating mammalian biology." *Cell* 104(4): 487-501.
191. Satoh, H., M. Nakamura, et al. (2004). "Expression and localization of tumour necrosis factor- $\alpha$  and its converting enzyme in human abdominal aortic aneurysm." *Clin Sci (Lond)* 106(3): 301-306.
192. Scheller, J., A. Chalaris, et al. (2011). "ADAM17: a molecular switch to control inflammation and tissue regeneration." *Trends Immunol* 32(8): 380-387.
193. Lohoefer, F., C. Reeps, et al. (2012). "Histopathological analysis of cellular localization of cathepsins in abdominal aortic aneurysm wall." *Int J Exp Pathol* 93(4): 252- 258.
194. Shi, G. P. (2007). "Role of cathepsin C in elastase-induced mouse abdominal aortic aneurysms." *Future Cardiol* 3(6): 591-593.

195. Gacko, M. and S. Glowinski (1998). "Activities of proteases in parietal thrombus of aortic aneurysm." *Clin Chim Acta* 271(2): 171-177.
196. Gacko, M., A. Guzowski, et al. (2006). "[Concentration and activity of cathepsin D in the blood plasma and serum of patients with abdominal aortic aneurysm]." *Przegl Lek* 63(5): 265-267.
197. Chamberlain, C. M., L. S. Ang, et al. (2010). "Perforin-independent extracellular granzyme B activity contributes to abdominal aortic aneurysm." *Am J Pathol* 176(2): 1038-1049.
198. Ballard DJ, Filardo G, Fowkes G, et al. Surgery for small asymptomatic abdominal aortic aneurysms (review). *Cochrane Database Syst Rev* 2008
199. Van der Vliet JA, Boll AP. Abdominal aortic aneurysm. *Lancet* 1997;349:863-866.
200. Reeps C, Essler M, Pelisek J, et al. Increased 18F-fluorodeoxyglucose uptake in abdominal aortic aneurysms in positron emission/computed tomography is associated with inflammation, aortic wall instability, and acute symptoms. *J Vasc Surg* 2008;48:417-424.
201. Vos FJ, Bleeker-Rovers CP, Corstens FH, et al. FDG-PET for imaging of non-osseous infection and inflammation. *Q J Nucl Med Mol Imaging* 2006;50:121-130.
202. Sakalihan N, Hustinx R, Limet R. Contribution of PET scanning to the evaluation of abdominal aortic aneurysm. *Semin Vasc Surg* 2004;17:144-153.
203. Bleeker-Rovers CP, de Kleijn EM, Corstens FH, et al. Clinical value of FDG PET in patients with fever of unknown origin and patients suspected of focal infection or inflammation. *Eur J Nucl Med Mol Imaging* 2004;31:29-37.
204. Rudd JH, Fayad ZA. Imaging atherosclerotic plaque inflammation. *Nat Clin Pract Cardiovasc Med* 2008;5(Suppl. 2): S11-S17.
205. Lòpez-Candales A, Holmes DR, Liao S, et al. Decreased vascular smooth muscle cell density in medial degeneration of human abdominal aortic aneurysms. *Am J Pathol* 1997;150:993-1007.
206. Laitinen I, Marjamäki P, Haaparanta M, Savisto N, Laine VJ, Soini SL, et al. Non-specific binding of [18F]FDG to calcifications in atherosclerotic plaques: experimental study of mouse and human arteries. *Eur J Nucl Med Mol Imaging* 2006;33:1461-7.
207. Boellaard R, O'Doherty MJ, Weber WA, Mottaghy FM, Lonsdale MN, Stroobants SG, et al. FDG PET and PET/CT: EANM procedure guidelines for tumour PET imaging: version 1.0. *Eur J Nucl Med Mol Imaging* 2010;37:181-200.

208. Rudd JH, Myers KS, Bansilal S, et al. Atherosclerosis inflammation imaging with 18F-FDG PET: carotid, iliac, and femoral uptake reproducibility, quantification methods, and recommendations. *J Nucl Med* 2008;49:871-878.
209. Rudd JH, Myers KS, Bansilal S, et al. 18Fluorodeoxyglucose positron emission tomography imaging of atherosclerotic plaque inflammation is highly reproducible implications for atherosclerosis therapy trials. *J Am Coll Cardiol* 2007;50:892-896.
210. Izquierdo-Garcia D, Davies JR, Graves MJ, Rudd JH, Gillard JH, Weissberg PL, et al. Comparison of methods for magnetic resonance-guided [18-F]fluorodeoxyglucose positron emission tomography in human carotid arteries: reproducibility, partial volume correction, and correlation between methods. *Stroke* 2009;40:86–93.
211. Ellison RC, Zhang Y, Wagenknecht LE, Eckfeldt JH, Hopkins PN, Pankow JS, et al. Relation of the metabolic syndrome to calcified atherosclerotic plaque in the coronary arteries and aorta. *Am J Cardiol* 2005;95:1180–6.
212. Siegel CL, Cohan RH, Korobkin M, Alpern MB, Courneya DL, Leder RA. Abdominal aortic aneurysm morphology: CT features in patients with ruptured and nonruptured aneurysms. *AJR Am J Roentgenol* 1994;163:1123–9.
213. Freestone T, Turner RJ, Coady A, Higman DJ, Greenhalgh RM, Powell JT. Inflammation and matrix metalloproteinases in the enlarging abdominal aortic aneurysm. *Arterioscler Thromb Vasc Biol* 1995;15:1145–51.
214. Davies MJ. Aortic aneurysm formation: lessons from human studies and experimental models. *Circulation* 1998;98: 193-195.
215. Choke E, Cockerill G, Wilson WR, et al. A review of biological factors implicated in abdominal aortic aneurysm rupture. *Eur J Vasc Endovasc Surg* 2005;30:227-244.
216. Sakalihasan N, Delvenne PH, Nusgens B, et al. Activated forms of MMP2 and MMP9 in abdominal aortic aneurysms. *J Vasc Surg* 1996;24:127-133.
217. Bouvet C, Moreau S, Blanchette J, et al. Sequential activation of matrix metalloproteinase 9 and transforming growth factor beta in arterial elastocalcinosis. *Arterioscler Thromb Vasc Biol* 2008;28:856-862.
218. Truijers M, Harrie AJ, Kurvers M, et al. In vivo imaging of abdominal aortic aneurysms: increased FDG uptake suggests inflammation in the aneurysm wall. *J Endovasc Ther* 2008;15:462-467.



219. Kotze CW, Menezes LJ, Endozo R, et al. Increased metabolic activity in abdominal aortic aneurysm detected by 18F-fluorodeoxyglucose (18F-FDG) positron emission tomography/ computed tomography (PET/CT). *Eur J Vasc Endovasc Surg* 2009;38:93-99.
220. Soret M, Bacharach SL, Buvat I. Partial-volume effect in PET tumor imaging. *J Nucl Med* 2007;48:932-945.
221. Menezes LJ, Kotze CW, Hutton BF, et al. Vascular inflammation imaging with 18F-FDG PET/CT: when to image? *J Nucl Med* 2009;50:854-857
222. Xu XY, Borghi A, Nchimi A, et al. High levels of 18F-FDG uptake in aortic aneurysm wall are associated with high wall stress. *Eur J Vasc Endovasc Surg* 2010;39:295-301.
223. Chaikof EL, Brewster DC, Dalman RL, et al. The care of patients with an abdominal aortic aneurysm: the Society for Vascular Surgery practice guidelines. *J Vasc Surg* 2009;50(Suppl. 4):S8-49.
224. Ogawa M, Ishino S, Mukai T, Asano D, Teramoto N, Watabe H, et al. (18)F-FDG accumulation in atherosclerotic plaques: immunohistochemical and PET imaging study. *J Nucl Med* 2004;45:1245–50.
225. Walter MA, Melzer RA, Schindler C, Müller-Brand J, Tyndall A, Nitzsche EU. The value of [18F]FDG-PET in the diagnosis of large-vessel vasculitis and the assessment of activity and extent of disease. *Eur J Nucl Med Mol Imaging* 2005;32:674–81.
226. Palombo D, Morbelli S, Spinella G, et al. A positron emission/ computed tomography (PET/CT) evaluation of asymptomatic abdominal aortic aneurysms: another point of view. *Ann Vasc Surg* 2011
227. Ocana E, Bohórquez JC, Pérez-Requena J, Brieva JA, Rodríguez C. Characterisation of T and B lymphocytes infiltrating abdominal aortic aneurysms. *Atherosclerosis* 2003;170:39–48.
228. Koch AE, Haines GK, Rizzo RJ, Radosevich JA, Pope RM, Robinson PG, et al. Human abdominal aortic aneurysms. Immunophenotypic analysis suggesting an immune-mediated response. *Am J Pathol* 1990;137:1199–213.
229. Henderson EL, Geng Y-J, Sukhova GK, Whittemore AD, Knox J, Libby P. Death of smooth muscle cells and expression of mediators of apoptosis by T lymphocytes in human abdominal aortic aneurysms. *Circulation* 1999;99:96–104.
230. Stella A, Gargiulo M, Pasquinelli G, Preda P, Faggioli GL, Cenacchi G, et al. The cellular component in the parietal infiltrate of inflammatory abdominal aortic aneurysms (IAAA). *Eur J Vasc Surg* 1991;5:65–70.

231. Tisell LE, Oden A, Muth A, Altiparmak G, Mölne J, Ahlman H, et al. The Ki67 index a prognostic marker in medullary thyroid carcinoma. *Br J Cancer* 2003;89:2093–7.
232. Annovazzi A, Bonanno E, Arca M, D'Alessandria C, Marcoccia A, Spagnoli LG, et al. <sup>99m</sup>Tc-interleukin-2 scintigraphy for the *in vivo* imaging of vulnerable atherosclerotic plaques. *Eur J Nucl Med Mol Imaging* 2006;33:117–26.
233. Zubal G, Fujibayashi Y, Maruoka N, Omata N, Yonekura Y. Automated kinetic analysis of FDG uptake in living rat brain slices from dynamic positron autoradiography. *Cancer Biother Radiopharm* 2003;18:405–11.
234. Colin S, Mascarelli F, Jeanny JC, Vienet R, Bouche G, Courtois Y, et al. Comparative study *in vivo* and *in vitro* of uniformly <sup>14</sup>Clabelled and <sup>125</sup>I-labelled recombinant fibroblast growth factor 2. *Eur J Biochem* 1997;249:473–80.